Structural and molecular determinants of the sensitivity of a4b2 nicotinic acetylcholine receptors to the allosteric ligand desformylflustrabromine

Constanza Alejandra Alcaino-Ayala

PhD 2015

"Soy,

Soy lo que dejaron,

Soy toda la sobra de lo que se robaron.

Un pueblo escondido en la cima,

mi piel es de cuero por eso aguanta cualquier clima.

Frente de frio en el medio del verano,

el amor en los tiempos del cólera, mi hermano.

Soy el desarrollo en carne viva,

un discurso político sin saliva.

Las caras más bonitas que he conocido,

soy la fotografía de un desaparecido.

Soy una canasta con frijoles,

soy Maradona contra Inglaterra anotándote dos goles.

Soy lo que sostiene mi bandera,

la espina dorsal del planeta es mi cordillera.

Soy lo que me enseño mi padre,

el que no quiere a su patria no quiere a su madre.

Soy América latina,

un pueblo sin piernas pero que camina.

¡Perdono pero nunca olvido!

Aquí estamos de pie

¡Que viva Latinoamérica!"

To my mother Alejandra

List of Publications

Mantione E, Micheloni S, **Alcaino C**, New K, Mazzaferro S and Bermudez Isabel (2012) Allosteric modulators of α4β2 nicotinic acetylcholine receptors: A new direction for antidepressant drug discovery. *Future Medicinal Chemistry*.

Benallegue N, Mazzaferro S, **Alcaino C**, and Bermudez I (2013). The additional acetylcholine binding site at the α4(+)/α4(-) interface of the $(\alpha4\beta2)_2\alpha4$ nicotinic acetylcholine receptor contributes to desensitisation. *British Journal of Pharmacology*.

Mazzaferro S, Gasparri F, New K, **Alcaino C**, Faundez M, Vasquez P.I, Vijayan, R, Biggin, P.C, Bermudez I (2014). Non-equivalent Ligand Selectivity of Agonist Sites in $(\alpha4\beta2)_2\alpha4$ Nicotinic Acetylcholine Receptors: A Key Determinant of Agonist Efficacy. *Journal of Biological Chemistry.*

Manuscript in Preparation

Alcaino C, Mazzaferro S, Faundez M, Vazquez P.I, Musgaard M, Biggin P.C, Bermudez I (2015). Role of the C-terminal domain in the modulatory effects of the transmembrane allosteric modulator Desformylflustrabromine in α4β2 Nicotinic Acetylcholine Receptors.

Poster Presentations

Biophysical Society (BPS) Annual Meeting 2013, San Francisco, CA, USA. **The role of the fifth subunit in the sensitivity of α4β2* Nicotinic Acetylcholine Receptors to Allosteric Modulators.**

Nicotinic Acetylcholine Receptors Meeting. Cambridge, UK, 2014. **The role of the fifth subunit in the sensitivity of α4β2* Nicotinic Acetylcholine Receptors to Allosteric Modulators.**

Table of Contents

List of Publications **1**
Poster Presentations 2
Table of Contents 3
List of Figures 6
List of Tables 9
List of abbreviations 10
Abstract 12

CHAPTER 1 ..... **13**

Introduction **13**

1.1 Signal transmission in the nervous system. 14
1.2 LGICs. 16
1.2.1 pLGICs. 17
1.2.2 pLGICs at the atomic level. 18
1.3 The ECD. 20
1.3.1 The agonist binding site. 23
1.4 The TMD. 28
1.4.1 The ECD-TMD interface. 29
1.4.2 The Ion Pore. 30
1.5 Structural Transitions during Gating. 31
1.5.1 Pre-opening conformational transitions. 33
1.5.2 Coupling Agonist Binding to Channel Gating. 34
1.5.3 Desensitisation in the pLGIC Family. 37
1.6 Allosteric Modulation of pLGICs 39
1.6.1 Allosteric sites in the ECD. 39
1.6.2 Allosteric sites in the TMD. 40
1.7 nAChRs. 41
1.7.1 nAChR types and distribution. 42
1.7.2 α4β2* nAChRs. 43
1.7.3 Subunit composition of α4β2 nAChRs. 44
1.7.4 α5α4β2 nAChRs. 47
1.7.5 α6-containing-α4β2 nAChRs. 48
1.8 α4β2* nAChRs in Brain Pathologies. 49
1.8.1 Nicotine addiction. 49
1.8.2 Cognition. 51
1.8.3 Mood disorders. 51
1.8.4 Analgesia. 53
1.8.5 ADNFLE. 53
1.9 Pharmacological Profile of α4β2* nAChRs. 54
1.9.1 Agonists. 54
1.9.2 Antagonists. 57
1.9.3 Allosteric Modulators of α4β2 nAChRs. 58
1.9.4 PAMs of α4β2 nAChRs. 59
1.9.5 NAMs of α4β2 nAChRs. 64

AIM OF THE THESIS 65

CHAPTER 2 ..... **66**

Materials and Methods **66**

2.1 Reagents. 67
2.2 Animals. 67
2.3 Molecular Biology. 67
2.3.1 Single Point Mutations 68
2.3.2 α4β2 and α3β2 nAChR models 70
2.3.3 Engineering mutant β2_α4_β2_α4_α4 and β2_α4_β2_α4_β2 receptors. 70
2.4 *Xenopus laevis* oocytes preparation. 71
2.4.1 Microinjection of cDNA and cRNA. 72
2.5 Electrophysiological Recordings. 73
2.5.1 ACh and dFBr concentration response curves (CRC). 73
2.6 Substituted cysteine accessibility method 75
2.6.1 Modification of dFBr putative binding sites using SCAM. 75
2.6.2 Covalent modification of introduced cysteines by MTSET reagent 76
2.6.3 MTSET reaction rates. 77
2.6.4 Protection assay. 78
2.7 Statistical analysis. 79
2.8 Homology Modelling and Docking. 79

CHAPTER 3 ..... **82**

Pharmacological Characterization of the Positive Allosteric Effects of dFBr on α4β2 nAChRs. 82

3.1 Introduction 83
3.2 Results 85
3.2.1 Effects of dFBr in $(\alpha4\beta2)_2\alpha4$ and $(\alpha4\beta2)_2\beta2$ nAChRs. 85
3.3 Discussion. 94

CHAPTER 4 ..... **95**

The TMD of the α4β2 nAChR mediates the potentiating effects of dFBr. **95**

4.1 Introduction 96
4.2 Results 98
4.2.1 Role of the TMD in the potentiation by dFBr. 98
4.2.2 SCAM approaches support the presence of a potentiating binding site for dFBr in the TMD of the α4 subunit 106
4.2.3 The α4 subunit is necessary and sufficient for dFBr potentiation of α4β2 nAChRs .. 110
4.3 Discussion 115

CHAPTER 5 ..... **118**

The C-terminal domain of the α4 subunit as a key determinant of the potentiating effects of dFBr on α4β2 nAChRs **118**

5.1 Introduction 119
5.2 Results 121
5.2.1 Sequence conservation and dFBr effects in nAChRs. 121
5.2.2 Role of the C-terminal in the potentiating effects of dFBr in α4β2 nAChRs. 122
5.2.3 Transduction mechanism: C-terminal domain and Cys loop interaction. 131
5.3 Discussion 136

CHAPTER 6 ..... **138**

Final Discussion **138**

Acknowledgments **143**

Bibliography **146**

List of Figures

CHAPTER 1 ..... **13**

Introduction **13**

Figure 1.1. Diagram of a typical chemical synapse. 15
Figure 1.2. Membrane topology of receptors from the family of pLGICs. 19
Figure 1.3. Crystal structures of all Pentameric Ligand-gated Ion channels. 22
Figure 1.4. Ribbon diagrams of the tridimensional structure of the whole *Torpedo* nAChR at 4Å resolution. 24
Figure 1.5. Ligand binding interface from the *Torpedo* nAChR at 4 Å resolution (Adapted from Unwin 2005) 25
Figure 1.6. Top view of the AChBP pentamers in presence of antagonist (A) and agonist (B). 28
Figure 1.7. The flipped states. 34
Figure 1.8. ECD-TMD interface of nAChR at 4 Å resolutions. 36
Figure 1.9. Subunit combinations in neuronal nAChRs. 43
Figure 1.10. Homology models of α4β2 nAChRs. 44

CHAPTER 2 ..... **66**

Materials and Methods **66**

Fig. 2.1. Diagram of three steps for receptor expression in *Xenopus* oocytes showing cRNA injection of β2_α4_β2_α4_β2 cRNA. 72

CHAPTER 3 ..... **82**

Pharmacological Characterization of the Positive Allosteric Effects of dFBr on α4β2 nAChRs. **82**

Figure. 3.1. Tridimensional structure of dFBr. 83
Figure 3.2. ACh and dFBr concentration response curves from α4β2 receptors expressed in

Xenopus oocytes in 1:1 ratios. 87

Figure 3.3. ACh concentration response curves of 1:1 α4β2 receptors in presence and absence of 10 μM dFBr. 89

Figure 3.4 Desensitization kinetics of α4β2 receptors elicited by ACh in presence and absence of dFBr. 90

Figure 3.5 Effects of dFBr in β2_α4_β2_α4_α4 and β2_α4_β2_α4_β2 concatenated receptors. 92

Figure 3.6. Effects of membrane potential on inhibitory effects of dFBr at concatenated α4β2 nAChRs. 93

CHAPTER 4 95

The TMD of the α4β2 nAChR mediates the potentiating effects of dFBr. 95

Figure 4.1. α4β2 nAChR Homology model and dFBr docking experiments. 100

Figure. 4.2. ACh and dFBr profiles of wild type and TMD mutant receptors. 101

Figure. 4.3. dFBr concentration response curves for α4F312Aβ2, α4F312Cβ2 and α4F312Yβ2 mutant receptors. 105

Figure. 4.4. Effect of MTSET on dFBr responses of wild type and mutant α4β2 receptors. 107

Figure. 4.5. Effect of low concentrations of MTSET in dFBr responses using Protection Assay with and without rates. 109

Figure. 4.6. Comparison of the conserved cavity hosting the putative binding site of dFBr in α4 and β2 subunits. 111

Figure. 4.7. Potentiation of concatenated α4β2 nAChRs is dependent on the number of α4 subunits. 113

CHAPTER 5 118

The C-terminal domain of the α4 subunit as a key determinant of the potentiating effects of dFBr on α4β2 nAChRs 118

Figure 5.1. Pair-wise Sequence alignment of relevant loops and domains present across α subunits. 122

Figure. 5.2. ACh and dFBr concentration response curves for α3β2 wild type and α3F310Aβ2

receptors. 123
Figure 5.3. Pharmacological profile of α3* and α4* chimeric receptors. 124
Figure 5.4. Changes in dFBr maximal potentiation by removal or introduction of a PP motif at the top of the M4 helix. 128
Figure 5.5. Effects of single point mutations in the C-terminal domain on potentiation by dFBr. 129
Figure. 5.6. Additive effects of dFBr and 17β-estradiol (17β-E) in α4β2 nAChRs. 130
Figure 5.7. Structure of Cys loop and C-terminal domain of an α4 subunit (From α4β2 model adapted from X-ray structure 5-HT_3 receptor) 132
Figure 5.8. ACh and dFBr responses of α4β2 receptors with modified α3 Cys loop and C-terminal domain. 133
Figure 5.9. Relative potentiation of α4β2 wild type and Cys loop mutants. 134

List of Tables

CHAPTER 1 ..... **13**

Introduction **13**

Table 1.1. Pharmacological profile of α4β2 nAChRs. 46
Table 1.2. Positive allosteric modulators of α4β2 nAChRs. 60

CHAPTER 3 ..... **82**

Pharmacological Characterization of the Positive Allosteric Effects of dFBr on α4β2 nAChRs. **82**

Table 3.1. Summary of ACh CRC of α4-containing nAChRs 88

CHAPTER 4 ..... **95**

The TMD of the α4β2 nAChR mediates the potentiating effects of dFBr. **95**

Table 4.1. Concentration effects of ACh and dFBr on wild type and TMD mutant α4β2 nAChRs. 102

CHAPTER 5 ..... **118**

The C-terminal domain of the α4 subunit as a key determinant of the potentiating effects of dFBr on α4β2 nAChRs **118**

Table 5.1. Concentration effects of ACh and dFBr on mutant α4β2 and α3β2 nAChRs. 125

List of abbreviations

5I-A5380	5-Iodo-3-[(2S)-2-Azetidinylmethoxy pyridine dihydrochloride
5-Br-Cys	5-bromo-cytisine
5-HT_3	Serotonin
5-HT_3R	Serotonin receptor
A-85380	3-[(2S)-2-Azetidinylmethoxy pyridine dihydrochloride
ACh	Acetylcholine
AChBP	Acetylcholine binding protein
AD	Alzheimer's disease
ADNFLE	Autosomal dominant nocturnal frontal lobe epilepsy
AMPA	α-amino-3-hydroxy-5-methyl-4-isoxazolepropionic acid
ANOVA	Analysis of variance
ATP	Adenosine triphosphate
C.elegans	*Caenorhabditis elegans*
C-terminal	Carboxy-terminus
cDNA	complementary deoxyribose nucleic acid
CI	Confidence interval
CNS	Central nervous system
CRC	Concentration response curve
cRNA	Complementary ribonucleic acid
Cyt	Cytisine
DA	Dopamine
dFBr	Desformylflustrabromine
dTC	[^{3}H]d-tubocurarine
dNTP	Deoxyribonucleotide triphosphate
DhβE	Dihydro-β-erythroidine
DMSO	Dimethylsulphoxide
DTT	Dithioerythritol
EC_{10}	Concentration producing 10% of maximal effect.
EC_{50}	Concentration producing half maximal effect
EC_{50_1}	Concentration producing half-maximal high sensitivity stimulatory effect in a biphasic CRC
EC_{50_2}	Concentrations producing half-maximal low sensitivity stimulatory effects in a biphasic CRC
ECD	Extracellular domain
ELIC	Prokaryotic pentameric ligand-gated ion channels from *Erwinia chrysanthemi*
Epi	Epibatidine
EPSP	Excitatory postsynaptic potential
GABA	γ-aminobutyric acid
$GABA_AR$	γ-aminobutyric acid receptor type A
GAs	General anaesthetics
GLIC	Prokaryotic pentameric ligand-gated ion channels from *Gloeobacter violaceus*
GluCl	Glutamate-gated chloride channels
Gly	Glycine
GlyR	Glycine receptor
HEK	Human Embryonic Kidney 293

HEPES	N-2-hydroxyethylpiperazine-N'-2-ethansulphonic acid
HS	High sensitivity
HPA	Hypothalamic-pituitary-adrenal axis
IC_{50}	Concentration producing half maximal inhibition
IACh	Acetylcholine current
IPSP	Inhibitory postsynaptic potential
KAB-18	Biphenyl-2-carboxylic acid 1-(3-phenyl-propyl)-piperidin-3-ylmethyl ester
Ki	Binding affinity constants
kDA	Kilo Dalton
LGIC	Ligand-gated ion channel
LS	Low sensitivity
LY-2087101	[2-(4-fluoroanilino)-4-methyl-1,3-thiazol-5-yl]-thiophen-3-ylmethanone
Mec	Mecamylamine
MTS	Methenothiosulphate reagents
MTSET	[2-(Trimethylammonium)ethyl] methanethiosulfonate
N-terminal	Amino-terminus
NA	Noradrenaline
NAc	Nucleus accumbens
nAChR	Nicotinic acetylcholine receptor
nH	Hill coefficient
NAMs	Negative allosteric modulators
Nic	Nicotine
NMDA	n-methyl-D-aspartic acid
NS9283	3-[3-(3-pyridyl)-1,2,4-oxadiazol-5-yl]benzonitrile
NS206	3-N-Benzyloxy-3-hydroxyimino-2-oxo-6,7,8,9-tetrahydro-1H-benzo[g]indole-5-sulfonamide
PAMs	Positive allosteric modulators
PCR	Polymerase chain reaction
PFC	Prefrontal cortex
pLGIC	Pentameric ligand-gated ion channel
PNS	Peripheral nervous system
PNU-120596	(5-Chloro-2,4-dimethoxyphenyl)-N'-(5-methyl-3-isoxazolyl)-urea)
REFER	Rate-equilibrium free energy relationships
Saz-A	Sazetidine-A
SCAM	Substituted Cysteine Accessibility Method
SEM	Standard error of the mean
SNP	Single nucleotide polymorphism
TC-2559	4-(5-ethoxy-3-pyridinyl)-N-methyl-(3E)-3-buten-1-amine difumarate
TC5214	S-(+) mecamylamine
TMA	Tetramethylammonium
TMD	Transmembrane domain
TPP	Tegmental pedunculopontine nucleus
UCI-30002	N-(1,2,3,4-tetrahydro-1-naphthyl)-4-nitroaniline)
Var	Varenicline
VTA	Ventral tegmental area
Zn^{2+}	Zinc

Abstract

Allosteric modulation of neuronal nicotinic acetylcholine receptors (nAChRs) is considered to be one of the most promising approaches for therapeutics. By binding to a site of the receptor distinct from the neurotransmitter binding site, allosteric modulators alter the response of the receptors to their agonists. There are two major locations of allosteric modulator binding sites. One is in subunit interfaces of the extracellular N-terminal domain. The other is in the transmembrane domain close to the channel gating machinery. This thesis focuses on a positive allosteric modulator of the human α4β2 nAChR, desformylflustrabromine (dFBr), which was found to exert its potentiating effects on this receptor by binding to a site in the transmembrane region of the α4 subunit.

α4β2 nAChRs are the most abundant nAChR type in the brain, where they modulate a range of brain functions such as mood, cognition, nociception and reward. This receptor subtype has been shown to be sufficient and necessary for the rewarding and reinforcing properties of nicotine. In addition, α4β2 nAChRs have been implicated in aging-related cognitive dysfunction, Alzheimer's and Parkinson's diseases, mood disorders and a rare type of family epilepsy. dFBr is a positive allosteric modulator of the α4β2 and α2β2 nAChRs that displays selectivity against all other nAChRs. Using functional mutagenesis and structural modelling, the molecular basis for the selective potentiation of α4β2 nAChRs has been identified. The potentiating binding site of dFBr is located in the top-half of a transmembrane cavity between the M3 and M4 helices of the α4 subunit. α4Y309, α4F312 and α4L617 influence dFBr potentiation in accord with a role in dFBr binding. Alanine substitutions of these residues annulled dFBr potentiation and experiments using MTSET showed that the residues in this putative site are accessible to MTSET and that dFBr competes with MTSET for the access to the cavity. These residues map to a highly conserved intra-subunit cavity in the pentameric ligand gated ion channel (pLGIC) family. In addition, the effector system for the potentiating effects of dFBr was also identified. The post-M4 region (C-terminal) and the Cys loop residues F167 and F170 of the α4 subunit play central roles in transducing dFBr binding to potentiation of the ACh responses of the α4β2 nAChR. Whilst the residues that contribute to the dFBr binding site in the α4 are conserved across all nAChR subunits, except for α7, the post-M4 region is not. It is this region that determines the selective potentiating effects of dFBr on α4β2 nAChR. This finding, together with recent data on the effect of propofol in bacterial and invertebrate evolutionary related pLGICs, suggest that for highly conserved transmembrane domain allosteric binding sites, the effector machinery associated with these sites, rather than the binding sites, define the receptor selectivity of the modulators.

CHAPTER 1

Introduction

1.1 Signal transmission in the nervous system.

In the nervous system, a synapse, a word derived from the Greek *synapsis*, is a structure that permits neurons to pass electrical or chemical signals to other cells such as neurons or muscle cells. Synapses can be chemical or electrical. In electrical synapses communication occurs between adjacent cells that are linked together by an intercellular specialization termed gap junction. Both ion currents and small molecules such as ATP and second messengers can pass through gap junctions and, the flow is bidirectional and has no delay. In chemical synapses, on the other hand, one neuron releases chemical messengers (neurotransmitter molecules) into a narrow space (the synaptic cleft) that is adjacent to another neuron. The neurotransmitter molecules are stored within small sacs called synaptic vesicles and are released into the synaptic cleft by exocytosis. Exocytosis is triggered when Ca^{2+} ions flow into the pre-synaptic terminals through voltage-gated Ca^{2+} channels. The latter activate when the pre-synaptic terminal is depolarized by the arrival of action potentials. The released neurotransmitter then binds to receptors on the plasma membrane of the post-synaptic cell and depending on whether the post-synaptic receptors are ligand-gated ion channels (LGICs) or metabotropic (G-protein coupled) receptors, neurotransmitter binding results in a transient change in either the membrane potential or the metabolic status of the post-synaptic cell, respectively. The signals generated by neurotransmitters on the post-synaptic cells can be depolarizing (excitatory post-synaptic potential, EPSP) or hyperpolarizing (inhibitory post-synaptic potentials, IPSP), depending on the ionic selectivity of the LGIC. The neurotransmitter-receptor complex dissociates within milliseconds and the receptors return to their resting state. Finally, neurotransmitter molecules are removed from the synaptic gap through one of several mechanisms including enzymatic degradation (cholinergic synapses) or re-uptake by specific transporters either on the presynaptic cell (e.g., biogenic aminergic

cells) or on glial cells surrounding the synapses (e.g., glutamatergic synapses) (Aidley, 1996) (Fig. 1.1).

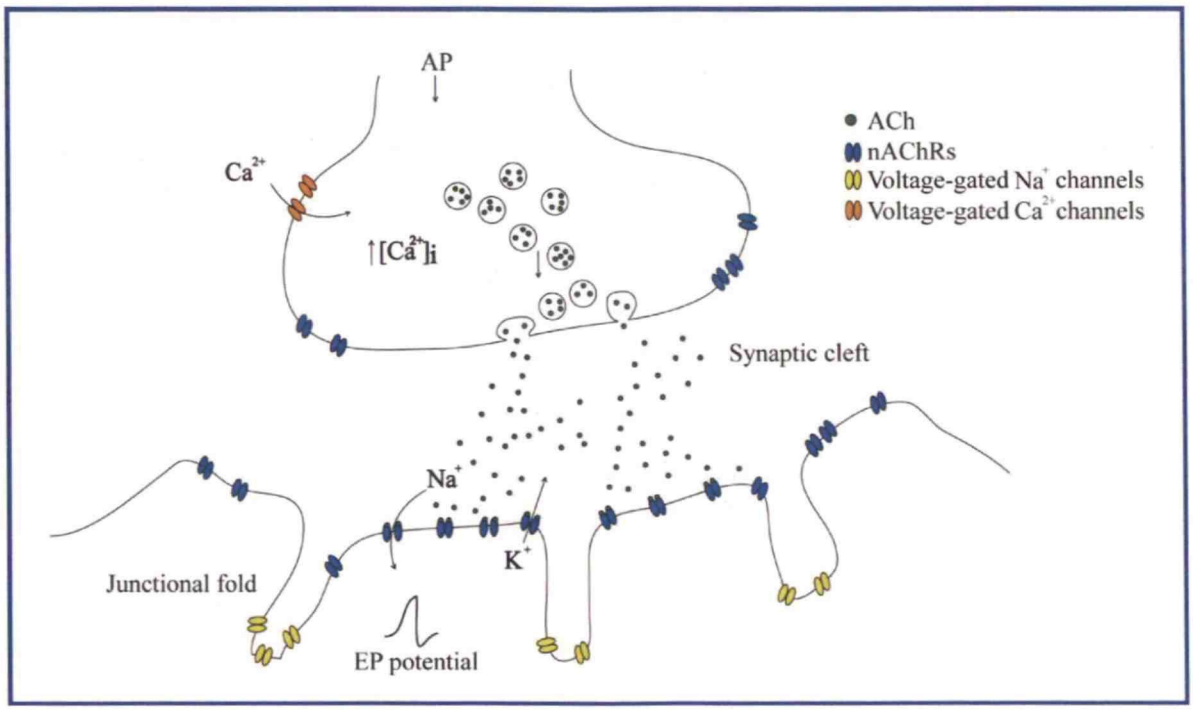

Figure 1.1. Diagram of a typical chemical synapse. The cartoon represents the neuromuscular junction, a chemical synapse that uses acetylcholine (ACh) as a neurotransmitter. In this synapse the post-synaptic receptors are LGICs, and the binding of ACh to this type of receptors leads to an excitatory transient response by the post-synaptic cell. Arrival of action potentials to the presynaptic terminal activates voltage-dependent Ca^{2+} channels (EPSP), which in turns induces the fusion of synaptic vesicles with the pre-synaptic membrane and hence release of the neurotransmitter into synaptic gap. The neurotransmitter binds post-synaptic receptors to trigger a response by the post-synaptic cell.

1.2 LGICs.

LGICs constitute an important class of integral membrane proteins responsible for fast signal transmission in excitable cells. LGICs are typically composed of at least two different regions: a transmembrane domain (TMD) that includes the ion pore and an extracellular domain (ECD) that houses the binding site for the neurotransmitter (agonist). LGICs are multimeric proteins whose component subunits assemble around a central ion channel through which ions move into or out of cells driven by their electrochemical gradients upon agonist-induced opening of the channel.

LGICs are classified into three super-families which are not related evolutionary: ATP-gated channels, ionotropic glutamate receptors and pentameric LGICs (pLGICs). A key structural characteristic of LGICs is the number of subunits that form the complexes and the membrane topology of each subunit. ATP-gated channels, termed P2X receptors, have a trimeric topology with permeability to Na^+, K^+ and Ca^{2+} ions. The composing subunits of P2X receptors have two membrane spanning segments (Alves et al., 2014). Ionotropic glutamate receptors are cationic tetramers and the TMD of each subunit is made of three membrane spanning segments. The ionotropic glutamate receptors are subdivided into three groups (AMPA, Kainate and NMDA receptors) based on their pharmacology and structural similarities (Karakas et al., 2015). pLGICs have a pentameric topology and comprise a large ECD (approx. 200 amino acids long) and a TMD made of four TM α helix segments (M1 to M4) organized in a bundle (Miller & Smart, 2010). This thesis is concerned with the α4β2 subtype of nicotinic acetylcholine receptors (nAChRs), a member of the pLGIC superfamily of signalling proteins.

1.2.1 pLGICs.

pLGICs are widely expressed in bacteria, invertebrates (e.g., insects, worms), birds, fish (*Torpedo*, zebrafish), mammals and humans. The amino acid sequence of Prokaryotic and Eukaryotic pLGICs show low sequence identity of typically 18%-20%, in accord with their phylogenetic distance. However, they share common structural and functional features such as transmembrane topology, N-terminal ECD and domain organization (Miller & Smart, 2010). They also conserve sequence motifs that are necessary for structure and function of this type of signalling proteins such as a cysteine bridge in a loop in the ECD involved in gating (Cys loop) and a W-X-P motif in a loop in the ECD. Eukaryotic pLGICs include nAChRs, GABA type A receptors ($GABA_ARs$), glycine receptors (GlyRs) and serotonin type 3 receptors ($5\text{-}HT_3Rs$). The invertebrate glutamate-gated chloride channel (GluCl) belongs to this group of ion channels as well (Miller & Smart, 2010). In mammals and humans, pLGICs mediate all fast synaptic inhibition in the central nervous system (CNS) and much of fast peripheral excitation. Human pLGICs are attractive targets for new drug development because of their many physiological roles, as in spinal nociception (GlyRs and nAChRs) (Harvey, 2004; Miwa et al., 2011), neuroprotection and cognition (neuronal nAChRs, $GABA_ARs$) (Miwa et al., 2011; Rudolph & Knoflach, 2011), appetite regulation and reward (neuronal nAChRs) (Mineur, Abizaid, et al., 2011; Mineur, Einstein, et al., 2011) and regulation of muscle tone (GlyRs) (Lynch, 2004). Thus, human pLGICs are the target of many common drugs, both medicinal (benzodiazepines, many anti-epileptics, neuromuscular blockers, general anaesthetics, the antiemetic ondansetron), and recreational (nicotine and alcohol). The related insect and worm GluCl channel is targeted by anti-parasitic drugs and by economically important insecticides (Wolstenholme & Rogers, 2005). The subunit composition of eukaryotic pLGICs is diverse, offering the opportunity and the challenge of

developing subtype-specific agents for therapeutic or pest-control purposes. Many drugs that act via pLGICs either directly activate them or enhance their activation.

pLGICs are homomeric or heteromeric pentamers and each subunit consists of an approximately 200 residue long N-terminal ECD with 10 β strands (β1 – β10) folded into β sandwich, four membrane spanning domains (M1 to M4) organized into a four α-helix bundle, connected by cytoplasmic and extracellular loops and a short extracellular C-terminus (Fig. 1.2). The group can be divided into excitatory or inhibitory receptors based on the permeability of the ion channel. For example, excitatory 5-HT_3Rs and nAChRs are cation selective and their permeability to sodium, potassium and/or calcium generates depolarizing membrane potentials, whereas inhibitory $GABA_A$Rs and GlyRs are anion selective and generate chloride hyperpolarizing currents (Miller & Smart, 2010; Lynagh & Pless, 2014). The remaining part of this chapter will review current understanding of the structure and function of pLGICs, with particular emphasis, towards the end, on the α4β2 nAChR, the focus of this thesis.

1.2.2 pLGICs at the atomic level.

The three dimensional structure of pLGICs is highly conserved from prokaryotes to humans. They all share a common topological organization with a molecular mass arranged around a central ion channel with a C5 (rotational symmetry of 5) axis perpendicular to the plasma membrane plane. The peptide subunits that form pLGICs have the same three dimensional fold comprising the ECD, the TMD and an intracellular part containing one α helix (Fig. 1.2). Available structures include those of prokaryotic pLGICs from *Gliobacter violaceous* (GLIC) and *Erwinia chrysanthemi* (ELIC) solved respectively at 2.9 Å (Bocquet et al., 2009) and 3.3

Å (Hilf & Dutzler, 2008; Hilf & Dutzler, 2009) and eukaryotic GluCl channel from *C. elegans* (in complex with a Fab antibody from mouse hybridoma cells and Ivermectin) solved at 3.3 Å (Hibbs & Gouaux, 2011), electron microscopy structure of *Torpedo* nAChR at 4-9 Å (Unwin, 1993; Miyazawa et al., 2003; Unwin, 2005; Unwin & Fujiyoshi, 2012), as well the recently solved structures of a human $GABA_AR$ β3 homomer and the mouse 5-HT_3A receptor (Miller & Aricescu, 2014; Hassaine et al., 2014). Prokaryotic structures have been solved in open and closed conformations at acidic pH (Hilf & Dutzler, 2008; Bocquet et al., 2009) as well as at neutral pH (Sauguet et al., 2014), thus providing crystal structures of closed, open and desensitised channels.

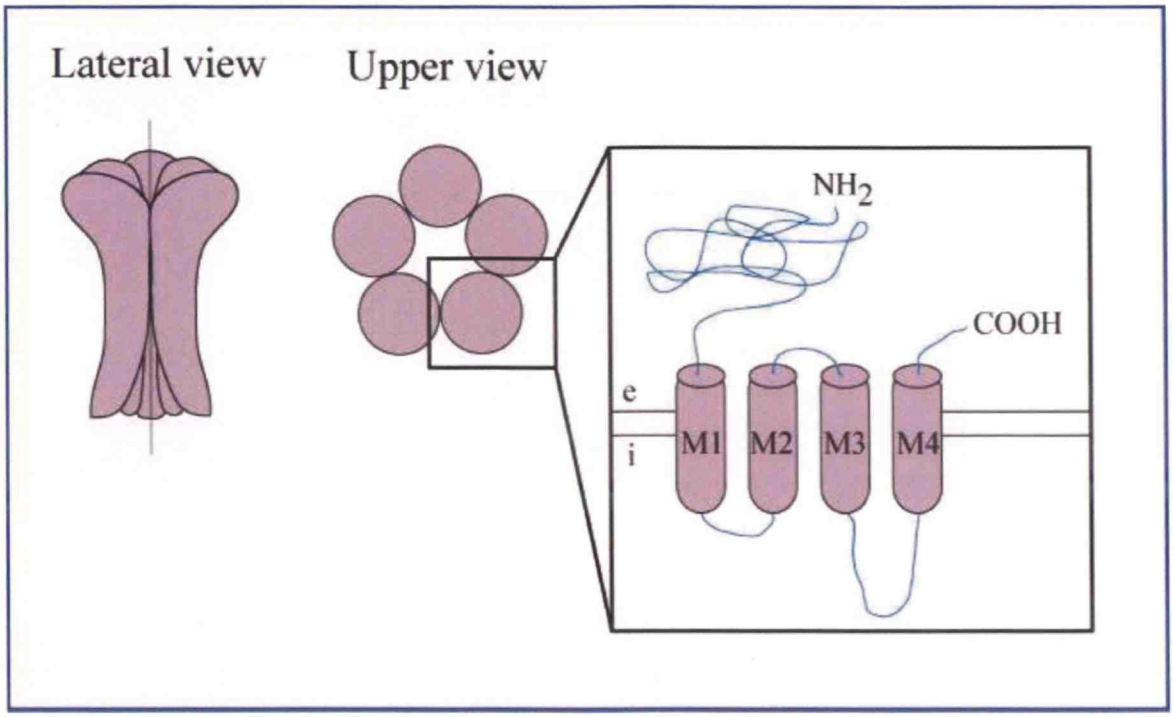

Figure 1.2. Membrane topology of receptors from the family of pLGICs. Lateral and upper view of the pentameric assembly and close-up of each subunit containing a large N-terminal domain, four trans-membrane helices, an intracellular loop of variable size connecting M3 and M4 helices and a short extracellular C-terminal tail. Extracellular (e) and Intracellular (i) compartments are indicated.

1.3 The ECD.

In the last fifteen years, several X-ray structures of isolated ECDs have been solved, leading to tremendous advances in our understanding of how pLGICs interact with competitive ligands and ECD-binding allosteric compounds. These are: the pentameric snail homolog ACh binding protein (AChBP) in complex with diverse nicotinic compounds, at resolutions as high as 2.05 Å (Brejc et al., 2001; Celie et al., 2004; Celie et al., 2005; Bourne et al., 2005; Hansen et al., 2005; Hibbs et al., 2009; Rucktooa et al., 2009; Brams et al., 2011); ECD of GLIC at 2.3 Å (Nury et al., 2010), ECD of the α1 nAChR subunit complexed to α-bungarotoxin at 1.94 Å (Dellisanti et al., 2007), α7 nAChR/AChBP chimera with and without an agonist at 2.8 Å (Li et al., 2011) and 3.1 Å (Nemecz & Taylor, 2011), respectively. More recently, the X-ray structure of the human α9 nAChR subunit ECD in both *apo* (1.8 Å resolution) and antagonist-bound conformations (Fig.1.3) has been published (Zouridakis et al., 2014). The complexes with antagonist methyllycaconitine or α-bungarotoxin were obtained at 1.7 Å and 2.7 Å resolutions, respectively.

In agreement with seminal structural studies of the snail AChBP (Brejc et al., 2001), it has been shown that the ECD of both Prokaryotic and Eukaryotic pLGICs is folded in a highly conserved immunoglobulin-like β sandwich fold. The two β-sheets composing the β sandwich are made of six inner strands (β1 to β6) and four outer strands (β7 to β10), and they are linked through a Cys loop disulphide bridge. The β strands in each β sheet are joined by loops that are important for agonist binding. These are: the Cys loop, loops A, B and C and the β1/β2 loop that connects the inner β-sheet to M2 (Miller & Smart, 2010). Eukaryotic ECD also contains an N-terminal α-helix that may play a role in receptor expression and in receptor-antibody interactions (Taly et al., 2009). The first high resolution image of a

mammalian pLGIC became available in 2007, when a 1.94 Å resolution atomic structure of the mouse α1 subunit ECD in complex with α-bungarotoxin was resolved (Dellisanti et al., 2007) (Fig. 1.3). This structure revealed the main regions of the domain together with the binding domain occupied by the toxin and most importantly it showed the presence of two buried hydrophilic residues at the core of the α1 subunit (T52 and S126), conserved throughout nAChRs, but that correspond to hydrophobic residues in AChBPs (F, L or V). This difference suggests that a more hydrophilic environment at positions 52 and 126 evolved for signalling functions (Dellisanti et al., 2007).

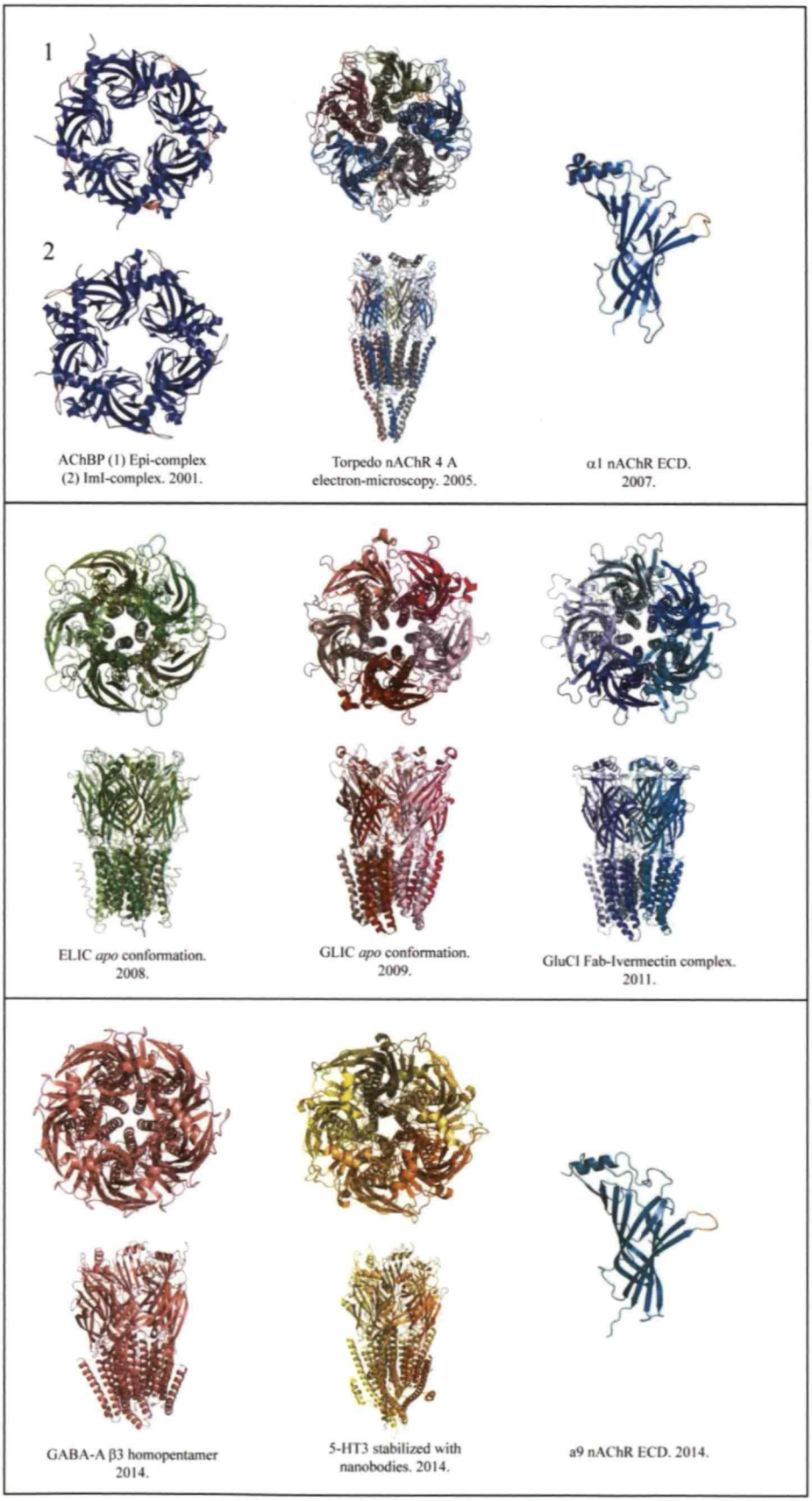

Figure 1.3. Crystal structures of all Pentameric Ligand-gated Ion channels. From top to bottom the crystal structures of pLGICs, in order of publication. Top box: AChBP structure Epi (1) and ImI (2) complexes (PDB code *apo* structure 1I9B), *Torpedo* nAChR structure

(Unwin, 2005. PDB code 2GB9) and ECD structure of α1 nAChR subunit (PDB 2QC1). Middle box: ELIC crystal structure in the *apo*-conformation (PDB 2VLO), GLIC crystal structure in *apo*-conformation (PDB 3EAM) and GluCl in complex with ivermectin (PDB 3RHW). Bottom box: $GABA_A$ β3 homopentamer structure (PDB 4COF), 5-HT_3 mouse structure (PDB 4PIR) and ECD of the α9 nAChR subunit (PDB 4D01).

1.3.1 The agonist binding site.

The agonist binding site in Eukaryotic pLGICs is located in the ECD at the interface of two adjacent subunits. One subunit contributes the principal (+) component of the binding site whereas the other acts as a complementary (-) face. The binding pocket is characterized by a core of aromatic and hydrophobic residues from both the principal and complementary subunits and loop C (Fig. 1.4).

Homomeric pLGICs have five agonist sites but heteromeric pLGICs host from 2 (nAChRs) to 3 ($(\alpha4\beta2)_2\alpha4$ nAChRs). Among the pLGIC family, the agonist binding sites of the muscle nAChR are the most functionally characterized. This 250 kDa heteropentamer is formed by two α1 subunits and three non-α subunits: β1, δ and ε or γ (ε in adult and γ in the fetal receptor). The subunit arrangement is δ-α1-γ-α1-β1 (Reynolds & Karlin, 1978; Lindstrom et al., 1979), with subunit interfaces α1-γ (ε in adult) and α1-δ each housing an ACh binding site (Blount & Merlie, 1989; Sine & Claudio, 1991) (Fig. 1.4). Diverse approaches have been applied to this domain, including affinity labelling, mutagenesis, substitution cysteine accessibility method (SCAM) (Czajkowski & Karlin, 1995; Zhang & Karlin, 1997; Karlin & Akabas, 1998), non-natural amino acid mutagenesis (Zhong et al., 1998; Xiu et al., 2009) and, as mentioned above, enhanced electron microscopy and crystallography (Unwin, 1993; Miyazawa et al., 2003; Unwin, 2005; Unwin & Fujiyoshi, 2012).

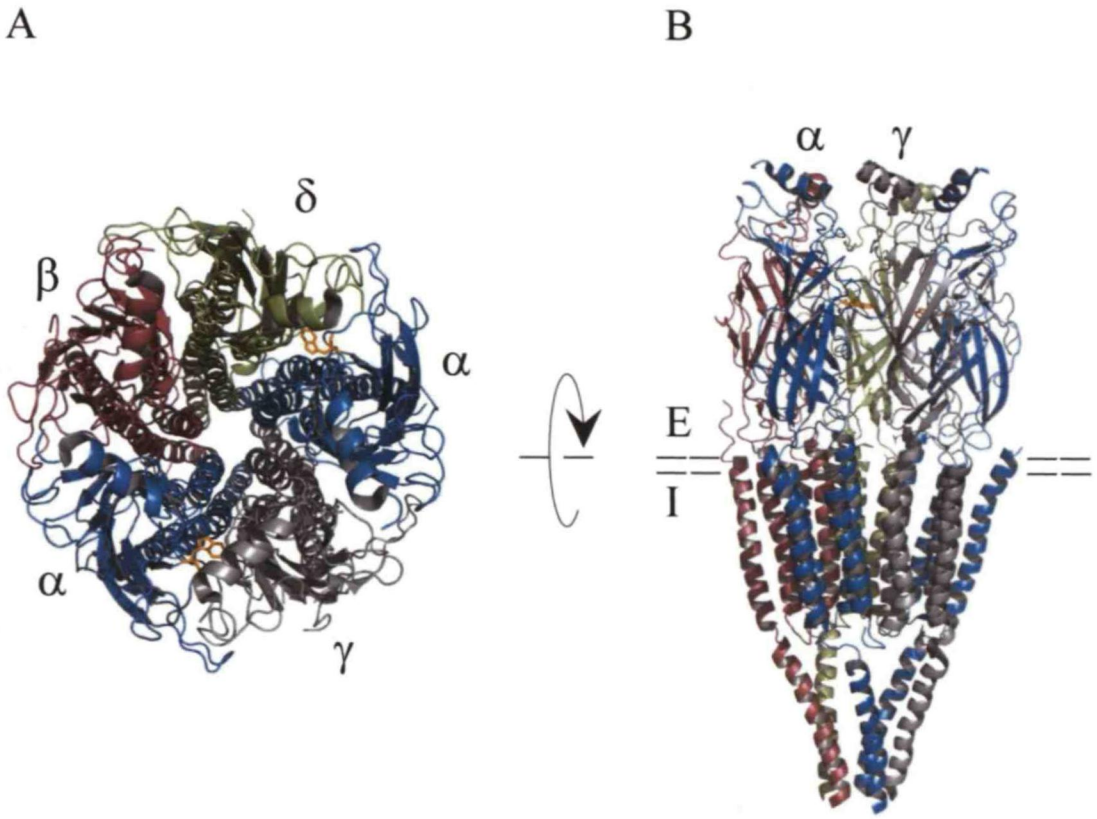

Figure 1.4. Ribbon diagrams of the tridimensional structure of the whole *Torpedo* nAChR at a 4Å resolution. (A) Anti-clockwise organization viewed from the extracellular side. (B) Lateral side view with the membrane plane. (Subunits: α, blue; β, red; γ, grey; δ, green; in yellow the locations of W149; E and I, show the extracellular an intracellular side respectively). (Adapted from Unwin, 2005).

The agonist binding site is contributed by loops A, B and C from the principal subunit, and four loops from the complementary subunit termed loops D, E, F and G (Bren & Sine, 1997; Sine, 2002; Beene et al., 2004; Miller & Smart, 2010) (Fig. 1.5). The complementary subunit is located anti-clockwise to the one providing the principal side (Fig. 1.5) (Lynagh & Pless, 2014; Nys et al., 2013). Aromatic residues from loops A, B, C and D form an aromatic box that interacts with the quaternary amine moiety of ACh. Particularly important is a cation π interaction between a conserved W residue (W149 in the *Torpedo* α1 nAChR subunit) in loop B and the quaternary amine group of ACh (Zhong et al., 1998). This interaction is a key determinant of agonist affinity and efficacy in nAChR (Zhong et al., 1998; Xiu et al., 2009) and is well conserved in eukaryotic pLGICs, although it may involve other loops, depending

on the type of pLGIC (e.g., loop B in nAChRs, GlyRs and 5HT-$_3$Rs or loop A in GABA$_A$Rs). Ligand binding interactions between ligand ammonium moieties and the aromatic residues of loops A, B and C have been also confirmed in crystal structures of both, *C. elegans* GluCl channel in complex with glutamate and prokaryotic pLGICs in complex with ligands (Zimmermann & Dutzler, 2011).

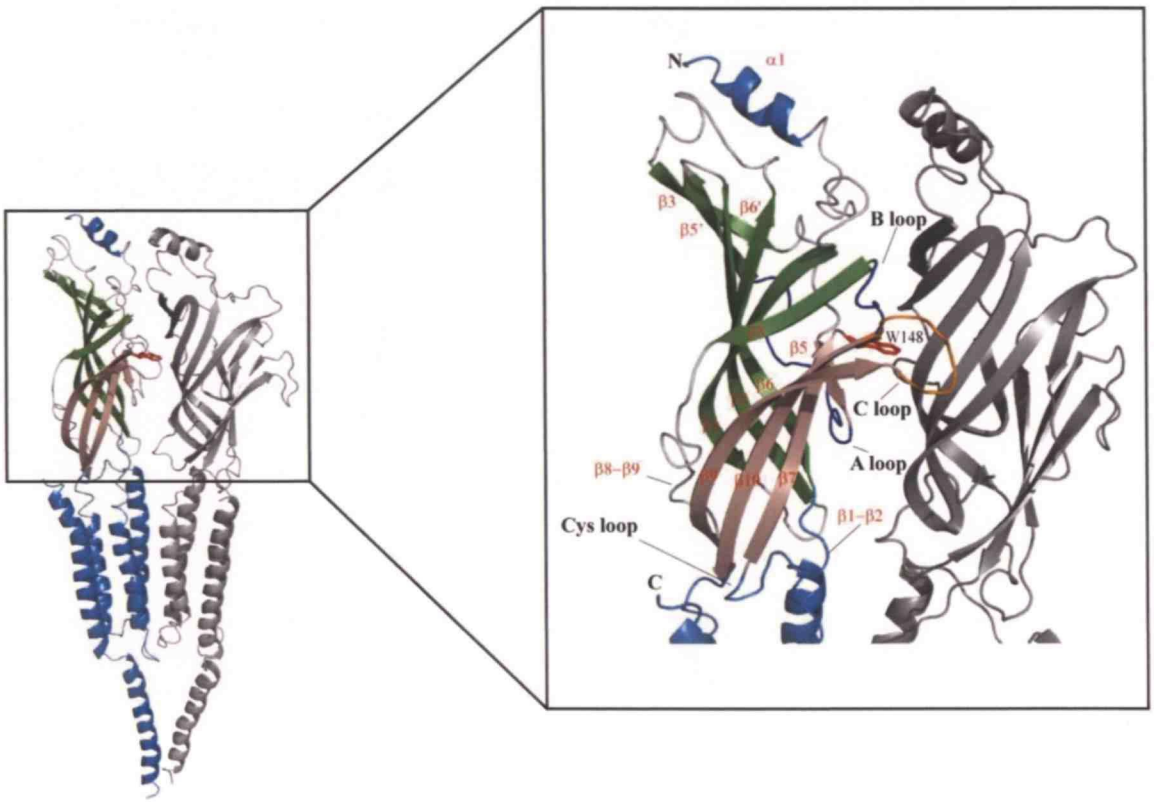

Figure 1.5. Ligand binding interface from the *Torpedo* nAChR at 4 Å resolution (Adapted from Unwin 2005). Left: full length interface α1/γ. Right: Close-up of the ligand binding domain with most important loops in α1 subunit and β-strands.

The acetyl functional group of ACh interacts with loops E and F (Albuquerque et al., 2009). Interactions with the complementary loops seem to be electronegative and hydrophobic (hydrogen bonding or van der Waals interactions), as suggested by crystal structures of agonist-bound AChBP (Hansen et al., 2005) and α7-AChBP chimeric receptors (Li et al., 2011). Key complementary face residues contributing to agonist binding in nAChRs are

L112, M114, and W53 (*Torpedo* sequence numbering). In the muscle nAChR, photo-affinity labelling studies that used [^{3}H]d-tubocurarine (dTC), a competitive antagonist, and [^{3}H]nicotine showed that loop C of the α subunit and γW55 (loop D) are critical for ligand binding (Chiara et al., 1999). Cross-linking experiments of αC192/C193 to a negatively charged residue showed that residue D180 (loop F) is also involved in ligand binding (Czajkowski & Karlin, 1995). Further studies in embryonic muscle nAChR from mice suggested that amino acid differences between loop E and loop F in γ and δ subunits account for site selectivity to competitive antagonists (Sine, 1993), whereas in the adult mouse antagonist affinity has been attributed mainly to the residue γE57 (Loop D) (Bren & Sine, 1997). Extensive mutagenesis and electrophysiological studies as well as crystal structures of the AChBP bound to different agonists and antagonists have led to the view that agonist interactions with the principal subunit primarily determine binding affinity, whereas interactions with key amino acids at the complementary subunit affect agonist efficacy (Hibbs et al., 2009; Brams et al., 2011; Billen et al., 2012; Rohde et al., 2012; Harpsøe et al., 2013). More recently, it has been shown that in heteromeric receptors that host three agonist sites, in which one of the site differs from the other two by having a different complementary subunit, agonist exclusion from this site is due to residues located in the complementary component of that particular site, and this agonist selectivity is an important determinant of agonist efficacy (Mazzaferro et al., 2014).

Currently, more than 50 structures of AChBP with diverse bound ligands are available, including full and partial agonists (Celie et al., 2004; Hibbs et al., 2009; Rucktooa et al., 2009) and antagonists (toxins) (Bourne et al., 2005; Brams et al., 2011). These structures have shown that loop C moves inwardly towards the bound binding site (loop C capping), leading to the view that loop C capping may trap the agonist into the binding site

(Mukhtasimova et al., 2009). Large ligands, such as antagonists, appear to induce loop C uncapping (an outward movement of loop C) (Figure 1.6). This finding suggests that loop C capping may be an early conformational transition leading to receptor activation. Uncapped loop C has also been observed in the high resolution electron microscopic images of unbound *Torpedo* nAChR (Unwin, 2005; Unwin & Fujiyoshi, 2012). In a different study, capping of loop C was studied using a chimeric pLGIC comprising the AChBP linked to the TMD of a 5-HT_3R. The chimeric receptor was sensitive to ACh, suggesting that the movement of loop C seen in AChBP once in contact with an agonist could trigger an activation similar to that of nAChRs (Bouzat et al., 2004). In $GABA_A$Rs an intra-subunit salt-bridge between two conserved charged residues was identified to be critical for the regulation of loop C position (Venkatachalan & Czajkowski, 2008), homologous to that found in muscle nAChRs (Mukhtasimova et al., 2005). However, it has also been shown that in presence of the potent nAChR antagonist dihydro-β-erythroidine (DhβE) the co-crystal of DhβE-Ls-AChBP had loop C in the capped conformation (Shahsavar et al., 2012). Thus, the role of loop C capping in the function of pLGICs is still not fully understood (Figure 1.6).

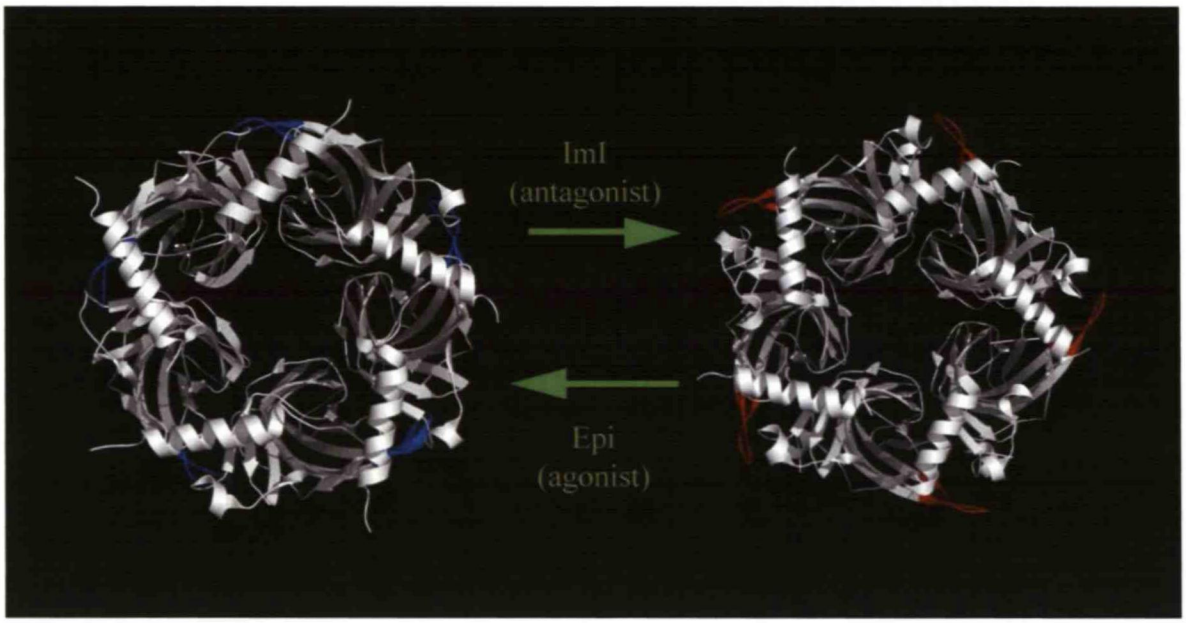

Figure 1.6. Top view of the AChBP pentamers in presence of antagonist (A) and agonist (B). Note the distinctive conformations for the antagonist (α-conotoxin ImI) and agonist (Epi) complexes. The loop C remains open in presence of antagonist (in red) and closed with agonist (in blue) (Adapted from Hansen at al., 2005).

1.4 The TMD.

Early structures of *Torpedo* nAChR (Unwin, 2005) and crystal structures of GLIC and ELIC (Hilf & Dutzler, 2008; Hilf & Dutzler, 2009; Bocquet et al., 2009; Nury et al., 2011), GluCl channels from *C. elegans* (Hibbs & Gouaux, 2011) and full length human and mice pLGICs (Miller & Aricescu, 2014; Hassaine et al., 2014) indicate that the four membrane-spanning segments of each subunit of pLGICs fold into α helices that arrange in the membrane forming concentric rings around a tapered water filled pore. There is an inner ring of helices (M2) lining the water filled pore, and an outer ring of helices (M1, M3 and M4) facing the membrane lipids. In the closed channel, M2 bends inwardly and make side-to-side contacts in the middle of the phospholipid bilayer. The outer M1 and M3 make side-to-side contacts and twist around each other. This packing produces a slight separation between the inner and

outer rings, particularly in the extracellular part of the TMD. The outermost M4 helices make limited contact with the rest of the protein but interact extensively with membrane lipids.

The TMD is not only the domain that contains the ion channel but abundant experimental evidence show that the various regions of the TMD play crucial roles in the function of pLGICs. For instance, post M4, the extracellular region of M4 (i.e., C-terminal), has been suggested as a key player in the coupling of agonist binding to channel gating through possibly interactions between M4 and the Cys loop (daCosta & Baenziger, 2009). Evidence from studies of the nAChR indicate that M4 is also an important lipid sensor, and lipid-nAChR interactions appear to play a pivotal role in receptor folding and trafficking as well as allosteric interactions with lipids such as cholesterol (Hénault et al., 2014). Although M4 is the segment of the TMD with highest lipid interactions, M1 has also been shown to present special motifs for cholesterol-mediating signalling (Baier et al., 2011). The TMD is also an important region for allostery and this will be discussed in more detail in section 1.7 of this chapter and Results Chapter 4.

1.4.1 The ECD-TMD interface.

From studies on *Torpedo* nAChRs, it appears that the region that couples agonist binding to channel gating is made up of several loops that come into close contact with TMD. These are, from the ECD, the Cys loop, the β1-β2 linker, the β8-β9 linker, the β10-M1 linker and, from the TMD, the M1-M2 linker (Unwin, 2005; Jha et al., 2007; Lee et al., 2009). M1 is connected to M2 through loop M1-M2 and, M2 is connected with M3 through the M2-M3 linker. Finally, a long intracellular loop connects helices M3 and M4 and the last segment is connected to the extracellular side of the membrane through post-M4. This arrangement is similar in the prokaryotic pLGIC, making it possible to engineer fully functional proteins

between GLIC and α1 GlyR (Duret et al., 2011).

1.4.2 The Ion Pore.

The dimensions of the pore vary across the lipid membrane. The helices traverse the membrane with a set of conserved residues that form concentric rings at each level. By convention, these rings are numbered from the intracellular side of the channel, starting with 0' (first positively-charged ring) and ending up with 20' for the last extracellular ring (Unwin, 2005). In *Torpedo* nAChR the upper part of the spanning pore is the widest and presents mostly non-polar amino acids except for two residues (S266 and E262) that are thought to influence cation transport by creating a negative electrostatic environment in this area. At the cytoplasmic side of the pore another group of negatively charged residues creates a vestibule of similar characteristics (Konno et al., 1991). In anion-selective pLGICs, these regions are electropositive, providing a conserved anionic attractive environment. Single point mutation studies altering the charge of this region in *Torpedo* nAChRs have shown to change ion conductance (Imoto et al., 1988) and the exchange of M2 residues from α7 nAChRs to GABA receptors converted the nAChR channel from cationic to anionic (Galzi et al., 1992).

The middle section is the narrowest, as the M2 helices come together by the presence of bulky hydrophobic side chains that symmetrically interact with each other. These contacts happen between L251 and its neighbour alanine or serine (presumably S252) and at the lower level between F256 and its corresponding valine or isoleucine residue (presumably V255), creating a highly hydrophobic region between rings 9' and 14' of a radial distance from the central axis of no more than 3.5 Å. This constriction would make impossible for a hydrated potassium or sodium ion to pass through. The unique characteristics of this section as a barrier for ion permeation along the conduction path strongly suggest it to be the channel gate

(Wilson & Karlin, 1998; Miyazawa et al., 2003). In ELIC, unlike what is seen in nAChRs, the middle section of the channel is made of bulky hydrophobic amino acids that constitute a physical barrier that obstruct the channel when is in a closed conformation (Hilf & Dutzler, 2008).

Converging evidence suggests that agonist binding makes M2 α-helices of all five subunits rotate sideways to open the pore. This rotation is possible due the proximity between M1, M3 and M4 with M2 and the flexibility of α helixes (Miyazawa et al., 2003; Unwin, 2005). Recent structural studies suggest that the upper portions of the M2 and M3 α helices and the M2-M3 loop move as a unit (Althoff et al., 2014), although rate-equilibrium free energy relations (REFER) analyses found that M2 presents higher energy levels than M3 and M4, suggesting these two helices move as a rigid body after M2 twists to open the channel (Auerbach, 2010). The latter is consistent with the idea of a quaternary twist of the M2 helices studied in α7 nAChRs (Taly et al., 2005).

1.5 Structural Transitions during Gating.

In pLGICs the agonist site and the ion channel are more than 50 Å apart, suggesting that agonist binding may trigger conformational transitions that are transmitted to M2 to induce channel gating. Early electron microscopy studies of *Torpedo* nAChR suggested that channel opening involves rotation of M2 accompanied by a kinked-to-straight change in α-helix conformation (Unwin, 1993; Unwin, 2005). These studies also suggested that α subunits β strands (especially β1 and β2) rotate clockwise by 15 degrees during activation (Miyazawa et al., 2003; Unwin, 2005). This rotation is transmitted to the channel domain via contact between loop-2 in the inner β sheet and the M2-M3 linker at the extracellular end of the pore.

More recently, Unwin and collaborators used a plunge-freezing technique in samples of *Torpedo* nAChR in combination with cryo-electron-microscopy to obtain high resolution images of ACh-bound nAChRs (Unwin & Fujiyoshi, 2012). These images suggest that ACh binding to the α subunits triggers a rearrangement and displacement of subunits that makes β subunits move and destabilize the symmetrical pore-lining helices arrangement (Unwin & Fujiyoshi, 2012). These events have not been experimentally validated. However, comparing open and closed structures of Prokaryotic pLGICs (GLIC and ELIC) (Hilf & Dutzler, 2008; Hilf & Dutzler, 2009; Bocquet et al., 2009) suggests a similar pattern of conformational changes. Thus, it appears that in Prokaryotic pLGIC the channel opens by an outward tilt of the extracellular end of the pore-lining M2 helix, probably because loop 7 and M2-M3 move outwards, pulling M2 back towards M1, M3 and M4. This is supported by the pattern of proton accessibility of pore residues in mammalian nAChRs (Cymes et al., 2005). What is the precise ECD conformational change that leads to channel gating in Eukaryotic pLGICs is less clear. The open and closed structures available come from pLGICs with modest sequence homology (Prokaryotic GLIC and ELIC and *Torpedo* nAChR) and most of the *apo*- and agonist-bound structures come from AChBP. It seems obvious that gating has to start with a motion of ECD loops surrounding the agonist binding site and that these changes have to bring about an increase in agonist affinity. One possibility is that loop C on the primary component of the binding site moves inwardly to cap the binding pocket. Different electrostatic interactions stabilize the capped and uncapped conformations of loop C (Mukhtasimova et al., 2005). In *C. elegans* GluCl, binding of the agonist glutamate makes loop C move closer to the agonist, but these data have to be taken cautiously because GluCl was crystallized in complex with a Fab molecule that appears to interact in the crystal with the ECD at loops C and F (Hibbs & Gouaux, 2011). Loop B has been proposed as an alternative or additional candidate for the earliest movement induced by agonist binding

(Auerbach, 2010).

1.5.1 Pre-opening conformational transitions.

The downstream transmission of the agonist-binding signal is essential for gating, and structural and single channel data suggests that the activation mechanism of pLGICs involves several intermediate states prior to channel opening, which adds more complexity to the three steps model of open, desensitised and closed conformations (Del Castillo & Katz, 1957). Evidence for these intermediate states comes from studies that have mapped the energy landscape of the channel proteins using single channel recording approaches as it proceeds from resting to activated. Rate constants values determined in these studies have been analysed by REFER, which was pioneered for muscle nAChRs by Auerbach and his team (Grosman et al., 2000). They showed that during activation a wave of conformational change spreads from the ECD towards the pore, probably with several distinct, successive motions, each of which involves a discrete set of residues (Purohit et al., 2007). The precise nature of these motions and the structures of the intermediate states in the chain remain largely unexplored. Studies by Sivilotti and her team at University College London detected and measured for the first time the properties of pre-opening intermediates in the GlyR (Burzomato et al., 2004). Their findings were confirmed in muscle nAChR by Sine and his team in the USA (Mukhtasimova et al., 2009). Their work on pre-opening conformational transitions ('priming') links priming to a conformational change in the ECD, as priming induced by agonist binding is reproduced by trapping the loop C in a partially activated state with a disulphide bridge. Analysis by Lape et al. (2008) showed that the pre-opening intermediates (termed flipped states) bind the agonist more tightly than the resting state of the channel, suggesting that it represents a distinct ECD conformation. It was also shown that this

state is important in the pharmacology of pLGICs because it is the ability to make the channel flip that determines how efficacious an agonist is (Lape et al., 2008), for a review see (Colquhoun & Lape, 2012) (Fig. 1.7). Recent single channel kinetic studies by Auerbach and his team that compared the rate and equilibrium constants for low affinity binding to nAChRs and channel gating for several different agonists of adult-type mouse nAChRs suggested that each binding site can undergo two conformational changes ("catch" and "hold") that connect three different structures (*apo*-, Low affinity-bound, and high affinity-bound) (Jadey & Auerbach, 2012).

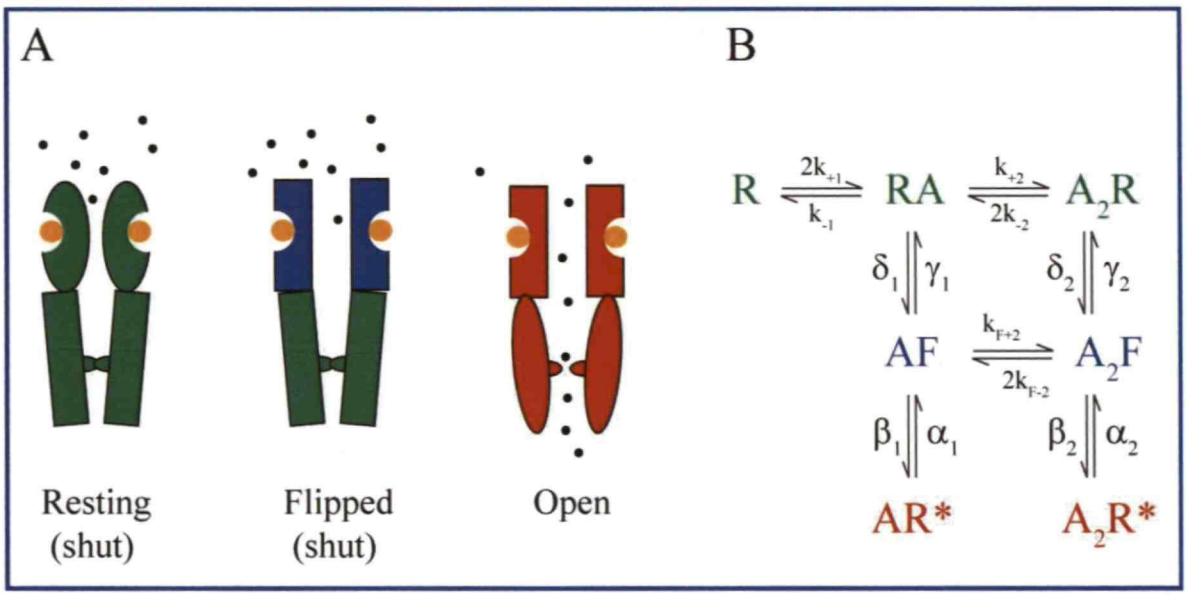

Figure 1.7. The flipped states. (A) The receptor at the resting state binds the agonist, then changes conformation to reach a flipped state. The flipped state has high affinity for the agonist but the channel is still close. Next the flipped receptor transits to the open conformation. (B) The flip mechanism in muscle nAChR activated by tetramethylammonium (TMA). The agonist is represented by A. R and R* are the receptor at the rest and activated states, respectively. F represents the flipped conformation (Adapted from Lape et al 2008).

1.5.2 Coupling Agonist Binding to Channel Gating.

Since the early 2000's several groups have investigated the connection between ligand

binding and channel gating (Fig. 1.8). The idea of a conformation wave proposed by Auerbach and colleagues was one of the first sets of evidence suggesting the existence of a coordinated pathway connecting the extracellular domain with the M2-lining helix, still in absence of a high resolution structure of the coupling region. In these studies, using single-channel kinetic analysis in conjunction with single point mutations in muscle nAChRs, they found that ligand binding triggers blocks of coordinated motions that connect the agonist binding site with the ion channel, starting from β4-β5 linker, β7-β8 linker, the loop C, down through the Cys-loop, β1-β2 linker, M2 and the channel gate (Grosman et al., 2000; Chakrapani et al., 2004; Purohit & Auerbach, 2009). Furthermore, their data suggested that areas located near the binding site move earlier in the opening process compared to those near the gate. The conformational wave propagates following Brownian movements in about 1 μs and the data suggested the M2 helix moves in three discrete steps, with the core of the channel serving as a gate to regulate the ion flux and also as a hub directing the propagation of the gating isomerization through the TMD (Grosman et al., 2000; Chakrapani & Auerbach, 2005; Purohit et al., 2007).

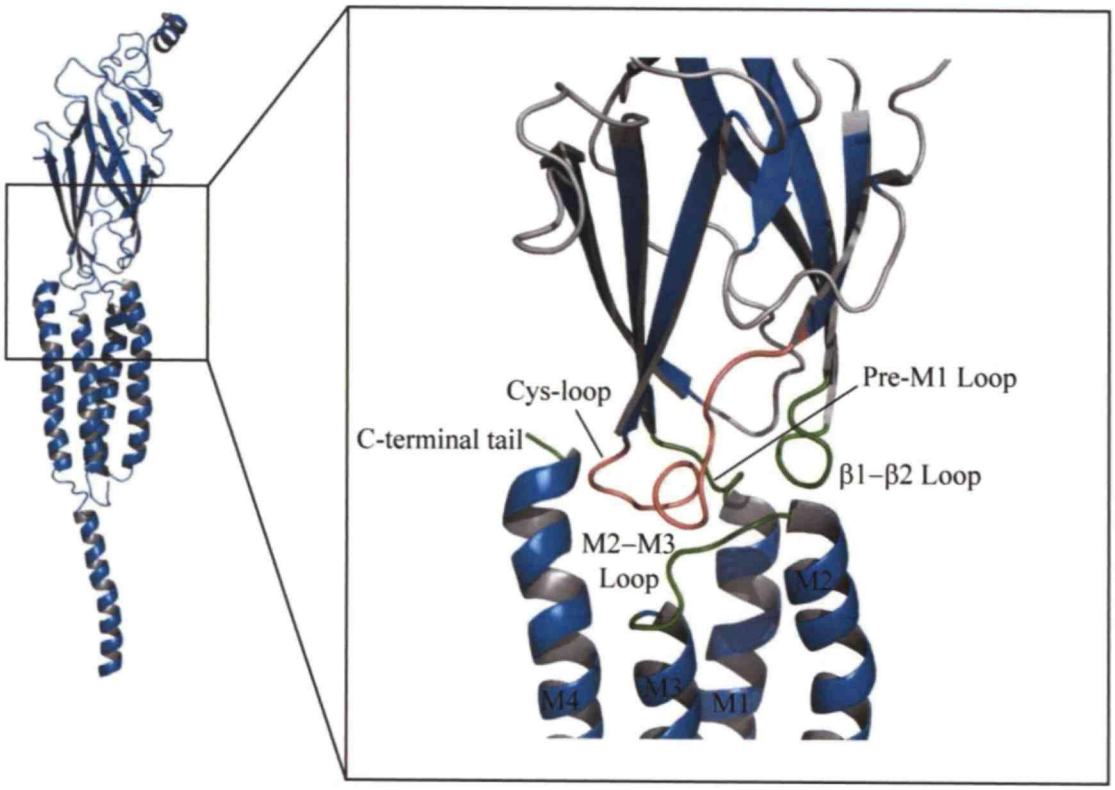

Figure 1.8. ECD-TMD interface of nAChR at 4 Å resolutions. Left-hand side ribbon diagram of a full length α1 subunit (lateral view). Right-hand side close-up of the Coupling region. In green M2-M3 Loop, β1-β2 Loop and Pre-M1 Loop. In light red Cys-Loop (Adapted from Unwin 2005, PDB code 2BG9).

A network of interacting loops in the interface between binding site and the ion channel has been probed to couple binding with gating in Eukaryotic pLGICs (Kash et al., 2003; Bouzat et al., 2004). Some of the initial studies in muscle nAChRs identified a triad of conserved residues which forms electrostatic interactions: in the absence of agonist, residues αK145 (β-strand 7) and αD200 (β-strand 10) form a salt bridge that has been be associated with the closed state of the channel and once in presence of agonist the movement of residue αY190 closer to αK145 breaks the contact with αD200. These movements, starting in β-strand 7 and β-strand 10, are thought to start the series of conformational changes prior to channel gating (Mukhtasimova et al., 2005). A most exhaustive mechanism defined as "The Principal Pathway" using the 4 Å resolution *Torpedo* structure (Unwin, 2005) defines a pathway that

starts with the capping of loop C and the subsequent movement of β-strand 10. In this region, a pair of invariant arginine (R209) and glutamic acid (E45) residues, present only in α subunits, form an electrostatic contact that links peripheral and inner β-sheets from the binding domain to the channel gate. E45 and a valine residue (presumably V46) present in β1-β2 hairpin, energetically couple to conserved proline and serine residues (P272 and S269) at the top of the M2-helix (Lee & Sine, 2005). In summary, this primary pathway suggests a link between the pre-M1 domain and the M2-M3 linker through the β1-β2 loop. Furthermore in 5-HT_3Rs a *trans* to *cis* side-chain isomerisation of a Proline residue (P303) in the M2-M3 loop appears to be critically involved in the opening of the channel (Lummis et al., 2005). The Cys-loop also plays a critical role in the transduction of the coupling signal. Its contribution is analogous to that of the β1-β2 loop by connecting the pre-M1 to the M2-M3 region and it constitutes a parallel pathway (Dellisanti et al., 2007; Jha et al., 2007; Lee et al., 2009). Moreover, there seems to be a concerted movement of β1-β2 loop and the Cys-loop, which act jointly on the M2-M3 linker to open the channel pore for ion conduction. REFER studies showed both loops have similar channel opening-closing rate equilibrium constants, which suggests they change conformation at the same time (Jha et al., 2007). Once the β-barrel relaxes and the loops return to their original positions the top of the pore constricts and the channel closes (Lee et al., 2009).

1.5.3 Desensitisation in the pLGIC Family.

In addition to activation, all Eukaryotic pLGIC desensitize when exposed to prolonged pulses of agonist. Among the various conformations of agonist-bound pLGIC, the desensitised agonist-bound pLGIC has the highest affinity for the agonist. Desensitization has also been reported for the Prokaryotic ELIC activated by cysteamine (Zimmermann & Dutzler, 2011) and for GLIC activated by protons, although GLIC desensitisation seems to be a slow process

in comparison to that of ELIC and Eukaryotic pLGICs (Gonzalez-Gutierrez & Grosman, 2010).

The mechanism of desensitisation is not fully understood but it is thought to be an important regulatory factor of chemical signalling (Giniatullin et al., 2005). Desensitisation is also relevant for drug discovery programmes. For example, some allosteric modulators such as PNU-120596, a selective positive allosteric modulator of α7 nAChRs, enhance the responses of this pLGIC by removing desensitisation (Hurst et al., 2005). Mutagenesis in combination with functional assays have shown that receptor regions involved in desensitisation of Eukaryotic pLGICs are the ECD (Bohler et al., 2001; Gay & Yakel, 2007; McCormack et al., 2010), the ECD-TMD interface (Bouzat et al., 2004), the hydrophobic rings that border the upper part of the ion pore (Revah et al., 1990) and the loop linking the M1 and M2 segment (Giniatullin et al., 2005). Time-resolved affinity labelling studies have suggested a reorganisation of the upper part of the TMD in the course of desensitisation (Forman & Miller, 2011), suggesting that desensitisation may underlie a local reorganisation of the TMD. This possibility is supported by voltage-clamp fluorimetry studies on GlyRs that show that the ECD-TMD region undergo large motions, whereas the structural changes undergone by ECD are less prominent (Wang & Lynch, 2011). Thus, although the exact mechanisms underlying desensitisation are not known, an increasing body of evidence indicates that there are discrete structural arrangements of the ECD and TMD associated with desensitisation, with structural perturbations at the level of the ECD-TMD being highly prominent.

1.6 Allosteric Modulation of pLGICs

In addition to ligands affecting pLGICs function by binding to the agonist sites or the lumen of the ion channel, pLGICs are allosterically modulated by diverse types of compounds, including general anaesthetics (GAs), neurosteroids, sex hormones, lipids, cholesterol and benzodiazepines. Over the last 20 years divergent accumulated evidence shows that pLGICs have two distinct regions that bind allosteric modulators. These are: a) sites located at non-agonist binding pockets that are homologous to the agonist binding sites (e.g., the benzodiazepine binding site in the $GABA_AR$ and Morantel in $\alpha3\beta2$ nAChRs; b) sites located in the TMD. The TMD contains a variety of allosteric sites making it a valid target for the development of novel therapeutic compounds.

1.6.1 Allosteric sites in the ECD.

The best-characterized example of an allosteric site in the ECD is the benzodiazepine binding pocket of $GABA_AR$. It is located in the $\alpha/\gamma2$ subunit interface, homologous to the GABA binding site in the β/α subunit interface. The benzodiazepine binding pocket is formed by residues in loops A through F and homologous to those forming the agonist binding pockets. Residues (with rat $\alpha1$ subunit numbering) identified from loop A H101 (Wieland et al., 1992; Duncalfe et al., 1996), loop B Y159 (Amin et al., 1997), and loop C G200 (Schaerer et al., 1998), T206, and Y209 (Buhr et al., 1997; Schaerer et al., 1998) are contributed by the α subunit and form the principal face of the binding pocket. Residues in loop D F77 (Buhr et al., 1997; Wingrove et al., 1997), A79, T81 (Teissére & Czajkowski, 2001; Kucken et al., 2003), loop E M130 (Buhr et al., 1997; Wingrove et al., 1997), and loop F E189, T193, and R194 (Sancar et al., 2007) are contributed by the γ subunit and form the complementary face

of the binding pocket. Recent structural studies of the prokaryotic ELIC pLGIC have shown that benzodiazepines also bind prokaryotic pLGICs (Spurny et al., 2012). Crystals of ELIC bound to flurazepam show that benzodiazepines engage two sites, depending on their concentration. One site is an inter-subunit site that partially overlaps the agonist binding pocket; this site is associated to potentiation and is occupied by low concentrations of flurazepam and matches with the benzodiazepine site found in eukaryotic $GABA_AR$. The other site is located in an intra-subunit region facing the channel vestibule; this site is associated with inhibition of ELIC. For nAChRs, a recent study shows that there is an amino-terminal non-canonical allosteric site for the positive allosteric modulator morantel in the α3β2 nAChR (Seo et al., 2009). This binding site for the allosteric modulator is located in the β/α subunit interface, in contrast to the α/β interface for the ACh binding site. The binding residues identified for morantel are located in what is equivalent to the upper half of the homologous agonist binding site.

1.6.2 Allosteric sites in the TMD.

Lipids, free fatty acids and steroids are known to allosterically modulate pLGIC nAChRs (daCosta & Baenziger, 2009; Nury et al., 2011). Although the TMD has been long known to house binding sites for allosteric modulators in eukaryotic pLGICs, the recent open structures of GLIC and GluCl have added an in-depth insight on the areas of the TMD involved in allostery. These studies have revealed three distinct allosteric binding site regions in the pLGIC TMD. These are: a) the intra-subunit cavity; b) the inter-subunit cavity; c) the lipid bilayer interface.

The intra-subunit cavity is located in the upper part of the TMD, at the centre of the α helix

bundle of each subunit. Structural studies that have applied X-ray electron density mapping and molecular dynamics to GLIC bound to the GAs Desflurane or Propofol have shown that GAs bind to this area mainly through van der Waals interactions (Nury et al., 2011). Extensive mutagenesis studies of Eukaryotic pLGICs indicate that this cavity is likely the binding site for GAs in nAChRs as well as for a variety of other synthetic compounds (e.g., (Young et al., 2008; daCosta et al., 2011; Gill et al., 2011). The recent structure of GluCl (Hibbs & Gouaux, 2011) bound to ivermectin revealed the upper part of the TMD of each subunit as a region that can bind large allosteric modulators such as ivermectin. Ivermectin contacts multiple residues from M2 and M3 of one subunit and from M1 of the adjacent subunit. Mutagenesis studies indicate that modulators such as neurosteroids bind an intra-subunit region located in the upper part of TMD (Hosie et al., 2009).

1.7 nAChRs.

nAChRs play critical physiological roles throughout the brain and body by mediating cholinergic excitatory neurotransmission (e.g., the neuromuscular junction, autonomic ganglia) (Albuquerque et al., 2009; Millar & Gotti, 2009), modulating the release of neurotransmitters (Wonnacott et al., 2000), and having longer-term effects on, for example, gene expression and cellular connections (Albuquerque et al., 2009; Millar & Gotti, 2009). nAChRs exist as a family of subtypes in the pLGIC superfamily of LGICs. Mammalian nAChR subunits are derived from a family of sixteen different genes (α1-α7, α9-α10, β1-β4, γ, δ) and have distinctive distributions (Albuquerque et al., 2009; Millar & Gotti, 2009). The functional and pharmacological properties of nAChRs are determined by the composing subunits (Albuquerque et al., 2009). nAChRs are very diverse in terms of subunit composition, which provides therapeutic opportunities, as it could be exploited to selectively

alter brain or body functions or deficits due to disease, using drugs that specifically or selectively target a given nAChR subtype.

1.7.1 nAChR types and distribution.

Five of the 17 vertebrate nAChR subunits form the muscle type: α1, β1, δ, γ and ε, and the neuronal type comprise subunits from α2 to α10 and β2 to β4. These subunits have been grouped as α and non-α, depending, as mentioned previously, on a signature cysteine bridge (Cys-loop) on the ECD, since α subunits have the Cys-Cys pair near the entrance of M1. Typically, α subunits contribute the principal component of the ACh binding site and thus critically influence agonist affinity (Albuquerque et al., 2009). Based on evolutionary criteria, the subunits are grouped in four subfamilies (I-IV). Subunits from subfamilies I and II are considered ancestral, whereas subfamily IV was the latest to emerge. Subfamily I contains α9 and α10 subunits, both found in epithelial tissues. Subfamily II contains the neuronal subunits α7, and α8, both able to form homomeric nAChRs. So far, subunit α8 has only been found in avian neurons (Lohmann et al., 2000). Homomeric α7 nAChRs are prevalent in the mammalian CNS and are highly permeable to Ca^{2+} (Fucile, 2004). Subfamily III comprises α2 to α6 and β2 to β4 subunits, a group of subunits that form αβ heteropentamers (Fig.1.9). This group can be found in autonomic neurons (mainly α3-β4 pairs, in some cases with α5) and in the CNS (Gotti et al., 2006; Albuquerque et al., 2009). Despite being classified as α subunits, neither the α5 or α10 subunits are able to form homomeric channels or contribute to the principal component of the agonist binding site (Gotti et al., 2009). The lack of residue Y198 in the loop C of α5 have been suggested to underlie its inability to form functional agonist sites (Marotta et al., 2014; Corringer et al., 2000).

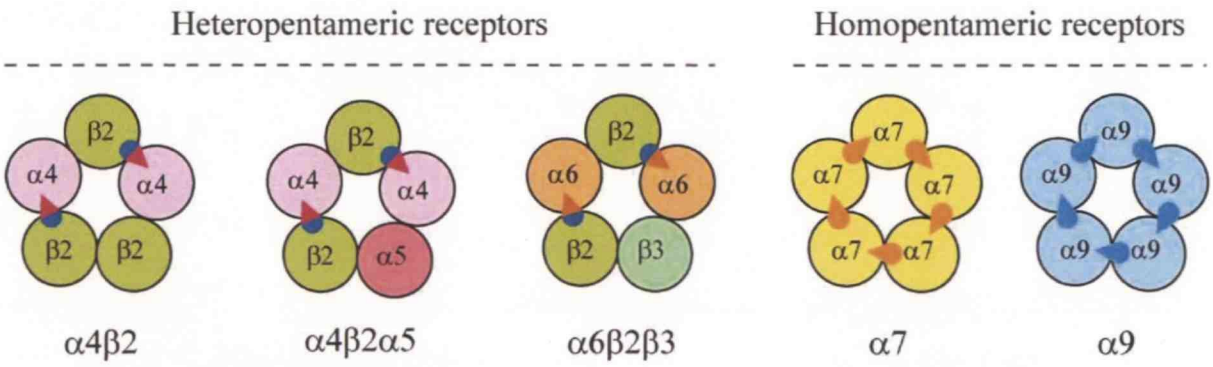

Figure 1.9. Subunit combinations in neuronal nAChRs. On the left examples of heteropentameric nAChRs and on the right homopentameric nAChRs. Triangles and semi-circles represent the principal and the complementary component of the binding site respectively.

1.7.2 α4β2* nAChRs.

nAChRs containing α4 and β2 subunits α4β2*-nAChRs (where the asterisk indicates that α4 and β2 plus other nAChR subunits are known or thought to be receptor constituents) are the most abundant nAChR in the mammalian brain (Moretti et al., 2004; Grady et al., 2009; Millar & Gotti, 2009) . For clarity purposes, in this thesis α4β2*- nAChRs will be used to note that the receptor contains two α4β2 pairs and a α4, β2 or α5 subunit, whereas the use of α4β2 nAChRs indicates that the receptors are composed of only α4 and β2 subunits (i.e., $(\alpha4\beta2)_2\alpha4$ and $(\alpha4\beta2)_2\beta2$ subtypes). The use of α5α4β2 nAChRs indicates that the receptor comprises two α4β2 pairs and a α5 subunit.

α4β2*- nAChRs are mostly located at peri-, pre- and extra-synaptic locations, from where they modulate the release of diverse neurotransmitters such as ACh, GABA, glutamate, dopamine (DA), serotonin and noradrenaline (NA) (Wonnacott et al., 2006; Jin et al., 2011). Because of its modulatory role in neurotransmitter release, α4β2*- nAChR signalling impacts a wide range of brain functions such as cognition, attention, nociception, mood and reward and has been implicated in various pathologies of these functions (Dani & Bertrand, 2007;

Alburquerque et al., 2009). As a result of their implications in various brain disorders, α4β2*-nAChRs have been the target of many drug discovery efforts (Taly et al., 2009).

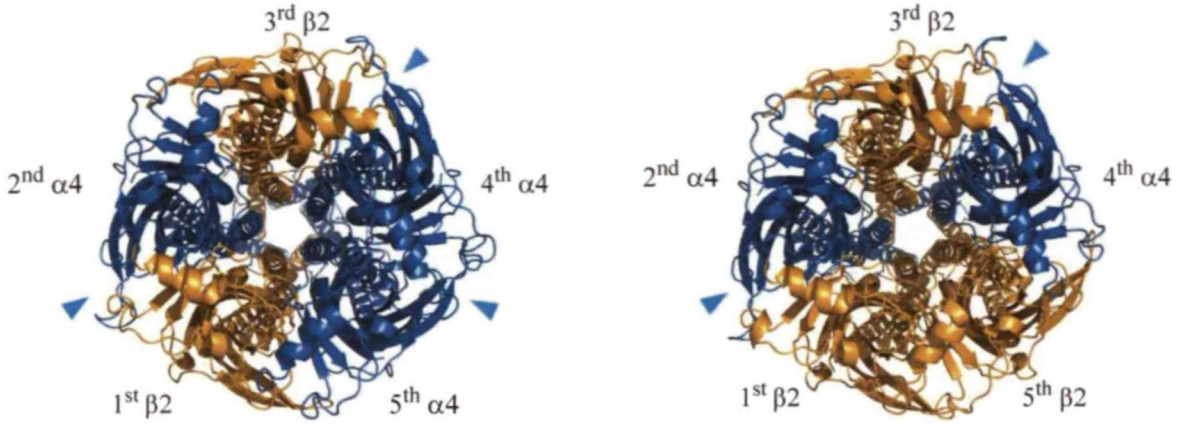

Figure 1.10. Homology models of α4β2 nAChRs. Homology model of α4β2 nAChRs constructed using the X-ray structure of the mouse 5-HT_3 receptor at 3.3 Å resolution. (A) $(\alpha4\beta2)_2\alpha4$; (B) $(\alpha4\beta2)_2\beta2$ receptors.

1.7.3 Subunit composition of α4β2 nAChRs.

α4 and β2 subunits combine with each other to form alternate $(\alpha4\beta2)_2\alpha4$ and $(\alpha4\beta2)_2\beta2$ receptors (Nelson et al., 2003; Moroni et al., 2006). As suggested by functional analysis and immunoprecipitation studies, both stoichiometries express in the cortex and thalamus (Marks et al., 1999; Marks et al., 2007; Gotti et al., 2009). More recently, the use of a selective positive allosteric modulator of the $(\alpha4\beta2)_2\alpha4$ nAChR (NS9283) has shown that although both receptor forms are expressed in the cortex and thalamus, only the $(\alpha4\beta2)_2\beta2$ type is expressed in the striatum (Timmermann et al., 2012; Rode et al., 2012), an important issue given the relevance of the α4β2 nAChR in mediating DA release in the striatum. Further evidence that the alternate α4β2 nAChRs may have some degree of location discrimination come from studies of motoneuron-Renshaw cells, that have shown that the $(\alpha4\beta2)_2\alpha4$ subtype

is most likely to occupy a post-synaptic position (d'Incamps & Ascher, 2014).

The alternate forms of the α4β2 nAChR display 100-fold difference in sensitivity to activation by ACh, and they also differ in sensitivity to exogenous nicotinic ligands (Nelson et al., 2003; Moroni et al., 2006; Zwart et al., 2008; Carbone et al., 2009). Table 1.1 shows the stoichiometry-specific pharmacology of α4β2 nAChRs. Agonists not only activate the receptor isoforms with different potencies but they also display strikingly different efficacies. For example, sazetidine-A, a highly potent α4β2 receptor agonist, displays full agonism at the $(\alpha4\beta2)_2\beta2$ receptor but its efficacy at $(\alpha4\beta2)_2\alpha4$ nAChRs is almost negligible (Zwart et al., 2008), and the agonist TC-2559 displays superagonism at $(\alpha4\beta2)_2\beta2$ but behaves as a partial agonist at $(\alpha4\beta2)_2\alpha4$ nAChRs (Moroni et al., 2006; Carbone et al., 2009). The isoforms also differ in unitary properties (Nelson et al., 2003), calcium permeability (Tapia et al., 2007), sensitivity to modulation by Zn^{2+} (Moroni et al., 2008; Carbone et al., 2009) and allosteric modulators developed by Neurosearch (Timmermann et al., 2012; Olsen et al., 2013; Olsen et al., 2014). The discovery that the alternate α4β2 nAChRs have different functional and pharmacological properties may provide a new impetus to drug discovery problems; however, in order to realize this potential, it is necessary to unravel the structural mechanisms that underlie the pharmacological properties of the alternate α4β2 nAChRs. The remaining part of this section will discuss current understanding of the structural mechanisms that define the pharmacological properties of the alternate α4β2 nAChRs.

Table 1.1. Pharmacological profile of α4β2 nAChRs. All values are means ± S.E.M/95% IC. from 5-10 cells. Key: NE, no effects; ND, not determined: IN: inhibition. Maximal response (I_{max}), apparent potency (EC_{50}) and Hill coefficient, were estimated from CRCs fit to the Hill equation as previously published (Moroni et al. 2006; Carbone et al. 2009). Data for ACh, A85380, 5I-A5380, Cyt, 5-Br-Cys, Epi, nicotine, TC-2559 and sazetidine-A are adapted from Moroni et al. 2006; Zwart et al. 2006 and Carbone et al., 2009. Data for estradiol, progesterone are from Mantione et al. 2012 and Zn^{2+} from Moroni et al. 2008. Data for NS9382 and NS206 are from Olsen et al., 2013. Data for dFBr have been taken from this thesis.

	$(\alpha4\beta2)_2\beta2$		$(\alpha4\beta2)_2\alpha4$	
	$I_{max}/IACh_max$	EC_{50} (μM)	$I_{max}/IACh_max$	EC_{50} (μM)
ACh	1	2.4±0.5	1	111 ± 15
A85380	1.86±0.1	0.3±0.07	1.32±0.06	2.7±0.05
5I-A85380	2.40±0.1	0.14±0.01	0.99±0.06	28.20± 5
Cyt	NE	-	0.27±0.04	55±8
5-Br-Cyt	NE	-	0.28±0.05	11±3
Epi	0.6±0.014	0.16±0.02	2.7±0.01	0.30±0.03
Nicotine	0.28 ±0.011	(0.8-1.3)	0.62 ±0.03	34 (23-50)
TC-2559	4.18±0.1	2±0.05	0.13±0.1	0.91±0.05
Sazetidine-A	1.01±0.01	0.007±0.0009	0.008±0.0004	ND
Progesterone	-	-7±0.04	-	-11±4
Estradiol	3 ± 0.9	18±8	1.8 ±0.6	18±6
Zn^{2+}		-17±2 (IN)	1.5±0.2	49±5
dFBr	2.3±0.17 (1.55-3.05)	1.94±0.5 (0.96-2.9)	12.81±3.54 (5.72-19.9)	3.2±1.4 (0.4-6.1)
NS9283	NE	NE	680 (534-834)	3.4 (1.5-7.9)
NS206	420 (340-500)	4.2 (2.7-6.6)	600 (490-700)	2.2 (1.3-3.6)

What are the structural basis of the pharmacological differences between the alternate forms of the α4β2 nAChRs? Functional assays combined with mutagenesis of conserved ECD aromatic residues in concatenated α4β2 nAChRs have shown that the α4β2 nAChR, like the prototype muscle nAChR, consists of two identical α4β2 subunit pairs and a fifth α4 or β2 subunit, all arranged quasi-symmetrically around a central cation pore (Mazzaferro et al., 2011; Mazzaferro et al., 2014). Each α4β2 subunit pair harbours a structurally identical ACh binding site formed at the interface between the two adjacent subunits. The principal or (+) face of the binding site at α4/β2 interfaces is contributed by the α4 subunit, whilst the β2 subunit contributes the complementary or (-) face. In addition, there are two structurally identical non-canonical α4/β2 interfaces (i.e. β2(+)/α4(-) interfaces) in both receptor forms (Mazzaferro et al., 2011; Mazzaferro et al., 2014). However, these receptors differ in their fifth subunit, which is α4 in $(\alpha4\beta2)_2\alpha4$ nAChRs and β2 in $(\alpha4\beta2)_2\beta2$ nAChRs. That the fifth subunit can be either α4 or β2 leads to signature interfaces. In the $(\alpha4\beta2)_2\beta2$ receptor there is a β2/β2 interface, whereas in the $(\alpha4\beta2)_2\alpha4$receptors there is a α4/α4 interface. Recently, it has been shown that the α4/α4 interface houses an operational agonist site that largely accounts for the ACh sensitivity (Harpsøe et al., 2011; Mazzaferro et al., 2011) and high-affinity desensitisation patterns (Benallegue et al., 2013) of the of the $(\alpha4\beta2)_2\alpha4$ nAChR. Further studies have shown that the ability of agonist to occupy the site at the α4/α4 interface impact significantly the ability of agonists to elicit maximal gating (Mazzaferro et al., 2014).

1.7.4 α5α4β2 nAChRs.

α4 and β2 subunits combine with α5 subunits to assemble as α5α4β2 nAChRs (Fig. 1.9). About 20% of the α4β2* nAChRs contain a α5 subunit (Brown et al., 2007), and α5(-) knock out mice display a decreased sensitivity for acute nicotine administration, compared to wild

type, suggesting that α5α4β2 nAChRs may regulate the rate of response to large doses of nicotine (Kedmi et al., 2004). Recently the α5 subunit has been of particular interest since it was found that a non-synonymous coding variant of this subunit is associated with an increased risk of developing nicotine dependence (Kuryatov et al., 2011; George et al., 2012). Further, the level of α5 in the medial habenula determines the aversive response to nicotine (Frahm et al., 2011), and receptors containing the α5 subunit along with α4 and β2 are critical in regulating DA release in the dorsal striatum (Exley et al., 2012). Studies of recombinant and native $(\alpha4\beta2)_2\alpha5$ receptors indicate there is little pharmacological difference between the $(\alpha4\beta2)_2\alpha5$ and $(\alpha4\beta2)_2\beta2$ receptor (Kuryatov et al., 2008; Marotta et al., 2014; Jin et al., 2014). This suggests that neither the β2 or α5 subunits affect the overall pharmacology of the agonist sites at the α4/β2 interfaces, which presents a formidable barrier for the full understanding of the physiological and pathological processes influenced by these two types of α4β2 nAChRs.

1.7.5 α6-containing-α4β2 nAChRs.

α4 and β2 subunits also combine with α6 and β3 subunits to assemble α4β2α6β2β3 nAChR (Millar & Gotti, 2009). The latter receptors, together with other possible α6-containing nAChRs such as α6β2β3 nAChRs, predominantly express in the midbrain dopaminergic neurons thought to constitute important elements in reward systems, as well as in motor control (Gotti et al., 2007). α6-containing nAChRs will not be discussed in further detail in the remaining part of this thesis.

1.8 α4β2* nAChRs in Brain Pathologies.

α4β2* nAChRs are considered valid targets for therapeutic intervention in diverse pathologic conditions, including addiction to tobacco smoking (nicotine addiction), cognitive deficit associated with ageing and Alzheimer's disease (AD), mood disorders, pain disorders and the rare familial epilepsy autosomal nocturnal front lobe epilepsy (ADNFLE).

1.8.1 Nicotine addiction.

Nicotine, the principle psychoactive component of tobacco, exerts its effects through brain nAChRs. The principal class of nAChRs that binds nicotine with high affinity in the mammalian brain is the α4β2* nAChR type (Picciotto et al., 2001). Studies with transgenic mice with knockout or hypersensitive nAChRs have shown that α4β2* nAChRs are necessary and sufficient for the rewarding and reinforcing effects of nicotine (Picciotto et al., 2001; Tapper et al., 2004; Maskos et al., 2005; Tapper et al., 2007). It is thought that the role of α4β2* nAChRs in nicotine addiction is due to their expression in midbrain dopaminergic neurones thought to be key elements in the pleasure/reward system of the brain. Furthermore, α4β2* nAChRs also express in midbrain GABAergic neurones, which project to the tegmental pedunculo pontine nucleus, and this pathway has also been reported to be involved in the rewarding and aversive physiological effects of nicotine (Laviolette & van der Kooy, 2004; Zhang et al., 2009).

Up-regulation of α4β2* nAChRs by long-term exposure to nicotine has been observed both in animal studies and human smokers, and it has been suggested that this effect of nicotine may play a role in the development/maintenance of nicotine dependence (Staley et al., 2006;

Lester et al., 2009). Up-regulation seems to result from both the ability of nicotine to bind and stabilise nascent α4β2 nAChRs during receptor assembly and receptor maturation in the endoplasmic reticulum and from nicotine-dependent reduction of nAChR degradation after insertion in the plasma membrane (Kuryatov, 2005; Srinivasan et al., 2011).

An interesting focus of research on nicotine addiction is the role of single nucleotide polymorphism (SNPs) of the subunits of α4β2* nAChRs on nicotine addiction susceptibility. In addition to the SNP (D398N) in the α5 subunit discussed above, genome-wide linkage studies and association studies have found significant effects of several human CHRNA4 variants on nicotine dependence (Han et al., 2011; Kamens et al., 2013). SNPs tend to affect the intracellular loop M3-M4, which suggest that the SNPs may affect the biogenesis of the receptors.

A long-standing question in the nAChR field is whether nicotine elicits its addictive effects via activation or desensitisation of α4β2* nAChRs. α4β2 nAChRs are prone to long-term desensitisation when exposed chronically to agonists (Benallegue et al., 2013), which is the case during smoking. A possible scenario is that nicotine first activates α4β2 nAChRs on midbrain dopaminergic terminals in the nucleus accumbens (NAc) and ventral tegmental area (VTA) causing an increase in reward. After chronic exposure to nicotine, as it occurs during smoking, the receptors become desensitised. However, because α4β2 nAChRs also modulate GABA release from midbrain GABAergic neurons that exert inhibitory effects on DA release from midbrain terminals in the NAc, desensitization of α4β2 nAChRs may also contribute to the mechanism of nicotine in the pleasure/reward system of the brain (Mansvelder & McGehee, 2002; Laviolette & van der Kooy, 2004; Picciotto & Zoli, 2008).

1.8.2 Cognition.

α4β2* nAChRs are highly expressed in brain regions thought to constitute important elements of the cognitive systems of the brain (e.g., cortex, hypothalamus, thalamus, VTA) (Gotti et al., 2007; Albuquerque et al., 2009). The cholinergic pathway is well-established as a key component of cognitive processes including memory, attention and even mediation of psychotic symptoms (Han et al., 2003; Sarter et al., 2005). The α4β2* nAChR, as well as the α7 nAChR, have been suggested as a positive influence for attention performance and improvement of cognitive function (Levin & Simon, 1998; Preskorn et al., 2014) and agonists of α4β2 nAChRs have been shown to enhance learning and memory (Cassels et al., 2005). The neuroprotective effects of α4β2 nAChRs combined with the involvement of this receptor type in cognition have suggested that they may be good targets for the therapeutic management of neurodegeneration-related or ageing-related cognitive dysfunction (Quik & Jeyarasasingam, 2000; Quik et al., 2007; Picciotto & Zoli, 2008; Quik et al., 2014).

1.8.3 Mood disorders.

Several lines of evidence support the involvement of α4β2 nAChRs in mood disorders, particularly depression. Firstly, the prevalence of smoking in depressed individuals is higher than in non-depressed subjects (Covey et al., 1998), and amelioration of anxiety by smoking seems to be one of the most common reasons why smokers relapse from abstinence (Ashare & McKee, 2012). Additionally, chronic nicotine exposure has been linked to an increase in the response to anti-depressive drugs (Andreasen et al., 2009). Secondly, antidepressants, such as bupropion and fluoxetine inhibit α4β2 nAChRs (Ashare & McKee, 2012), which suggests that some of the effects of these drugs may be due to α4β2 nAChR inhibition. This

possibility is supported by the observation that nicotinergic inhibitors such as the channel blocker mecamylamine or the competitive inhibitor DhβE reduce measures of depression in rodents (Mineur & Picciotto, 2010). Thirdly nAChRs are present in the hypothalamic-pituitary-adrenal axis (HPA), which suggests that nAChRs contribute to the regulation of cortisol release (Raber et al., 1995), a hormone linked to anxiety and stress. It has been indeed shown that chronic smokers have high levels of cortisol, growth hormones and prolactin (Wilkins et al., 1982) and exposure to mecamylamine produces a decrease in circulating cortisol (Newman et al., 2001). From these data, it appears that inhibition of α4β2* nAChRs enhances mood; however, partial agonists such as Cyt have been shown to have anti-depressant effects (for a review, see (Mantione et al., 2012)), suggesting that receptor desensitisation may be necessary for α4β2* nAChR-mediated mood elevation.

It is not known how α4β2* nAChRs influence mood. It may be that they contribute to mood due to their critical role in modulating the activity of the VTA- NAc- prefrontal cortex pathway (Gotti et al., 2006). In addition to their role in regulating DA release, the regulation of GABAergic signalling by α4β2 nAChRs may also be relevant for depression therapies (Laviolette & van der Kooy, 2004). GABAergic neurons have been implicated in the anxiolytic effects of nicotine and miss-function of GABAergic transmission is associated with affective disorders (O'Neill & Brioni, 1994).

1.8.4 Analgesia.

The analgesic effects of nicotine have long been known, which suggests that α4β2* nAChRs contribute to nociceptive pathways in the mammalian CNS. This is supported by the discovery that epibatidine, a potent agonist of α4β2* nAChRs, is a potent analgesic (Daly et al., 2000). Experiments with transgenic mice with knocked out nAChR subunits suggest that the animal show reduced sensitivity to pain stimuli, further supporting a role for α4β2* nAChRs in nociception. There is evidence the $(\alpha4\beta2)_2\alpha5$ subtype may play a key role in analgesia; for example, there is an increase in expression of α5 subunits following spinal nerve ligation (Vincler & Eisenach, 2004) and transgenic mice with knockout α5 subunit are not sensitive to the analgesic effects of nicotine (Jackson et al., 2010). As for other functions or pathologies, the exact mechanisms α4β2* nAChR may produce analgesia are not known. Recent studies have shown that compounds that highly desensitise α4β2* nAChRs are more effective at producing analgesia (e.g., sazetidine-A), which suggests a link between desensitisation of nAChRs and analgesia (Zhang et al., 2012). Other nAChRs such as α9α10 receptors located in sensory dorsal root ganglion neurones may also contribute to nociception, further complicating the nociceptive nicotinergic scenario (Gotti et al., 2009).

1.8.5 ADNFLE.

Rare mutations in the α4 and β2 subunits are linked to ADNFLE (Steinlein et al., 1995; Phillips et al., 2001; Bertrand et al., 2002). Most of the mutations found are located within TM2 and have been shown to modify the receptor responses to agonists, Ca^{2+} permeability and desensitisation (Weiland et al., 1996; Steinlein et al., 1997; Bertrand et al., 1998). However, it is not yet understood how ADNFLE mutations cause epileptic discharges during sleep.

1.9 Pharmacological Profile of α4β2* nAChRs.

The characterisation of the pharmacological profile of α4β2* nAChRs has been carried out on native (Marks et al., 1999; Marks et al., 2007) and recombinant receptors (Chavez-Noriega et al., 1997; Moroni et al., 2006; Carbone et al., 2009). Although expression of α4 and β2 subunits in expression cell systems such as HEK-293 cells or *Xenopus* oocytes typically leads to the expression of both forms of the α4β2 nAChR type, Lindstrom and his team (Nelson et al., 2003) as well as Bermudez and her team have managed to express individual stoichiometries by using reduced temperature (Nelson et al., 2003), altered ratios of transfecting α4/β2 ratios (Nelson et al., 2003; Moroni et al., 2006) and partial (Zhou et al., 2003) or fully concatenated (Carbone et al., 2009) α4β2 nAChRs. Studying native α5α4β2 nAChRs is challenging, particularly because α5α4β2-selective pharmacological probes have not been found as yet, thus typically this receptor type is separated from α4β2 nAChRs using transgenic animals with knock out for α4, β2 or α5 subunits (Grady et al., 2010) or by using concatenated receptors (Zhou et al., 2003; Tapia et al., 2007; Kuryatov et al., 2008). The discussion that follows focuses on the pharmacological profile of $(\alpha4\beta2)_2\alpha4$ and $(\alpha4\beta2)_2\beta2$ nAChRs, given emphasis to key agonists, antagonists and allosteric modulators (Table 1.1).

1.9.1 Agonists.

Agonists bind the ACh binding sites and a direct consequence of this binding is the activation of the receptors, which, depending on the agonists, may be fully efficacious (e.g., ACh), moderately efficacious (e.g., nicotine) or poorly efficacious (Cyt on $(\alpha4\beta2)_2\beta2$ receptors). A key structural element of agonists is a quaternary ammonium, which engages in π-cation interactions with a tryptophan residue present in loop B of the ACh binding site

(Albuquerque et al., 2009). As shown in Table 1.1 nicotinergic agonists displaying high affinity for α4β2 nAChRs include nicotine, sazetidine-A, varenicline, epibatidine, TC-2559, A-85380 and 5-Iodo A-853805. A brief description of the effects of these agonists follows below.

Nicotine is the alkaloid that gives name to this family of receptors. It is found in tobacco plants of the *Solanaceae* family and it presents high affinity for α4β2* nAChRs (except in presence of a α5 subunit) (Kedmi et al., 2004). The reported binding affinity constants (Ki) and potency values (EC_{50}) of nicotine for α4β2* nAChRs are in the nanomolar range, in contrast to the low affinity and potency show in α7 nAChRs (Carbone et al., 2009).

Cyt is an alkaloid that displays almost no efficacy in the high sensitivity types of α4β2* nAChRs $(\alpha4\beta2)_2\beta2$ and $(\alpha4\beta2)_2\alpha5$ and a higher efficacy in the low sensitivity $(\alpha4\beta2)_2\alpha4$ receptor (Moroni et al., 2006; Carbone et al., 2009; Mazzaferro et al., 2014). Both potency and efficacy of this compound are enhanced by halogenation of the pyridine ring at position 3 in Cyt, which reduces the restricted conformation that Cyt adopts when bound (Slater et al., 2003).

Sazetidine-A was proposed to be a highly desensitising α4β2* nAChR agonist due to lack of sazetidine-A-evoked responses in native neurones (Xiao et al., 2006). However, work on recombinant α4β2 nAChRs by Zwart and colleagues (Zwart et al., 2008) showed that sazetidine-A displays differential efficacy at the two forms of the α4β2 nAChR. Thus, sazetidine-A displays full efficacy at $(\alpha4\beta2)_2\beta2$ nAChRs but almost no efficacy at $(\alpha4\beta2)_2\alpha4$ nAChRs (Zwart et al., 2008). It is not known why sazetidine-A does not display efficacy at $(\alpha4\beta2)_2\alpha4$ nAChRs but recent work by Mazzaferro and colleagues (Mazzaferro et al., 2014)

showed that sazetidine-A does not bind the agonist site at the α4/α4 interface, which suggest that the agonist sites at the α4/β2 interfaces in the α4β2 nAChRs are not functionally equivalent. Perhaps, the presence of a third binding site in $(\alpha4\beta2)_2\alpha4$ nAChRs changes the gating of this receptor in comparison to that of the $(\alpha4\beta2)_2\beta2$ nAChRs.

Varenicline (Chantix™ or Chanpix™) is used world-wide to aid smoking cessation (Cahill et al., 2008). It is a partial agonist at α4β2 nAChRs with a higher efficacy at $(\alpha4\beta2)_2\alpha4$ than at $(\alpha4\beta2)_2\beta2$ nAChRs (Table 1.1). In addition to its effects on nicotine addiction, varenicline appears to have anti-depressant like effects in animal models (Rollema et al., 2011), however it seems to have severe psychiatric side effects (Cahill et al., 2013).

Epibatidine is a potent agonist of all types of nAChRs, with the highest affinity at α4β2 nAChRs. This promiscuity makes it highly toxic, which prevents its use as a therapeutic agent. However, it is widely used as a template to characterize other nAChR ligands as well as in competitive binding assays as a radio ligand (Niessen et al., 2013).

TC-2559 is a selective α4β2 agonist. It behaves as a partial agonist at $(\alpha4\beta2)_2\alpha4$ receptors and as a "super-agonist" at the $(\alpha4\beta2)_2\beta2$ type (Zwart et al., 2006; Carbone et al., 2009). It is not known why TC-2559 is a super agonist at $(\alpha4\beta2)_2\beta2$ nAChRs but it is known that at $(\alpha4\beta2)_2\alpha4$ TC2559 cannot occupy the agonist site at the α4/α4 interface, thus failing to elicit maximal activation of the receptor (Mazzaferro et al., 2014).

1.9.2 Antagonists.

Antagonists can act by different mechanisms, depending on the location of their binding site. Antagonists that bind the agonist site are competitive antagonists (Hansen et al., 2005), whereas antagonists that occupy other sites in the receptor are named non-competitive antagonists. Pharmacological studies indicate that when a molecule inhibits agonist responses competitively, it right-shifts agonist concentration responses curves (CRC) in a parallel fashion with no effects on the maximal agonist responses. In contrast, non-competitive antagonists reduce the maximal responses of agonists and have little effect on the sensitivity of the receptors for the agonists. Non-competitive inhibition may be the result of ion channel blockade or binding of the antagonist to an inhibitory allosteric site (Revah et al., 1990; Wyllie & Chen, 2007).

DhβE is a classic example of a reversible competitive antagonist of nAChRs. It is obtained from seeds of the flowering plant *Erythrina Americana*, and it mostly blocks β2-containing nAChRs, with a higher potency at both α4β2* and α3β2* subtypes and much lower potency at α3β4* or α7 nAChRs (Chavez-Noriega et al., 1997; Jensen et al., 2005). Similar competitive inhibitory profiles have been described for other erythrina alkaloids such as **Erysodine**.

Recently homology modelling studies in combination with alanine substitutions and functional assays have suggested that DhβE interacts with a β2 residue in loop E (β2D169), a mechanism that could allow it to keep loop C in the uncapped position (Iturriaga-Vásquez et al., 2010).

Established non-competitive inhibitors include mecamylamine and bupropion. Although mecamylamine was originally used as a ganglionic blocker in the treatment of hypertension (Shytle et al., 2002), it has been proposed as an anti-depressant in view of its blocking effects on α4β2* nAChRs (Rabenstein et al., 2006). The antidepressant Bupropion also behaves as a non-competitive antagonist of α4β2* nAChRs. It was originally classified as an inhibitor of DA and NA transporters and therefore used as antidepressant, but its emerging role as a nicotinic antagonist amplified its potential as an anti-depressant (Jensen et al., 2005).

1.9.3 Allosteric Modulators of α4β2 nAChRs.

Allosteric ligands modulate the action of the endogenous agonist generally with no effect of their own or on the unoccupied receptor. Therefore, the agonist effect can be enhanced or decreased by allosteric ligands. Allosteric modulators (AMs) of LGICs are classified as positive allosteric (PAMs) or negative allosteric (NAMs) modulators depending on the effect they exert on receptor function. AMs are further classified according to the region they bind pLGICs. Thus, there are AMs that bind the ECD or the TM domain. Although generally PAMs have no agonist activity, some may activate LGICs but at a concentration range much higher than that at which only allosteric effects are observed and they do so through a site distinct from the agonist site (e.g., barbiturates at $GABA_A$Rs (Forman & Miller, 2011)). In receptors that contain structurally different agonist sites, AMs may bind one type of agonist site without causing activation of the receptor, however, in the presence of the agonist they may enhance the currents elicited by the agonist. An example of this type of PAMs is the compound NS-9283, a specific PAM of the $(\alpha4\beta2)_2\alpha4$ nAChR. It has been reported that NS-9283 exert its potentiating effects by binding the ACh binding site located at the α4/α4 interface but not those on the α4/β2 interfaces (Grupe et al., 2013; Olsen et al., 2013; Olsen et

al., 2014).

nAChRs were among the first membrane proteins in which allostery was studied (Taly et al., 2009; Changeux, 2012). According to the allosteric model for nAChR signalling, nAChRs can exist in multiple inter-convertible conformations in the absence of agonist, which include a resting state, an active state and multiple inactive (desensitised) states. The equilibrium between these states is determined by the differences in their free energy. Agonists and antagonists binding to the agonist sites can decrease or increase, respectively, the probability of the transition from one conformational state to another, thus having a profound influence on the function of nAChRs. Binding of ligands to allosteric sites located elsewhere from agonist sites can modulate nAChR signalling via an effect on the equilibrium between the resting, active or inactive states. PAMs increase agonist potency (e.g., benzodiazepine effects in $GABA_ARs$) and/or increase the maximal responses of agonists (e.g., barbiturate effects on $GABA_ARs$). PAMs can exert these effects by: a) enhancing agonist binding to the resting receptor conformation; b) increasing agonist efficacy through reducing the energy barrier to flipped states; c) by increasing the energy required for the transition from the active to the desensitised states. NAMs, on the other hand, appear to increase the energy tariff for activation, which decreases or inhibits the effects of agonists. NAMs could also reduce the energy tariff to the desensitised receptor conformation.

1.9.4 PAMs of α4β2 nAChRs.

A diverse group of ligands are known to act as PAMs at α4β2 nAChRs, including the divalent cation Zn^{2+} (Hsiao et al., 2006; Moroni et al., 2008) , 17β-estradiol (Paradiso et al., 2001; Curtis et al., 2002; Jin & Steinbach, 2011), desformylflustrabromine (dFBr) (Sala et al., 2005; Weltzin & Schulte, 2010) and a variety of compounds developed by drug discovery

companies (Table 1.2). With the exception of dFBr, the binding site and/or the downstream pathways associated to the effects of the above mention PAMs have been identified (Paradiso et al., 2001; Moroni et al., 2008; Young et al., 2008; Timmermann et al., 2012; Grupe et al., 2013).

Table 1.2. Positive allosteric modulators of α4β2 nAChRs.

Compound	PAM Effect	Reference
17-β-Estradiol	Potentiation of human receptors containing α4 subunit with a C-terminus end sequence WLAGMI	Paradiso et al., 2001
dFBr	Bell-shaped CRC effect	Sala et al., 2005; Weltzin & Schultze, 2010
Galanthamine	Bell-shaped CRC effect	Samochocki et al., 2003
HEPES	Only potentiates $(\alpha4\beta2)_2\beta2$	Weltzin et al., 2012
LY2087101	Potentiates α4-containing nAChRs	Broad et al., 2006
NS206	Bell-shaped CRC effect	Olsen et al., 2013
NS9283	Potentiates only $(\alpha4\beta2)_2\alpha4$	Olsen et al.,2013
S(+)mecamylamine (TC5214)	Potentiates $(\alpha4\beta2)_2\alpha4$	Fedorov et al.,(2009)
Zn^{2+}	Potentiates $(\alpha4\beta2)_2\alpha4$	Moroni et al., 2008

Zn^{2+} effects on α4β2 nAChRs are stoichiometry-selective. Zn^{2+} exerts an inhibitory modulatory effect on $(\alpha4\beta2)_2\beta2$ receptors, but it enhances or decreases, depending on its concentration, the function of $(\alpha4\beta2)_2\alpha4$ receptors (Table 1.1) (Moroni et al., 2008).

Zn^{2+} potentiation on $(\alpha4\beta2)_2\alpha4$ is exerted through a site housed at the signature α4/α4 interface of this receptor type, whereas Zn^{2+} inhibits both receptor types by binding a site located at β2(-)/α4(+) interfaces, which are present in both α4β2 receptor types. Key amino residues contributing to the potentiating site are α4H195 on the 'negative' side of the α4/α4 interface and α4E224 on the 'positive' side of the α4/α4 interface (Moroni et al., 2008). Regardless of the relevance of Zn^{2+} potentiation to the signalling functions of α4β2 nAChRs, the identification and mapping of a potentiating Zn^{2+} site on the α4/α4 interface of the

$(\alpha4\beta2)_2\alpha4$ showed for the first time the potential of this signature interface for the development of stoichiometry-specific α4β2 nAChR ligands.

17β-Estradiol displays PAM activity at both types of α4β2 nAChRs (Paradiso et al., 2001) (See Table 1.2). 17β-Estradiol displays higher efficacy at $(\alpha4\beta2)_2\alpha4$ than at $(\alpha4\beta2)_2\beta2$ nAChRs, likely because $(\alpha4\beta2)_2\alpha4$ receptors have three 17β-estradiol binding sites, in comparison to $(\alpha4\beta2)_2\beta2$ nAChRs that have only two sites. The binding sites are located at the C-terminus of α4 subunits (Paradiso et al., 2001) and its effects on α4β2 nAChRs are characterised by a left-shift of the ACh CRC with no changes in the maximal ACh responses (Paradiso et al., 2001; Curtis et al., 2002) .

NS9283, a benzonitrile compound developed by Neurosearch, enhances the agonist-evoked responses of $(\alpha4\beta2)_2\alpha4$ receptors but not those of $(\alpha4\beta2)_2\beta2$ receptors, a receptor that is inhibited by NS9283 (Timmermann et al., 2012; Grupe et al., 2013). NS9283 increases cognitive function (Timmermann et al., 2012) and enhances the effects of α4β2* nAChRs in nociception (Rode et al., 2012). Furthermore, when co-administered with ABT594, NS9283 enhances the analgesic efficacy of well tolerated clinical doses of ABT-594 (Lee et al., 2011), suggesting that administration of low doses of agonist and NS9283 could decrease the unacceptable side effects. The receptor subtype specificity of NS9283 is based on the binding of this compound to the agonist site at the α4/α4 interface of the $(\alpha4\beta2)_2\alpha4$ receptor as mentioned previously (Grupe et al., 2013; Olsen et al., 2013; Olsen et al., 2014). It is not known why binding of NS9283 to the agonist site on the α4/α4 interface is not efficacious (at least at the range of concentrations at which it has been tested) and how this non-efficacious binding enhances the responses of ACh. Taken into account that NS9283 binds the ECD of the $(\alpha4\beta2)_2\alpha4$, in a region that is equivalent to that of the benzodiazepine site in $GABA_A$Rs,

and that NS9283 left-shift the ACh CRC with no effects on maximal ACh responses (Timmermann et al., 2012), it is tempting to suggest that binding of NS9283 to the α4/α4 interface stabilises the ACh-bound agonist sites at the α/β interfaces, thus slowing down receptor deactivation, analogously to what has been proposed for the allosteric effects of benzodiazepines on $GABA_A$Rs (Bianchi & Macdonald, 2001).

NS206 (3-N-Benzyloxy-3-hydroxyimino-2-oxo-6,7,8,9-tetrahydro-1H-benzo[g]indole-5-sulfonamide), a PAM developed by NeuroSearch, potentiates both forms of the α4β2 nAChRs, although shows higher efficacy at the $(\alpha4\beta2)_2\alpha4$ receptor (Olsen et al., 2013). NS206 has only a minor effect on ACh potency but has a significant effect on ACh efficacy. Its binding site is thought to be located within the TM of the receptors (Olsen et al., 2013), since chimeric receptors containing the TMD of α3 subunits and ECD of α4 subunits are not sensitive to modulation by NS206, whereas chimeric receptors containing the TMD of α4 and ECD of α3 show potentiating responses similar to those of wild type α4β2*receptors. Interestingly, introduction of mutations in the ECD-TMD interface, impair the potentiating effects of NS206, suggesting this region (Cys loop) could be involved in the signal transduction mechanism of the PAM effects of this compound in α4β2*receptors.

LY2087101 ([2-[(4-Fluorophenyl)amino]-4-methyl-5-thiazolyl]-3-thienylmethanone), a compound developed by Eli Lilly displays PAM activity at α4β2 nAChRs but its receptor specificity is rather broad as it also potentiates α7 nAChRs (Broad, 2006). However, LY2087101 displays selectivity against α3-containing nAChRs, which resembles the receptor selectivity of 17β-Estradiol and dFBr. LY2087101 has marked effects on both ACh potency and efficacy (Broad, 2006). Work by Young and colleagues (Young et al., 2008) on α7 nAChRs has shown that the binding site of LY2087101 is located in a cavity within the TM

that is conserved in all pLGICs.

dFBr, a tryptamine derivative that is a metabolite of the marine bryozoan *Flustra foliacea*, potentiates, in the micromolar range, α4β2 nAChRs by increasing the efficacy of ACh with a minor effect on ACh potency (Weltzin & Schulte, 2010). At concentrations higher than those exerting potentiation, dFBr inhibits α4β2 nAChRs, presumably by ion channel blockade (Weltzin & Schulte, 2010). dFBr also enhances the function of α2β2 nAChRs (Pandya & Yakel, 2011) but inhibits all other nAChRs, including muscle and α3-containing nAChRs. Further information on the action of dFBr on nAChRs is given in the Results sections of this thesis.

Galanthamine and **physostigmine** are acetylcholine esterase inhibitors but they have also proposed to act as positive allosteric modulators of nAChRs, including α4β2 nAChRs (Samochocki et al., 2003). However, there is controversy as to whether they are PAMs of α4β2 nAChRs. Galanthamine has been reported to increase the potency of ACh responses of α4β2 nAChRs expressed heterologously in HEK cells without changes in ACh maximal responses (Samochocki et al., 2003) but this effect has not been replicated on α4β2 nAChRs expressed in *Xenopus* oocytes.

(+/-) Mecamylamine is a racemic mixture of a widely used non-competitive inhibitor of nAChRs. Work by Targacept, a company that focuses its drug discovery programs on neuronal nAChRs, found that [S-(+) mecamylamine (TC-5214) potentiates agonist-induced responses of $(\alpha4\beta2)_2\beta2$ nAChR but not those of $(\alpha4\beta2)_2\alpha4$ nAChRs (Fedorov et al., 2009), suggesting that this compound may exert potentiation of $(\alpha4\beta2)_2\beta2$ by binding to the signature interface β2/β2 of this receptor type, although it may also be possible that subtle

differences in the gating of the alternate α4β2 nAChRs underlies the subtype specificity of this compound.

1.9.5 NAMs of α4β2 nAChRs.

NAMs of α4β2 nAChRs include progesterone and several compounds with higher selectivity for other ion channels. An example of α4β2 nAChR-preferring NAMs is UCI-30002 [N-(1,2,3,4-tetrahydro-1-naphthyl)-4-nitroaniline)], which decreases nicotine self-administration in rats (Yoshimura et al., 2007). Another α4β2-selective NAM is KAB-18 (Henderson et al., 2010; Pavlovicz et al., 2011). KAB-18 inhibits α4β2 nAChRs at low micromolar concentrations and its binding site is located in α4/β2 interfaces about 10 Å away from the agonist binding site (Henderson et al., 2010). The anthelmintic oxantel also behaves as a selective α4β2 nAChR NAM and appears to bind a site in the β(+)/α(-) subunit interfaces (Cesa et al., 2012). Here, it appears that NAMs do not discriminate between the alternate forms of α4β2 nAChRs.

AIM OF THE THESIS

The overall aim of this thesis was to identify and map the potentiating binding site of dFBr on α4β2 nAChRs. Intermediary aims were:

- Use homology modelling of α4β2 nAChRs to identify receptor regions that may house a binding site for dFBr.
- Alanine substitution of putative dFBr binding amino acid residues and functional assays to determine effects of the substitutions on dFBr potentiating effects.
- Use SCAM to further identify the putative dFBr binding site.
- Compare effects of dFBr on α4β2 and α3β2 nAChRs to elucidate determinants that define the structural determinants of the effects of dFBr on these two nAChR types.

CHAPTER 2

Materials and Methods

2.1 Reagents.

Standard laboratory chemicals were of Analar grade. Collagenase Type IA and ACh were purchased from Sigma-Aldrich (UK). dFBr was purchased from Tocris Chemicals (UK). The cationic methanethiolsulfonate reagent [2-(Trimethylammonium)ethyl]methanethiosulfonate (MTSET) was purchased from Toronto Chemicals (Canada). 100 mM stocks were prepared and stored at -80 C° until experiments.

2.2 Animals.

Xenopus laevis (*X. laevis*) were purchased from Portsmouth University. *Xenopus* toad were housed and cared by the Biomedical Services at Oxford University. Ovaries were dissected from the toads using procedures in accordance with the Home Office regulations and approved by the Animal Use Committee of Oxford Brookes University and Oxford University.

2.3 Molecular Biology.

DNA ligations, maintenance and growth of *Escherichia coli* bacterial strains and the use of restriction enzymes were carried following the procedures described by Carbone et al., 2009. Plasmid isolation and DNA gel purification were carried out using commercially available kits (Promega, UK). Capped cRNA coding for wild type and mutant concatenated receptors was synthesized by in vitro transcription from *SwaI*-linearized cDNA template using the mMessage mMachine T7 kit (Ambion, UK.). The integrity and size of the cRNA transcripts

was confirmed using RNA gel electrophoresis.

2.3.1 Single Point Mutations.

Point mutations were carried out using the QuikChangeTM Site-Directed Mutagenesis Kit (Stratagene, The Netherlands). Oligonucleotides for PCR reactions were purchased from Eurofins (UK). The full-length sequence of wild type and mutated subunit cDNAs were verified by DNA sequencing (BiosourceScience, Oxford). In order to increase the number of positive transformants, the protocol used was slightly modified from the manufacturer's instructions, as described below.

Oligonucleotides primers (35 to 45 long, Melting T° > 80 C°) were synthesised carrying the desired mutations in the middle.

The synthesised primers were diluted to a final concentration of 125 ng/µl and used in the subsequent PCR reaction.

The PCR mix consisted of the following:

1) 5 µl Pfu Buffer 10X
2) 1 µl DNA template (stock 50 ng/µl)
3) 1 µl of sense primer (125 ng)
4) 1 µl of antisense primer (125 ng)
5) 3 µl DiMethyl Sulphoxide
6) 5 µl dNTPs (from 2 mM stocks)
7) 1 µl High fidelity Pfu DNA polymerase
8) 33 µl Nuclease free water

The parameters for the PCR run were as follows:

Segment	Number of Cycles	Holding Temperature (C)	Time (minutes)
1	1	95	1
2	16	95	0.5
		55	1
		68	1 min per kbp
3	1	68	1 min per kbp

1µl of the enzyme *DpnI* was added to the PCR mixture in order to degrade the parental methylated DNA, which corresponds to the template (non-mutated DNA), and to leave intact only the newly formed DNA (non-methylated and likely containing the desired mutation).

In general, X-Gold Competent cells were transformed with 5 ng/µl of DNA, with the exception of PCR products for single point mutations in individual subunits where the total reaction volume (25-30 µl) was added to the cells. After overnight incubation, 3 colonies were picked and amplified by growing them in 10 ml of CircleGrow medium (Anachem, UK) at 37 C°. After overnight growth, the cDNA was isolated from the bacteria using commercially available DNA purification kits (Promega, UK). The purified plasmid was fully sequenced to confirm the presence of the desired mutation and verified the sequence of the non-mutated regions.

The residue numbering used throughout this thesis includes the signal sequence. To obtain the position in the mature form, subtract 28 for α4 and 26 for β2.

2.3.2 α4β2 and α3β2 nAChR models.

The studies described in this thesis were carried out using both receptors made from loose α4, α3 and β2 subunits or concatenated β2_α4_β2_α4_α4 or β2_α4_β2_α4_β2 cDNAs. The former were used for screening the effects of amino acid residue substitutions on the effect of dFBr, whereas the latter were used to determine if the effects of dFBr were receptor α4β2 nAChR subtype specific and to assess the stoichiometry of the effect of dFBr. The engineering of concatenated α4β2 nAChRs has been described in detail elsewhere (Carbone et al., 2009).

2.3.3 Engineering mutant β2_α4_β2_α4_α4 and β2_α4_β2_α4_β2 receptors.

Fully concatenated $(\alpha4\beta2)_2\alpha4$ and $(\alpha4\beta2)_2\beta2$ nAChRs (β2_α4_β2_α4_β2_α4 and β2_α4_β2_α4_β2, respectively) were used to assess the stoichiometry of dFBr action on α4β2 nAChRs. In these studies, the mutation α4F312A was introduced in the α4 subunit of the receptors, one at a time, and the effects of the single substitutions on dFBr potentiating effects were assessed using the two electrode voltage-clamping procedures described below. The construction of concatenated α4β2 nAChRs has been described in detail by Carbone et al. (2009). To introduce the F312A mutations into specific α4 subunits of β2_α4_β2_α4_α4 and β2_α4_β2_α4_β2 receptors, the mutation was first introduced into the appropriate individual subunit sub-cloned into a modified pCI plasmid (Carbone et al., 2009; Mazzaferro et al., 2011). After confirming the presence of the desired mutation by full-length DNA, the

subunit cDNA was digested with appropriate unique flanking restriction enzymes and then ligated into the desired position in the concatenated pentamer using standard cDNA ligation protocols with T4 ligase (New England Biolabs, UK). The presence of the mutant subunit was also confirmed by DNA sequencing. Thus, following ligation and DNA amplification, the appropriate subunit was cut by enzyme restriction digestion from the concatenated receptor and sequenced by standard DNA sequencing. The same standard procotol was used to introduce mutantions in α3 and β2 subunits (α3F310A and β2F303A). Chimeric receptors containing variable C-terminal tails of both α3 and α4 subunits were obtained by single amino acid exchanges as described for single point mutations in Section 2.3.1.

2.4 *Xenopus laevis* oocytes preparation.

Xenopus oocytes were collected from adult female *Xenopus laevis*, anaesthetised and sacrificed according to Home Office guidelines. A visceral incision was made through the skin and body wall. The ovaries were removed and stored in OR2 solution (82 mM NaCl, 2 mM KCl, 2m M MgCl 2.5 mM HEPES adjusted to pH 7.6 with NaOH). Only oocytes at the stage V and VI of maturation were isolated. The theca and epithelial layers were removed enzymatically by incubating the oocytes for about 2 h in Type IA collagenase (1 mg/mL) dissolved in OR2 and placed on a rotating platform at room temperature. Oocytes were maintained at 18 C° in an incubator in a modified Barth's medium (88 mM NaCl, 1 mM KCl, 2.4 mM $NaHCO_3$, 0.3 mM $Ca(NO_3)_2$, 0.41 mM $CaCl_2$, 0.82 mM $MgSO_4$, 15 mM HEPES) supplemented with Streptomycin 1 μg/ml, 1 IU/ml Penicillin and 50 μg/ml Neomycin, pH 7.6 (adjusted with HCl).

2.4.1 Microinjection of cDNA and cRNA.

Needles for microinjection were prepared from Drummond glass capillaries (Sartorius, UK), which were pulled in one stage using a Narishige PC-10 micropipette puller (Narishige, Japan). Prior to use the tip of a selected needle was broken using fine forceps to give a narrow tip length of approximately 3 mm with an external diameter ranging from 1.0 to 1.5 μm. The needle was back-filled with light mineral oil and loaded on to a Nanoject II microinjector (Drummond, USA). Wild type or mutant concatameric receptor cRNA were injected into the oocyte cytoplasm (50.6 nl at 0.1 ng/nL) as illustrated in Fig 2.1. Wild type and mutant single subunits cDNA were mixed in equal ratios (1:1) and injected into the nucleus of the oocytes. Injected oocytes were transferred to 96 well sterile dish (one oocyte per each well) containing modified Barth's solution containing 5% Horse Serum and incubated at 18 C° for a maximum of 7 days. The Barth's solution was changed daily and oocytes that had degraded were removed in sterile conditions from the plate.

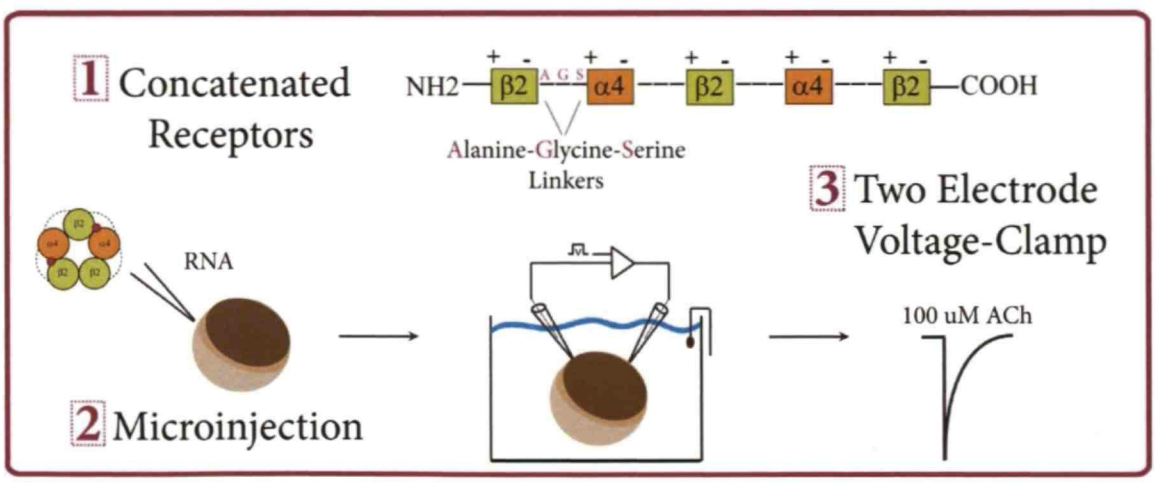

Fig. 2.1. Diagram of three steps for receptor expression in *Xenopus* oocytes showing cRNA injection of β2_α4_β2_α4_β2 cRNA. After 2-3 days post-injection currents were recorded using two-electrode voltage clamp technique.

2.5 Electrophysiological Recordings.

From 2-3 days post-injection oocytes were selected according to their appearance. Only oocytes with integral membrane and no signs of degradation were chosen for electrophysiological recordings. Oocytes were placed in a 30 µL recording chamber (Digitimer Ltd, UK) and bathed with a modified Ringer's solution (in mM: NaCl 150, KCl 2.8, Hepes 10, $BaCl_2$ 1.8; pH 7.2, adjusted with HCl). A gravity driven perfusion system was used for all the experiments. All solutions were freshly made prior to recordings.

Oocytes were impaled by two electrodes connected to an Oocyte Clamp OC-725C (Warner Instruments, USA) for standard voltage clamp recordings as illustrated in Fig. 2.1. Briefly, electrodes were made from borosilicate capillary glass (Harvard Apparatus, GC 150 TF) using a vertical two stage electrode puller (Narishige PP-83) to give a top diameter of 1-2 µm. Prior to recordings electrodes were filled with 3 M KCl and only electrodes with a resistance between 0.5 and 2 MΩ were used for voltage clamping. Oocytes were continually perfused with fresh Ringer's solution at a rate of 10 mL/min. Switching between different solutions occurred through manually activated valves.

2.5.1 ACh and dFBr concentration response curves (CRC).

CRC for ACh were obtained by normalizing agonist-induced responses to the control responses induced by a near-maximum effective ACh concentration. A minimum interval of 5 min was allowed between agonist applications to ensure reproducible recordings. The ACh CRC data were first fitted to the one-component Hill equation $I = Imax/[1 + (EC_{50}/x)nH]$ where EC_{50} represents the concentration of agonist inducing 50% of the maximal response (I_{max}), x is the agonist concentration and nH the Hill coefficient. In case of agonist induced

biphasic receptor activation, CRC were fitted with the sum of two Hill equations a two-component Hill equation. Data were fit to the following equation from Prism v 5 (GraphPad 5 software):

Y=Bottom + (Top-Bottom) *Frac/(1+10^((LogEC$_{50_1}$-X)*nH1)) + Top-Bottom

* (1-Frac)/(1+10^((LogEC$_{50_2}$-X)*nH2))

Where, LogEC$_{50_1}$ and LogEC$_{50_2}$ are the concentrations that give half-maximal stimulatory effect in the same units as X.

nH1 and nH2 are the unitless slope factors or Hill slopes. Frac is the proportion of maximal response due to the more potent phase.

ACh CRC in presence of dFBr were obtained following the same protocol but co-applying a constant concentration of dFBr (I_{max}) with each ACh concentration and fitted to the same equation. Because dFBr makes ACh responses more efficacious a constraint was introduced in this equation to fit a Top >1.0.

CRC for dFBr were obtained by normalizing dFBr-induced potentiation of ACh currents to the ACh control responses that elicited 10% (EC_{10}) of the maximal response (I_{max}). To achieve this, a co-application of increasing concentrations of dFBr with ACh EC_{10} was performed with a minimum interval of 5 mins between applications. Each dFBr response was normalized by the average IACh(EC_{10}) before and after the co-application. Data were fit to the following equation from Prism v 5 (GraphPad 5 software):

Y= (plateau1 + ((Imax-1)/(1+10^((logEC$_{50}$-X)*nH1))))/(1 + 10^((logIC$_{50}$-X)*nH2))

Where, LogEC$_{50}$ and LogIC$_{50}$ are the concentrations that give half-maximal stimulatory and inhibitory effects in the same units as X.

Plateau1 represents the baseline before potentiation (activating component) and I_{max} represents the maximum level of potentiation. nH1 and nH2 are the unitless slope factors for both activating and inhibitory components.

2.6 Substituted cysteine accessibility method.

SCAM was used to assess whether an intra-subunit pocket between TM4 and TM3 of the α4 subunit could bind dFBr. SCAM comprises the introduction of cysteines, one at a time, into a protein region and the subsequent application of thiol-specific reagents to the engineered residues to determine whether they are modified by the thiol reagents. Modification of the introduced cysteine is monitored using electrophysiological or biochemical assays. The method was first used to study residues lining the ion channel pore in muscle nAChRs and ever since it has been considered a powerful technique in the study of pLGICs structure and ligand binding interaction (Karlin & Akabas, 1998).

2.6.1 Modification of dFBr putative binding sites using SCAM.

MTSET was used to modify covalently a cysteine residue introduced at the transmembrane level of α4 subunits. The amino acids mutated, one at a time, to cysteine were α4L617C and α4F316C. Mutant α4 subunits and wild type β2 subunits were mixed and expressed in *Xenopus* oocytes, and characterised using two electrode voltage clamping procedures, as described above. Stocks of 100 µL, 100 mM of MTSET reagent in RNAase free water were prepared in dry ice. Stocks were stored at -80 °C. To get a final concentration of 1 mM these stocks were quickly diluted in 10 mL of Ringer's solution seconds prior application. Experiments were design so the speed of perfusion would allow at least 10 mL of perfusion for each 120 seconds of application.

2.6.2 Covalent modification of introduced cysteines by MTSET reagent.

The effect of MTSET on dFBr responses was assessed. Oocytes expressing receptors with a free cysteine or wild type receptors were first challenged with a control ACh EC_{10} concentration every 5 min until a stable response was obtained. Subsequently, dFBr responses were assessed by co-applying ACh EC_{10} together with 10 μM dFBr (corresponds to dFBr I_{max}). Oocytes were then perfused with Ringer's solution containing MTSET (1 mM) for 120 s after which time the impaled cells were washed with Ringer's solution for 90 s. After washing, ACh EC_{10} was applied again every 5 min until the amplitude of the responses was constant and another co-application of ACh EC_{10} and 10 μM dFBr was given to determine accessibility to the modified cysteine residue by the MTS reagent.

The (ACh EC_{10} + 10 μM dFBr) current amplitude prior to application of MTS was the control response current ($I_{initial}$), and the (ACh EC_{10} + 10 μM dFBr) current amplitudes after rinsing was the average response after MTSET application (I_{after} MTS). The effect of the MTS reagents was estimated using the following equation: % Change = ((I_{after} MTS/$I_{initial}$) – 1) x 100.

For both mutants $\alpha4^{L617C}\beta2$, $\alpha4^{F316C}\beta2$ and wild type α4β2 receptors the concentration of MTSET used was equal to 1 mM (the optimal concentration for MTSET; Zhang & Karlin 1997). All mutants were also tested for the specificity of the MTSET reaction by treating the oocytes with DTT (1 mM, 120 s), which reversed the inhibition caused by covalent modification.

2.6.3 MTSET reaction rates.

To determine whether dFBr binds the putative allosteric site located within α4 subunits, we assayed the effect of dFBr on the rate of MTSET modification of C617. If dFBr reduced MTSET reaction rates, it was inferred that it binds the site, thus impeding, likely by steric hindrance, the modification of the introduced Cys residue by MTSET.

The rate of MTSET covalent modification of the introduced cysteine was first determined by measuring the effect of sequential applications of sub-saturating concentrations of MTSET on IACh+dFBr responses. The concentrations of MTSET reagent used were 20 μM. Preliminary experiments established that these concentrations of MTSET were optimal to describe adequately the early and plateau phases of the MTS reaction rate data. The concentrations of dFBr used were those that elicited the maximum ACh potentiation (I_{max}) that for L617C was 10 μM. ACh EC_{10} concentrations were used to stabilised current level and to assess dFBr potentiation as a protectant (ACh EC_{10} + 10 μM dFBr).

Responses to ACh and (ACh + dFBr) prior to MTS reagent applications were first stabilised as follows: ACh (EC_{10}) pulses were applied for 5 s, followed by a recovery time of 70 s. The protectant (ACh EC_{10} + 10 μM dFBr) was then applied for 10 s followed by a washing period of 3 min and 40 s with ringer solution. The cycle was repeated until the responses to ACh were stable to (<5% on four successive applications of ACh EC_{10} + 10 μM dFBr). MTS reagent was then applied using the following sequence of reactions: at time 0, ACh (EC_{10}) was applied for 5 s, followed by a period of recovery of 70 s; MTSET was then applied for 10 s, followed by a recovery period of 10 s. Immediately after the recovery time, the protectant (ACh EC_{10} + 10 μM dFBr) was applied for 10 s, after which time the cell was washed with Ringer's solution for 3 min and 40s. This cycle was repeated until MTSET applications produced no further changes between currents elicited by ACh EC_{10} alone and by the

protectant (ACh EC_{10} + 10 μM dFBr) (approx. 40 seconds). To exclude receptor desensitisation as responsible for decreases in IACh, ACh and protectant pulses (following the same scheme used to stabilize the ACh responses prior the MTSET application) were applied at the end of the protocol as a control.

2.6.4 Protection assay.

The effects of dFBr on the rate of MTSET modification was tested by co-applying MTSET with dFBr (10 μM). The protocol used was identical to the one used to determine the rate of MTSET reaction, except that the reversible ligand (dFBr) was co-applied with MTSET reagent but its ability as a protectant was assessed in the same way by co-applying it with ACh EC_{10}.

Responses to ACh and (ACh + dFBr) prior to MTS reagent applications were first stabilised as follows: ACh (EC_{10}) pulses were applied for 5 s, followed by a recovery time of 70 s. The protectant (ACh EC_{10} + 10 μM dFBr) was then applied for 10 s followed by a washing period of 3 min and 40 s with ringer solution. The cycle was repeated until the responses to ACh were stable to (<5% on four successive applications of ACh EC_{10} + 10 μM dFBr).

The sequence of MTSET reactions was as follows: at time 0, ACh (EC_{10}) is applied (5 s), followed by a brief period of recovery (70 s); MTSET and dFBr (10 μM) were then co-applied for 10 s, and followed by a recovery period of 3 min and 40 s. This cycle was repeated for about 40 seconds.

The change in current was plotted versus cumulative time of MTSET exposure. A pseudo–first-order rate constant was calculated from the change in IACh+dFBr normalized by IACh. Peak values at each time point were normalized to the initial peak at time 0 s, and a pseudo–first-order rate constant (k1) was determined by fitting the data with a single exponential

decay equation: y = span x e-kt + plateau using Prism v.5.0 (GraphPAD, CA, USA). Because the data are normalized to values at time 0, span = 1 - plateau. The second order rate constant (k2) for MTSET reaction was determined by dividing the calculated pseudo–first-order rate constant by the concentration of MTSET reagent used.

2.7 Statistical analysis.

Data analyses were performed using GraphPAD-Prism software (GraphPAD, CA, USA). Data were pooled from at least three different batches of oocytes. An F-test determined whether the one-site or biphasic model best fit the data; the simpler one-component model was preferred unless the extra sum-of-squares F test had a value of p less than 0.05. Log EC_{50} values for ACh, changes in current response amplitudes in response to mutations, dFBr or MTS application were analysed using one-way analysis of variance (ANOVA) with a Dunnett or Bonferroni post hoc correction for the comparison of all mutated receptors, to determine significance between wild type and mutant receptors. Significance levels between mutant receptors were determined using unpaired t tests. Data are plotted as mean ± SEM/ 95% IC. Fit parameter values are the best fitting values with the SEM values estimated from the fit.

2.8 Homology Modelling and Docking.

Homology modelling of the α4β2 nAChRs and docking data shown in this study were supplied by Professor Phil Biggin and Dr Maria Musgaard from the Biochemistry Department, Oxford University. Their contribution to this study was part of a long-term collaboration between Professor Biggin and Professor Bermudez. After the construction of the Homology models of both $(\alpha4\beta2)_2\alpha4$ and $(\alpha4\beta2)_2\beta2$ nAChRs our observations of the

model, together with the experimental data led us to suggest a series of locations for our modellers to perform molecular docking experiments. Additional docking experiments performed in this model and in initial studies with the α4β2 homology model from *Torpedo* nAChR were performed by Dr. Patricio Iturriaga-Vazques, from University of Chile, Santiago, Chile.

Briefly, homology models of the $(\alpha4\beta2)_2\alpha4$ and $(\alpha4\beta2)_2\beta2$ were constructed using MODELLER 9.12 and were based on the 5-HT_3 receptor X-ray structure (Hassaine et al., 2014). The models comprise the ECD, the TMD and part of the intracellular domain. Four residues are missing in the extracellular M2-M3 loop, and more than 60 residues are missing in the intracellular linker between M3 and M4. Sequences of the human α4 and β2 nAChR subunits were obtained from the ExPASy proteomics server with accession numbers P43681 (α4) and P17787 (β2) and aligned to the 5-HT_3R subunits using the alignment function of MODELLER (align2d) and, for comparison, also using two different alignment tools from the European Bioinformatics Institute (EBI), EMBOSS Stretcher and EMBOSS Needle, respectively. The sequence identity is approximately 25% and the sequence similarity is around 45%. The three alignments were compared and the final alignment constructed with manual changes in regions where the alignment algorithms were not optimal. Disulphide bonds are included, and 50 models were constructed. The models mainly vary in regions where the template was missing, and the best models were chosen based on analysing the MODELLER scores (molpdf, DOPE and GA341). The 3-4 best models were further assessed with QMEAN and these results were used together with the MODELLER scores to choose the appropriate model for docking.

A 3D model of dFBr was constructed in Maestro version 9.7 (Schrödinger, LLC, New York, NY, 2012 (academic version)) in both positively charged and neutral state. Protein and ligand models were prepared for docking using Autodock Tools and docking calculations were

performed with Autodock Vina. A large box of 74x74x40 Å3 centered in the extracellular half of the ion channel and covering a large part of the TMD of all five chains was used as the search space for docking calculations. 20 binding models were generated for each ligand docked into each protein model, i.e. 80 poses were generated in total. The binding models were analysed visually as the docking scores were all very similar (best score among 80 posed was -7.5 and the worst -6.2).

CHAPTER 3

Pharmacological Characterization of the Positive Allosteric Effects of dFBr on α4β2 nAChRs.

3.1 Introduction.

dFBr is a potent PAM of the α4β2 nAChR subtype. dFBr was first isolated as a tryptamine derivate from the marine algae *Flustra foliacea* (Peters et al., 2002). This group of tryptamines are also known for their inhibitory effects on the formation of bacterial biofilms (Bunders et al., 2011). As shown in Figure 3.1 dFBr is a hydrophobic molecule containing two aromatic rings, a bromide group and two amino-groups that at physiological pH are probably protonated (pKa: 10.39).

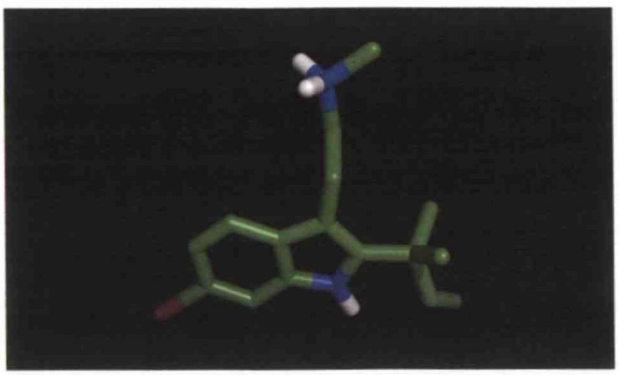

Figure. 3.1. Tridimensional structure of dFBr. Tryptamine structure containing two aromatic rings. N-groups are shown in blue and Bromide group in red.

dFBr also displays PAM activity at α2β2 nAChRs, albeit with decreased efficacy (Pandya & Yakel, 2011). In contrast, dFBr inhibits α7 nAChRs, α3-containing nAChRs and muscle nAChRs and this effect occurs at concentrations higher than 10 μM and in a voltage-dependent manner, indicative of ion channel blockade (Sala et al., 2005; Kim et al., 2007). dFBr also induces voltage-dependent inhibition of α4β2 nAChRs but at concentrations greater than 30 μM. This effect produces a bell-shaped CRC at the α4β2 nAChRs (Kim et al., 2007). Most α4β2 nAChR PAMs produce bell-shaped CRCs; for example, HEPES (Weltzin et al., 2014), galanthamine (Samochocki et al., 2003), atropine, scopolamine and physostigmine (Smulders et al., 2005). Typically, the inhibitory component of the bell-shaped

CRC is produced by moderate to high μM concentrations of PAM, suggesting ion channel blockade or the presence of potentiating and inhibiting AM binding sites (e.g., Zn^{2+} sites; Moroni et al., 2008).

dFBr increases the maximal responses of ACh with minor effects on ACh potency (Sala et al., 2005; Kim et al., 2007). Single channel studies of a mixed population of α4 and β2 assemblies expressed in oocytes, suggested that dFBr potentiates α4β2 nAChRs by increasing the channel open-probability, most likely by increasing the ratio of the rate constants of opening and closing (Sala et al., 2005).

dFBr may offer new opportunities for drug discovery. For example, dFBr has been shown to reduce nicotine self-administration in animal models of nicotine addiction (Liu, 2013). However, unlike agonists, dFBr cannot replace nicotine. These findings suggest that positive allosteric modulation of α4β2 nAChRs could be a promising target for the treatment of nicotine addiction and may present clinical advantages compared to agonists because of its lack of reinforcing actions when administrated on its own and the little liability for abuse that this implicates (Liu, 2013). In addition, the potentiating effects of dFBr on α4β2 and α2β2 nAChRs prevent the inhibition of these receptors by β-amyloid peptide, suggesting that dFBr, or similar PAMs, may be useful in the therapeutic management of Alzheimer's disease and related disorders (Pandya & Yakel, 2011).

As listed in Table 1.2, the structural and functional diversity of PAMs of α4β2 nAChRs suggests that multiple binding sites exist in the receptor. So far, binding sites or regions have been identified for NS9283 and NS206 (Olsen et al., 2013), Zn^{2+} (Moroni et al., 2008), galanthamine (Hansen & Taylor, 2007), 17β-estradiol (Paradiso et al., 2001) and LY2087101

(Young et al., 2008). In contrast, the binding site of dFBr on α4β2 nAChRs has not been identified yet. The studies reported in this thesis are concerned with the identification and mapping of the potentiating binding site of dFBr in α4β2 nAChRs. In this chapter, the general characteristics of the effects of dFBr on human α4β2 nAChRs were determined in order to establish an experimental approach that would facilitate the identification and mapping of the binding site of dFBr in this nAChR subtype.

3.2 Results.

3.2.1 Effects of dFBr in $(\alpha4\beta2)_2\alpha4$ and $(\alpha4\beta2)_2\beta2$ nAChRs.

The effects of dFBr on α4β2 nAChRs were examined using the two-electrode voltage clamping procedures (see Chapter 2, section 2.6) on α4β2 nAChRs expressed in oocytes following nuclear injection of equal amounts of α4 and β2 subunit cDNAs (1:1 ratios). This procedure yields a mixed population of α4β2 nAChRs made of approximately 80 % of $(\alpha4\beta2)_2\alpha4$ nAChRs and 20% of $(\alpha4\beta2)_2\beta2$ nAChRs (Moroni et al., 2006), resulting in bi-phasic ACh CRC (Fig. 3.2A). The biphasic responses comprise a low sensitivity component (ACh $EC_{50\text{-}1}$ = 129±0.1 μM) and a high sensitivity component (ACh $EC_{50\text{-}2}$ 3.95±1.6 μM). The high sensitivity component is produced not only by the presence of $(\alpha4\beta2)_2\beta2$ nAChRs (Moroni et al., 2006) but also by a relatively small high sensitivity component in the ACh CRC of $(\alpha4\beta2)_2\alpha4$ nAChRs (Harpsøe et al., 2011). This component is due to the presence of an additional ACh binding site at the α4(+)/(-)α4 interface of the $(\alpha4\beta2)_2\alpha4$ nAChR, which defines the agonist sensitivity (Harpsøe et al., 2011; Mazzaferro et al., 2011) and high-sensitivity desensitisation profile of this receptor type (Benallegue et al., 2013). The α4(+)/(-)α4 interface also accommodates the potentiating binding site for Zn^{2+} (Moroni et al., 2008)

and NS9283 (Olsen et al., 2013). For simplicity in the analysis of the results of all thesis chapters, α4β2 1:1 wild type and mutant receptors CRC were analysed as a monophasic.

At a concentration range of 1 – 10 μM, dFBr enhanced the responses to 10 μM ACh. A maximal potentiation of 850 ± 200 % (n = 5 cells) was achieved with 10 μM dFBr, with an EC_{50} for potentiation of 1.62±0.43 μM. At concentrations higher than 10 μM, the potentiating effect of dFBr decreased. dFBr inhibited the ACh responses with an IC_{50} of 39.2±13.8 (Fig. 3.2). The dFBr CRC was best fitted with an equation derived from the Hill equation to fit bell-shaped CRC data (see Chapter 2, Section 2.5.1) (p = 0.001; F test; n = 5). CRC parameters are summarised in Table 3.1.

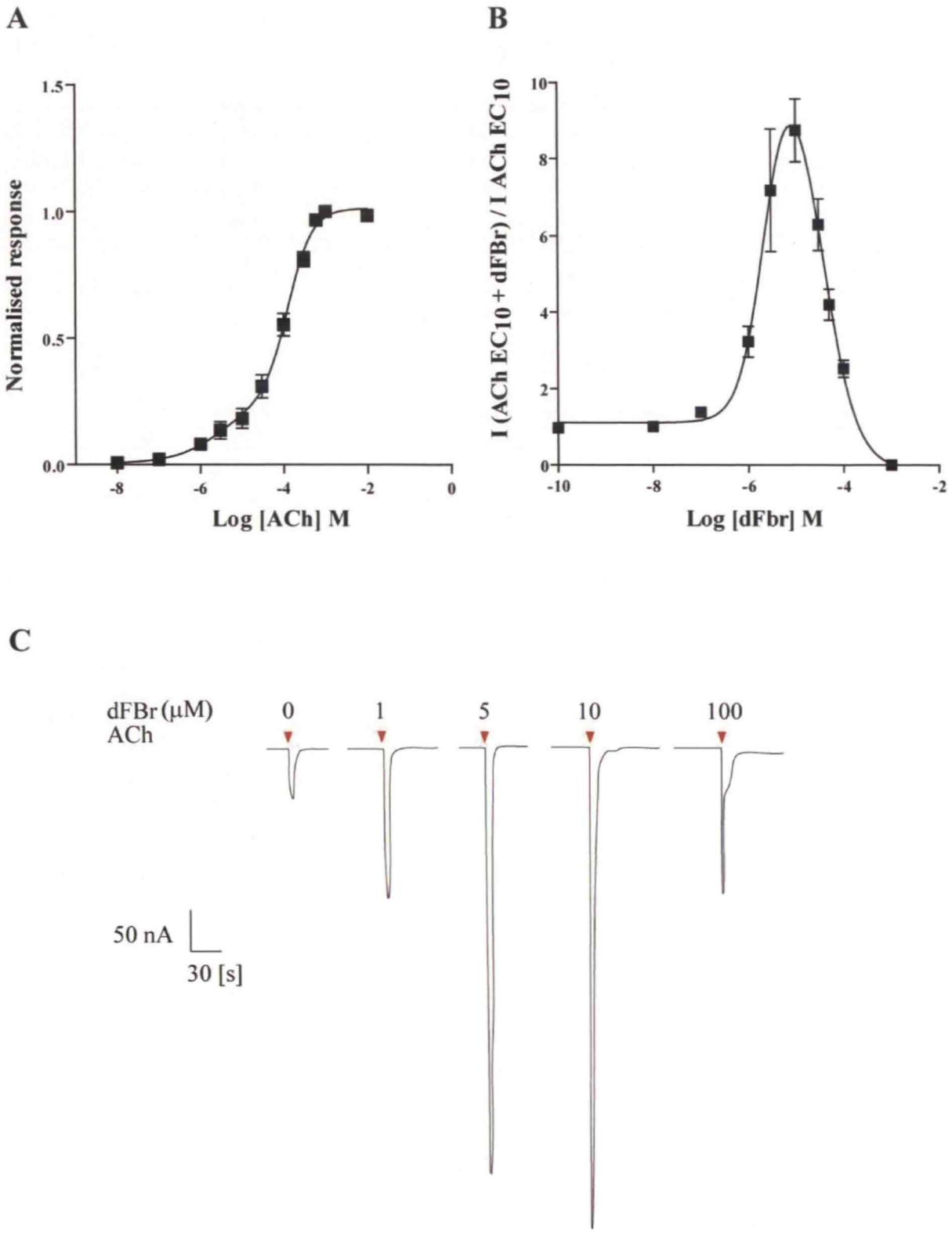

Figure 3.2. ACh and dFBr concentration response curves from α4β2 receptors expressed in *Xenopus* oocytes in 1:1 ratios. A) ACh CRC at α4β2 nAChRs assembled from loose α4 and β2 subunits. B) Bell-shaped CRC produced by dFBr at α4β2 nAChRs. C) Representative traces of ACh responses in presence of increasing concentrations of dFBr (μM). Red arrows represent ACh applications (▼).

Table 3.1. Summary of ACh CRC of α4-containing and α3β2 nAChRs. Data are the mean ± SEM and/or 95% IC for 3 -18 experiments. ACh and dFBr EC_{50} values, fractions, Hill coefficients and Imax are indicated. α4β2, α4β4 and α3β2 nAChRs represent receptors assembled from loose subunits, whereas β2_α4_β2_α4_α4 and β2_α4_β2_α4_β2 are fully concatenated α4β2 nAChRs. CRCs for ACh and dFBr were constructed as detailed in Chapter 2. The CRC parameters EC_{50}, IC_{50}, nH and Imax were estimated from CRC data from at least three different batches of oocytes (n = 3-8). IN indicates only inhibitory responses.

Receptor	ACh		dFBr		
	EC_{50}	nH	EC_{50}	IC_{50}	I_{max}
α4β2	97.99 (81-112)	0.94 ±0.07	1.62±0.43 (0.7-2.5)		10.6±2.1 (6.2-14.9)
β2_α4_β2_α4_α4	120±13.7 (92.7-147)	0.71±0.05	3.2±1.4 (0.4-6.1)		12.81±3.54 (5.72-19.9)
β2_α4_β2_α4_β2	7.5±1.03 (5.4-9.4)	0.7±0.07	1.94±0.5 (0.96-2.9)		2.3±0.17 (1.55-3.05)
α4β4	9.2±1.04 (7.8-10.5)	0.9±0.1	0.14±0.05 (0.03-0.26)	5.8±1.5 (2.5-9.0)	2.01±0.19 (1.53-2.5)
α3β2	12.8±3.0 (6.5-18.9)	0.6±0.06	IN	118±16.4 (83.5-153)	IN

The macroscopic mechanism of the potentiating effects of dFBr was next investigated testing the effect of dFBr on the ACh CRC at α4β2 nAChRs. For these experiments, the ACh CRC at α4β2 nAChRs was obtained in the absence and presence of a maximally potentiating concentration of dFBr (10 μM). Maximally potentiating dFBr had a pronounced effect on ACh efficacy, enhancing maximal ACh responses by 300% (Fig. 3.2). dFBr had a minor effect on ACh sensitivity with a small but not significant left shift.

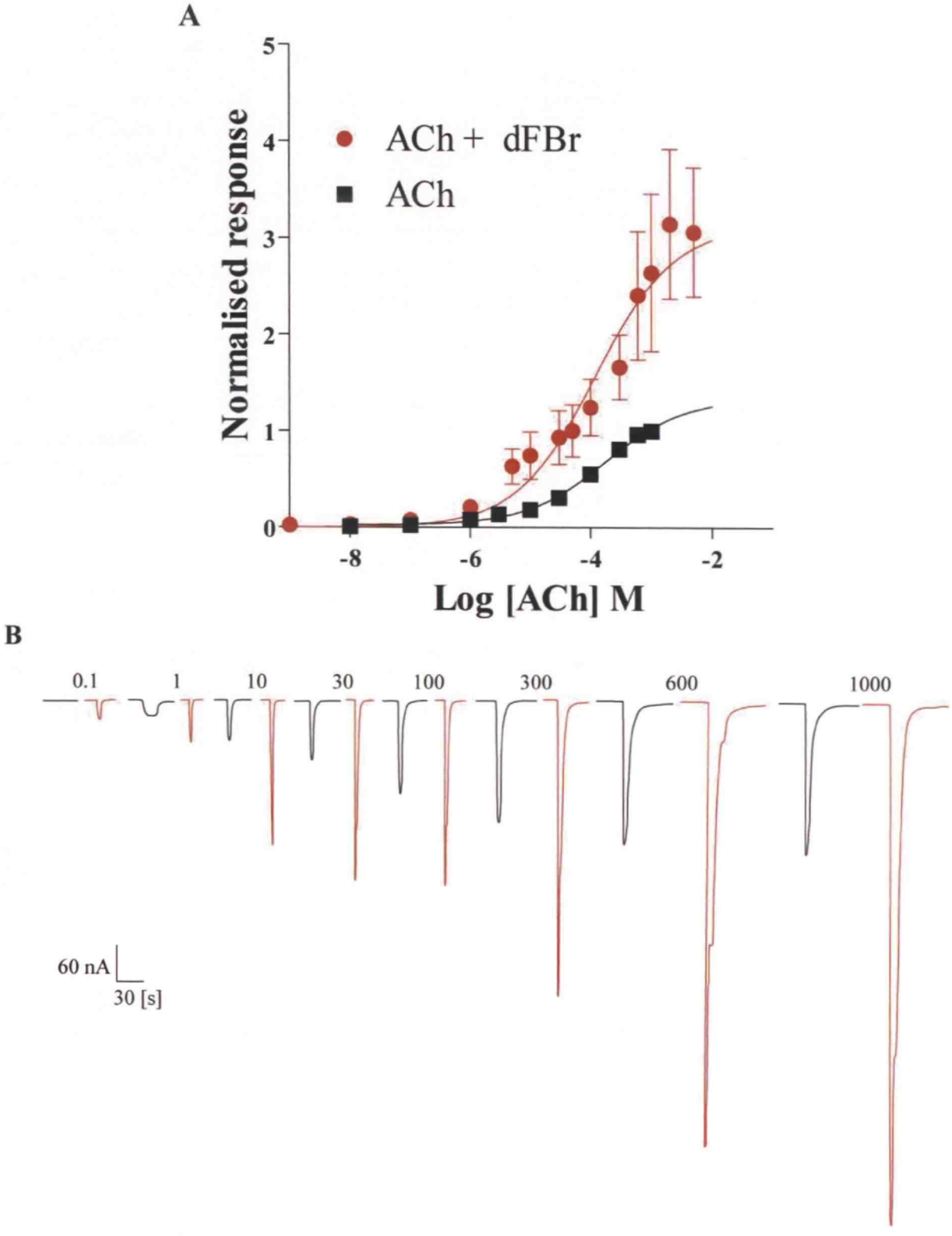

Figure 3.3. ACh concentration response curves of 1:1 α4β2 receptors in presence and absence of 10 μM dFBr. In A, plot of ACh CRC in presence (●) and absence (■) of 10 μM dFBr. In B: representative traces of ACh applications in presence (red trace) and absence (black trace) of dFBr, values are in micromolar range (μM).

The increase in ACh efficacy caused by dBFr at α4β2 nAChRs has been proposed to be due to the ability of this PAM to rescue α4β2 nAChRs from desensitisation (Weltzin & Schulte, 2010). To test this suggestion, the effects of dFBr on the turn-off kinetics of α4β2 receptors were inspected visually. As shown in Figure 3.4, dFBr seems to rescue α4β2 nAChRs from desensitisation.

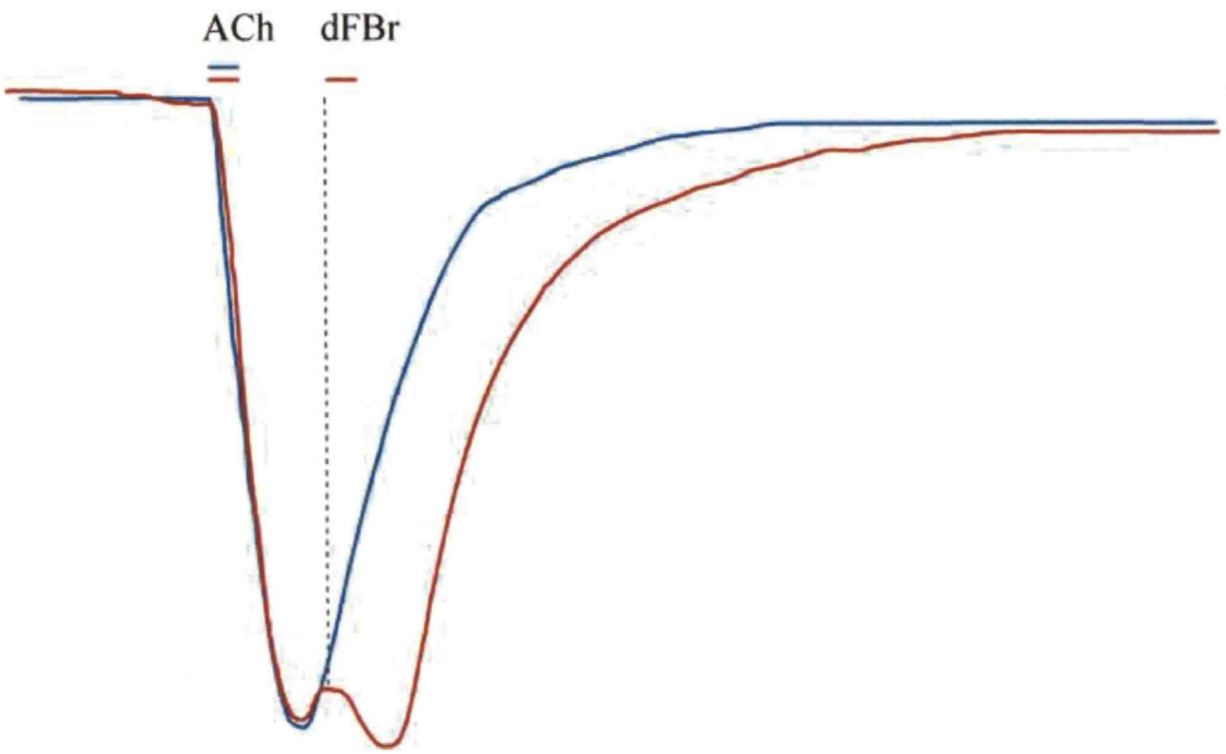

Figure 3.4 Desensitisation kinetics of α4β2 receptors elicited by ACh in presence and absence of dFBr. Representative traces after 5 seconds applications of either ACh or co-application of ACh and dFBr. Blue trace represents response elicited by 1 mM ACh and red trace represents co-application of 1 mM ACh and dFBr EC_{10}.

PAMs may have different selectivity for $(\alpha4\beta2)_2\alpha4$ and $(\alpha4\beta2)_2\beta2$ nAChRs (see Table 1.2) and differences may indicate the presence of more than one type of PAM binding site on α4β2 nAChRs (e.g., Moroni et al., 2008). To explore this possibility, the effects of dFBr were tested on the ACh responses of fully concatenated $(\alpha4\beta2)_2\alpha4$ and $(\alpha4\beta2)_2\beta2$ nAChRs. The use of these types of α4β2 nAChRs obviate uncertainties about receptor stoichiometry and subunit order (Carbone et al., 2009) and these receptors have been shown to replicate the

functional properties of $(\alpha4\beta2)_2\alpha4$ and $(\alpha4\beta2)_2\beta2$ nAChRs assembled from loose α4 and β2 subunits (Carbone et al., 2009) (see Table 3.1). As shown in Figure 3.5, both types of α4β2 nAChRs were potentiated by dFBr, albeit dFBr was 5-fold more efficacious at the $(\alpha4\beta2)_2\alpha4$ type. The EC_{50} values for the potentiating effects of dFBr at concatenated $(\alpha4\beta2)_2\alpha4$ and $(\alpha4\beta2)_2\beta2$ nAChRs were similar, and these were not different from the equivalent EC_{50} value obtained for α4β2 nAChRs assembled from loose α4 and β2 subunits (CRC parameters are summarised in Table 3.1), suggesting that the binding site for dFBr occupies the same region in both receptor types.

The findings above suggested that the α4 subunit plays a dominant role in conferring sensitivity to potentiation by dFBr. To explore this possibility further, the effect of dFBr was tested on receptors assembled from α3 and β2 subunits (α3β2 nAChRs) and α4 and β4 subunits (α4β4 nAChRs). As shown in Table 3.1, α3β3 nAChRs (see also Chapter 5) were not sensitive to potentiation by dFBR, whereas α4β4 receptors were. These findings, together with previously published data on α7 and α3β4 nAChR (Sala et al., 2005), further support the suggestion that the α4 subunit confers sensitivity to potentiation by dFBr.

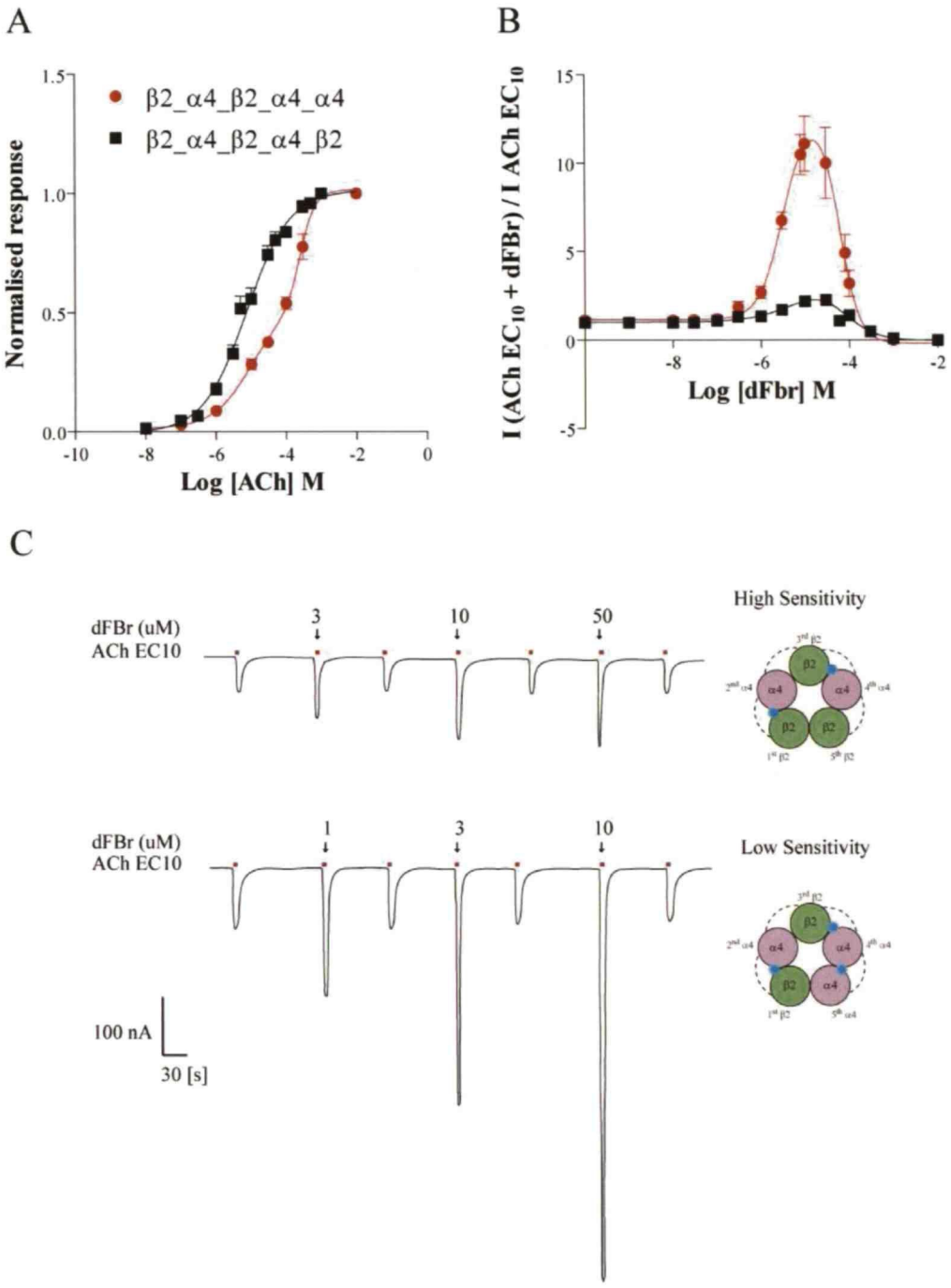

Figure 3.5 Effects of dFBr in β2_α4_β2_α4_α4 and β2_α4_β2_α4_β2 concatenated receptors. In A and B: ACh and dFBr concentration response curves for β2_α4_β2_α4_α4 (●) and β2_α4_β2_α4_β2 (■). In C representative traces of ACh (red lines) with increasing concentrations of dFBr (arrows) of both High (top) and Low Sensitivity (bottom) α4β2 concatenated receptors. dFBr concentrations in μM range.

Finally, to determine whether ion channel blockade could account for the inhibitory component of the dFBr CRC at α4β2 nAChRs, the effect of the holding potential on levels of dFBr-induced inhibition was assessed. Typically, blockade of Cys loop channels by ligands is voltage-dependent. For these studies, the current responses elicited by ACh EC_{10} at both types of concatenated α4β2 nAChRs were elicited in the absence and presence of the appropriate dFBr IC_{50} concentration at a range of holding potentials (-60 to -120 mV). For both types of receptors, the extent of dFBr-induced inhibition of the ACh current responses decreased with depolarisation of the holding potential, suggesting dFBr acts as an ion channel blocker at high μM concentrations (Fig.3.6A). Additionally, at high concentrations of dFBr a rebound effect on the ACh responses was found (Fig.3.6B).

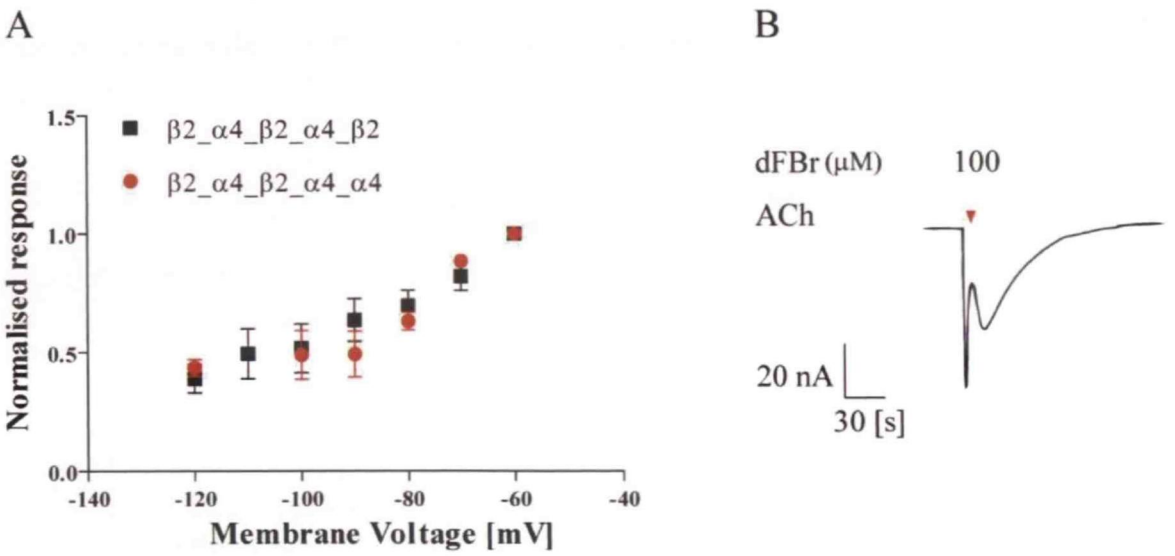

Figure 3.6. Effects of membrane potential on inhibitory effects of dFBr at concatenated α4β2 nAChRs. In A, β2_α4_β2_α4_α4 (●) and β2_α4_β2_α4_β2 (■) responses to inhibitory concentrations of dFBr (IC_{50}) co-applied to ACh EC_{10} at membrane voltages from -120 to -60 mV. In B, representative trace of a rebound current elicited by a saturating concentration of dFBr (100 μM) co-applied to an EC_{10} ACh. Red arrow represents application of ACh (▼).

3.3 Discussion.

The main finding of this chapter is that dFBr potentiates the ACh responses of α4β2 nAChRs by increasing the maximal responses of ACh. This effect is a hallmark feature of PAMs that exert their effects through binding sites in the TM domain of ion channels. dFBr effects on agonist efficacy appear to be due to disruption of the desensitisation of the receptors and this is consistent with its effect on agonist efficacy. PAMS that exert their action through sites located in the ECD typically increase agonist sensitivity with no effects on agonist efficacy. Examples of compounds of this type acting on α4β2 nAChRs include NS9283, 17β-Estradiol and galanthamine (Paradiso et al., 2001; Hansen & Taylor, 2007; Olsen et al., 2013).

dFBr is more efficacious at $(\alpha4\beta2)_2\alpha4$ nAChRs than at $(\alpha4\beta2)_2\beta2$ nAChRs. Previous work (Sala et al., 2005) and this study (Table 3.1) have found that the α4 subunit is necessary for sensitivity to potentiation by dFBr. Thus, the differential potentiating effects of dFBr on α4β2 nAChRs may be due simply to the number of α4 subunits present in both receptor forms. Single channel studies of the effects of the PAM compound PNU-120596 on α7 nAChRs have suggested that the efficacy of PNU-120596 depends on the number of PAM binding sites available (daCosta & Sine, 2013). It is thus tempting to suggest that the efficacy of dFBr is greater at $(\alpha4\beta2)_2\alpha4$ than at $(\alpha4\beta2)_2\beta2$ because there are more α4 subunits in the former receptor type. On the basis of this suggestion, the identification and mapping of the dFBr potentiating binding site on α4β2 nAChRs focused on the α4 subunit, specifically on the TM domain of this subunit. These studies are described next in Chapter 4.

CHAPTER 4

The TMD of the α4β2 nAChR mediates the potentiating effects of dFBr.

4.1 Introduction

The studies described in Chapter 3 suggested that dFBr may potentiate α4β2 nAChRs by binding to a site in the TMD of this receptor type. As previously discussed, the TMD is a three-ring cylinder of concentrically arranged M1-M4 α-helices that form a multifunctional complex. The pLGIC TMD contributes the ion channel and the gating machinery to control channel opening, acts as a lipid-sensor, is involved in both the assembly and trafficking of pLGICs to the cell surface and, of relevance to this thesis, houses the binding site for several classes allosteric compounds (for a review see, Henault et al., 2014). AMs that bind the TMD of pLGICs include ethanol and other short-chain alcohols, neurosteroids, barbiturates, GAs and some α7 nAChR PAMs (Hosie et al., 2006; Young et al., 2008; Forman & Miller, 2011). Typically, these type of allosteric compounds bind to a conserved cavity near the channel pore-lining domain, M2, and thus more directly influence channel gating than AMs that bind the ECD.

Compared to $GABA_A$Rs, only a few PAMs of the nAChR have been found to bind the TMD. PAMs for the α7 nAChR are the best-developed examples of nAChR modulators. α7 nAChR has fast desensitisation kinetics. PAMs for α7 nAChR can be classified into two types: type I and type II, according to their influence on current kinetics. Type I PAMs mainly potentiate current without significantly influencing receptor desensitisation. Ivermectin (Krause et al., 1998), 5-hydroxyindole (5-HI) (Zwart et al., 2002) and NS-1738 (Timmermann et al., 2007) are examples of type I PAMs. 5-hydroxyindole is also an allosteric modulator for 5-HT_3Rs. The binding site of 5-HI in 5-HT_{3A}Rs is located at L293 of the M2 domain (Hu & Lovinger, 2008). In contrast, type II PAMs can dramatically reduce desensitisation or even re-activate desensitised receptors. PNU-120596 is the best-characterized representative of this type

(Hurst et al., 2005). Its binding pocket is located in the transmembrane domain (Young et al., 2008), and is formed by five residues: S222 (M1), A225 (M1), M253 (M2, 15' position), F455 (M4), and C459 (M4). Each α7 subunit harbours one such site. These residues are located in a cavity that is conserved in the pLGIC family and that has been shown to house binding sites for neurosteroids and volatile anaesthetics on $GABA_A$Rs and GlyRs (Ye et al., 1998; Hosie et al., 2006). Another PAM of α7 nAChRs that occupies this TMD cavity is LY2087101 (Young et al., 2008). However, LY2087101 displays PAM-1 effects on α7 nAChRs (i.e., increases in peak current with little effect on the time course of the agonists-evoked responses), suggesting differences in the binding sites of these two AMs.

This Chapter describes the findings of dFBr docking simulations on homology models of full length α4β2 nAChRs, mutagenesis, electrophysiological assays and SCAM studies. The findings described here account for the dominant role of the α4 subunit on sensitivity to potentiation by dFBr by identifying residues in the TMD of this subunit that abolish or markedly reduce the potentiating effect of dFBr and compete with MTSET when cysteine-substituted. These residues map to a crevice between M3 and M4 in the TMD of the α4 subunit.

4.2 Results

4.2.1 Role of the TMD in the potentiation by dFBr.

In order to aid the identification of regions in the TMD of the α4β2 nAChR that might be responsible for the potentiating effects of dFBr, docking stimulations with this ligand on homology models of the TMD of the α4β2 nAChR were performed. As shown in Fig.4.1A, docking stimulations suggested that dFBr may occupy a crevice between M3 and M4 of the α4 subunit. The side chain of F312, T313 and Y309 of α4 M3 and L617 and F606 in α4 M4 are predicted to orientate towards this crevice (Fig. 4.1B, C) suggesting that these residues might directly contribute to dFBr binding, forming part of the dFBr potentiation site. This possibility was examined by alanine substitution. For all mutated α4 subunits, the potentiating effect of a range of concentrations of dFBr was examined on a submaximal (EC_{10-15}) concentration of ACh (Table 4.1 summarises the ACh and dFBr CRC parameters estimated from the data obtained in these studies). This strategy showed that alanine substitutions of M3 residues α4Y309, α4F312, α4T313 and α4F316 significantly affected the ability of dFBr to potentiate the ACh responses of α4β2 nAChRs (Fig.4.2), in comparison to wild type. α4Y309A and α4F312A abolished dFBr potentiation ($p < 0.001$; n =5). α4T313A and α4F316A also decreased the potentiating efficacy of dFBr but by a factor of 5 and 2.8 respectively ($p < 0.001$; n = 4). Alanine substitutions of M4 residues also reduced the extent of dFBr potentiation in comparison to wild type. Thus, α4F606A and α4L617A reduced the potentiating efficacy of dFBr by a factor of 2.7 and 8, respectively. Y309A, F312A and F617A decreased the sensitivity of the receptor to potentiation by dFBr ($p < 0.001$; n = 4-6) (Table 4.1), suggesting that these mutations selectively affected the dFBr potentiating binding site and did not exert a general perturbation of on α4β2 nAChR function. This conclusion is

supported by the observation that none of these mutations affected the sensitivity of the α4β2 nAChR to activation by ACh (Table 4.1). In contrast, α4T313A, α4F316A and α4F606A had less effect on the potency of dFBr potentiation, suggesting that these residues do not directly bind dFBr. Both α4F316A and α4F606A significantly affected sensitivity to ACh, suggesting that the effects of these mutations on potentiation by dFBr are due to a general perturbation of receptor function. The conclusions from this part of the work are supported by the observation that alanine substitution of M4 residue α4F618, a residue whose side chain points towards the phospholipid layer away from the M3-M4 crevice had no effect on potentiation by dFBr but significantly reduced sensitivity to ACh (Table 4.1).

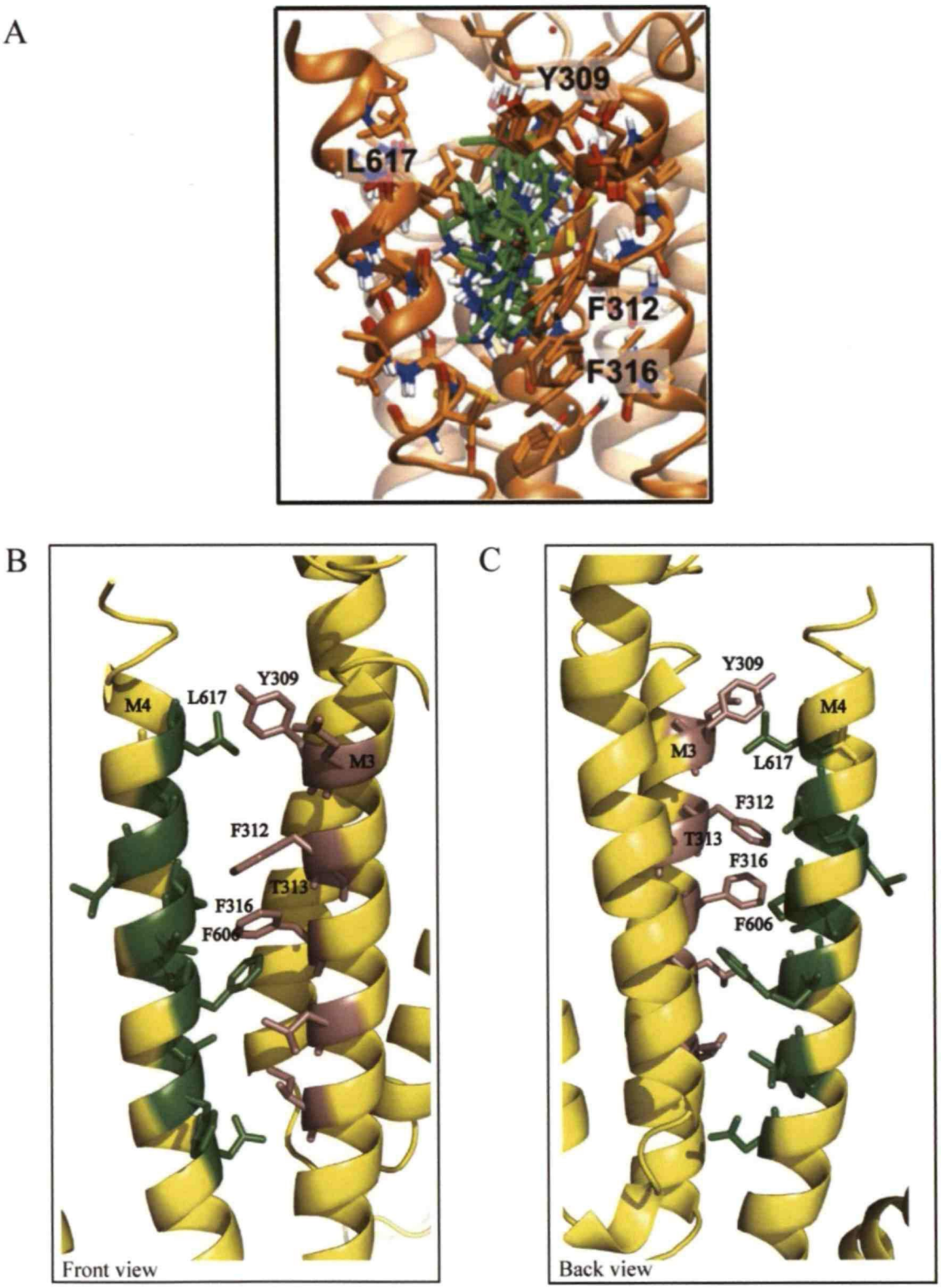

Figure 4.1. α4β2 nAChR Homology model and dFBr docking experiments. A) Binding of dFBr to a crevice between M3 and M4 of the α4 subunit. Different poses of dFBr docking are shown in green. B) and C) show the side chains of M3 (In pink) and M4 (in green) residues pointing towards the crevice between M3 and M4.

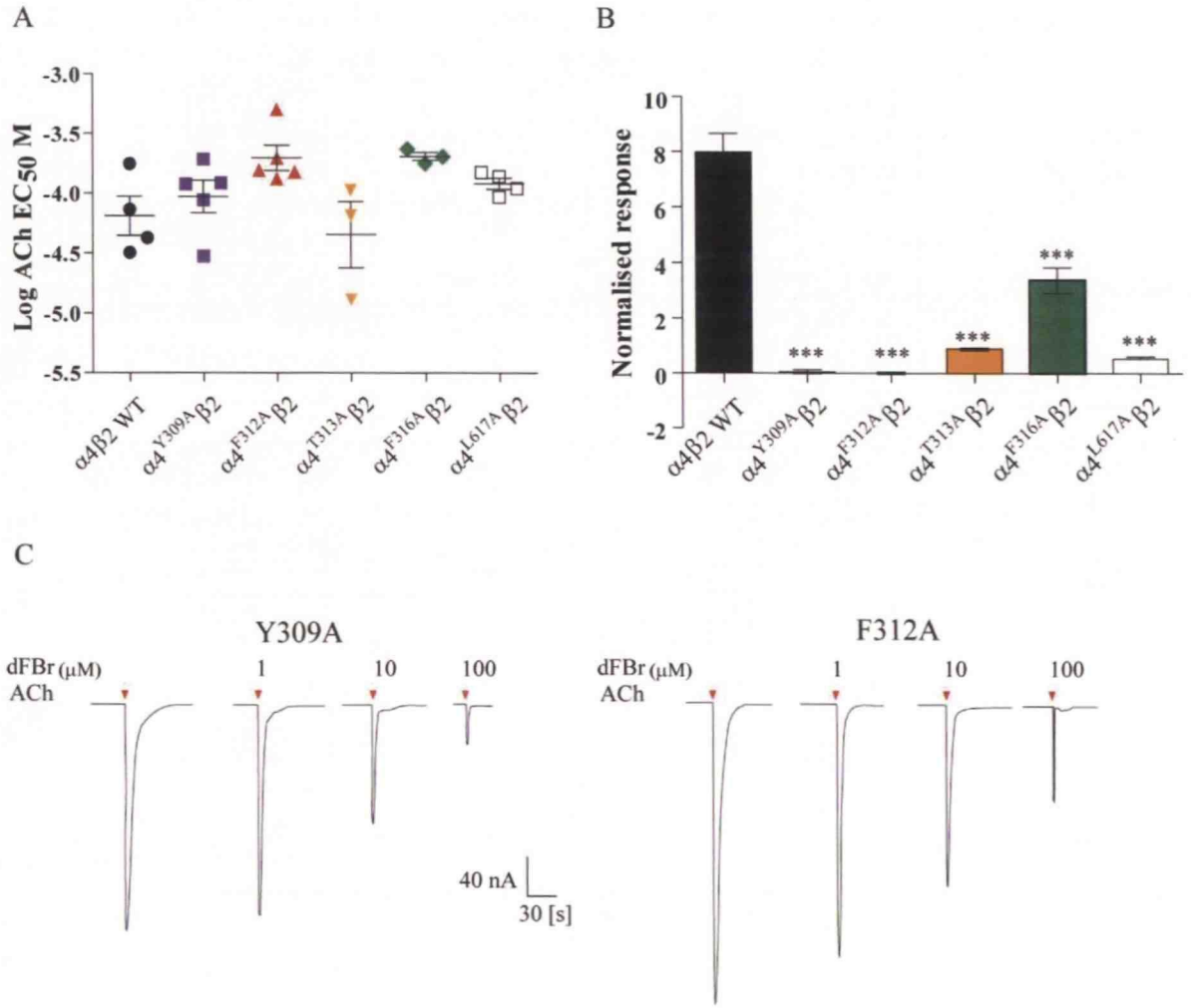

Figure. 4.2. ACh and dFBr profiles of wild type and TMD mutant receptors. In A, Dispersion plot of ACh $LogEC_{50}$ [M] values for wild type α4β2 and mutants $α4^{Y309A}β2$, $α4^{F312A}β2$, $α4^{T313A}β2$, $α4^{F316A}β2$ and $α4^{L617A}β2$. In B, Histogram of dFBr I_{max} of wild type α4β2 and mutants $α4^{Y309A}β2$, $α4^{F312A}β2$, $α4^{T313A}β2$, $α4^{F316A}β2$ and $α4^{L617A}β2$. As described in Chapter 2, dFBr I_{max} values represent responses to applications of ACh EC_{10}+ dFBr. ***$p<0.01$ (ANOVA). In C, representative traces of responses of mutants $α4^{Y309A}β2$ and $α4^{F312A}β2$ to co-applications of ACh EC_{10} and increasing concentrations of dFBr. Red arrows represent ACh applications (▼).

Table 4.1. Concentration effects of ACh and dFBr on wild type and TMD mutant α4β2 nAChRs. Oocytes expressing wild type or mutant α4β2 nAChRs were exposed to a range of concentrations of ACh or dFBr, as described in the Methods Chapter. The concentration effects of dFBr were determined on responses to ACh elicited by EC_{10} ACh concentrations. The data points were used to generate CRCs from which EC_{50}, Hill coefficient (nH) and maximal potentiation (I_{max}) values were estimated. Values represent the mean ± SEM (I_{max} and nH) and 95% CI of at least 3 independent experiments. Statistical differences were determined by Student's t-test or one-way analysis of variance. *$p < 0.05$; **$p < 0.01$. IC_{50} values are represented as negative EC_{50} values (concentration of dFBr that elicits 50% of the inhibitory response).

Receptor	ACh		dFBr	
	EC50 μM	nH	EC50	Imax
α4β2	97.99 (81-112)	0.94 ±0.07	1.62 (0.7-2.5)	10.6±2.0
M3 Residues				
$\alpha4^{Y309A}\beta2$	116 (77-173)	0.77±0.01	-93.91*** -(41-146)	1±0.03**
$\alpha4^{Y309C}\beta2$	112 (81-114)	0.81±0.09	-88*** (-38-150)	1±0.06
$\alpha4^{Y309F}\beta2$	110 (57-214)	0.69±0.11	-82 -(255-400)	1±0.03**
$\alpha4^{F312A}\beta2$	110 (73-163)	0.61±0.05	-97.14 -(52-142)	1±0.001**
$\alpha4^{F312Y}\beta2$	111 (71-174)	0.76±0.09	0.98 (0.07-10)	3±1**
$\alpha4^{F312C}\beta2$	102 (65-160)	0.67±0.09	-11*** -(7-15)	1±0.06**

$\alpha4^{I313A}\beta2$	114 (80-162)	0.81±0.09	1.7 (0.8-5)	2.2±0.4**
$\alpha4^{F316A}\beta2$	180* (100-322)	0.76±0.12	2.2 (0.9-5.2)	3.9±0.3**
$\alpha4^{F316C}\beta2$	122 (63-236)	0.67±0.10	2.5 (0.8-4.1)	4.2±0.44**
M4 Residues				
$\alpha4^{L617A}\beta2$	139 (99-147)	0.99±0.08	11* (9-13)	1.3±0.4**
$\alpha4^{L617C}\beta2$	143 (112-182)	1.2 ±0.15	10.84* (4-31)	3±0.21**
$\alpha4^{F606A}\beta2$	68* (37-124)	0.54±0.06	2 (0.5-2.6)	3.8±1.2**
$\alpha4^{F606C}\beta2$	115 (61-218)	0.61±0.08	1.8 (0.8-2.3)	4.01±1.4**
$\alpha4^{F618A}\beta2$	230* (190-359)	1.01±0.5	2.8 (2-4)	9.8±3

The alanine substitution experiments suggested that α4Y309, α4F312 and α4L617 play a pivotal role in the potentiating effects of dFBr. If these residues interact with dFBr directly, substitutions with other amino acids should affect those interactions in a manner consistent with the type of interactions they establish with dFBr. To determine whether aromaticity is essential for interactions between α4F312 and α4Y309 with dFBr, the effects of α4F312Y and α4Y309F were tested on dFBr potentiation. As shown in Fig.4.3, α4F312Y did not abolish the potentiating effect of dFBr, although the presence of a tyrosine residue at this

position reduced the potentiating effect of dFBr by a factor of 3.4 (Table 4.1). In contrast, α4Y309F completely abolished the potentiating effect of dFBr (Table 4.1). Mutating F312 and Y309 to a non-charged but polar residue such as cysteine completely abolished the potentiating effects of dFBr, suggesting the importance of aromaticity for dFBr potentiation. Thus, together the substitutions made at F312 and Y309 positions suggest that F312 may interact with dFBr through aromatic interactions (e.g., π-stacking interactions with one of the aromatic rings of dFBr) and that tyrosine 309 possibly establish hydrogen bonds. Interestingly, the effects of α4F316C, α4T313C or α4F606C on the efficacy of dFBr potentiation were similar to those observed with alanine substitutions, which, together with the observation that none of these mutations abolish the potency of dFBr potentiation, suggest that none of these residues directly interact with dFBr. Cysteine substitution of M4 L617, which would reduce hydrophobicity in this position, reduced both the efficacy and potency of dFBr, further suggesting that α4L617 contacts dFBr directly within a potentiating binding.

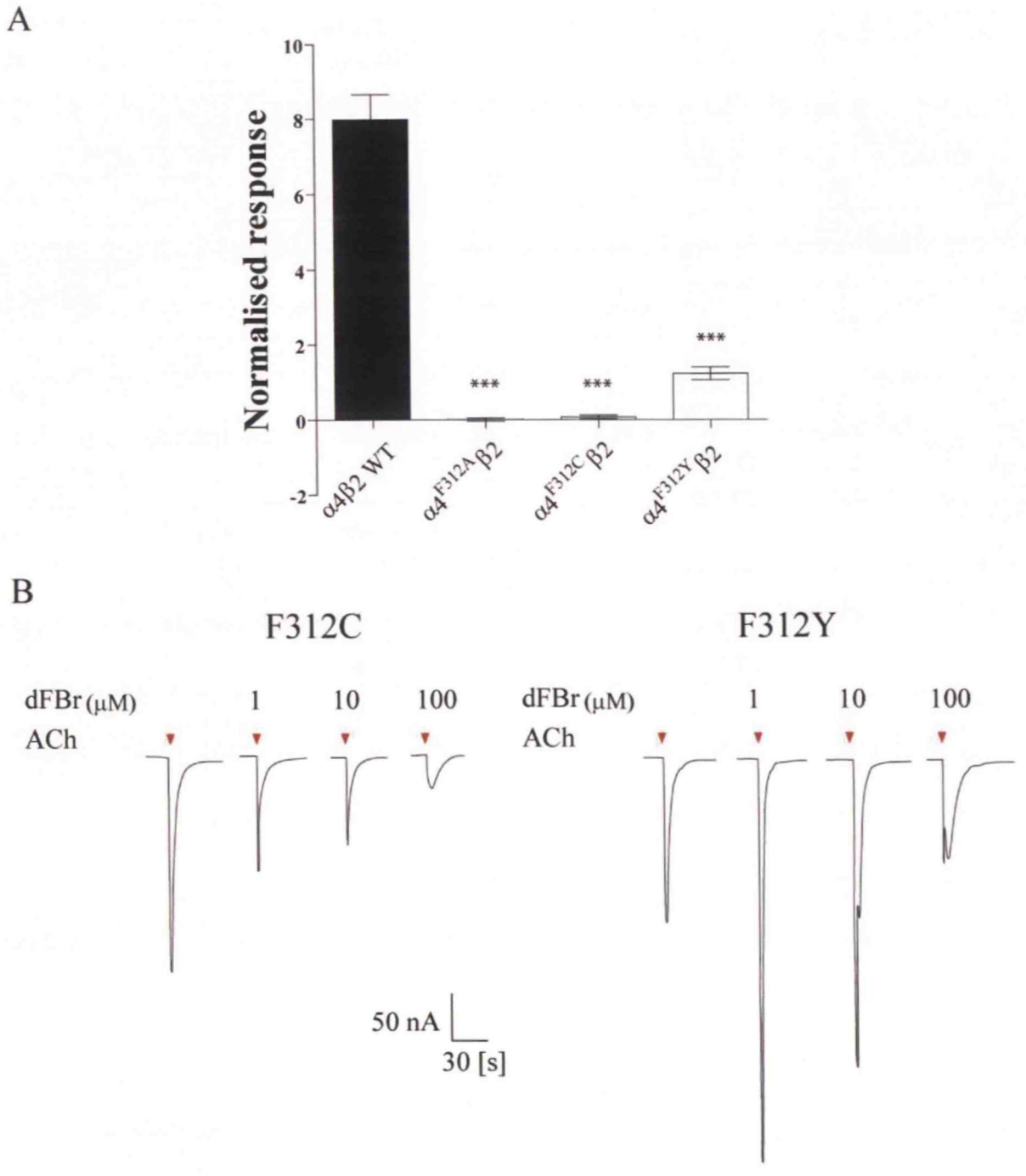

Figure. 4.3. dFBr concentration response curves for $\alpha4^{F312A}\beta2$, $\alpha4^{F312C}\beta2$ and $\alpha4^{F312Y}\beta2$ mutant receptors. In A, histogram of maximum potentiation of α4β2 wild type and mutants $\alpha4^{F312A}\beta2$, $\alpha4^{F312C}\beta2$ and $\alpha4^{F312Y}\beta2$. Data represent the mean from at least three independent experiments. ***$p < 0.01$ (ANOVA). In B Representative traces for inhibitory effects of dFBr on mutant α4F312C and potentiating effects on mutant α4F312Y. Red arrows represent ACh applications (▼).

4.2.2 SCAM approaches support the presence of a potentiating binding site for dFBr in the TMD of the α4 subunit.

To further examine the possibility that the crevice between M3 and M4 in the α4 subunit houses a binding site for dFBr, protection assays using the cationic methanethiolsulfonate reagent compound MTSET and dFBr were carried out. First, it was established whether α4L617C, at the entrance to the putative binding site, or α4F316C, below the putative binding site could be used for the protection assays. For this, it was determined the accessibility of α4L617C and α4F316C to MTSET by exposing the substituted cysteines to a saturating concentration of MTSET (1 mM). As shown in Fig. 4.4, 1 mM MTSET completely abolished the effect of dFBr when α4L617C was present, indicating that a cysteine at this position is fully accessible to MTSET. In contrast, the reaction of α4F316C with 1 mM MTSET reduced dFBr potentiation by only 30% (Fig. 4.4), indicating that a cysteine at this position has limited accessibility to MTSET. Our results not only confirm accessibility to the putative site by the introduction of α4L617C but strongly suggest this residue contributes to the binding of dFBr. Introduction of α4L617C alone significantly reduces potentiation elicited by dFBr (efficacy is 1.8), which may imply that the residue is either directly interacting with dFBr or structurally modifying the pocket once mutated. As shown in Fig. 4.4B (Before and After reaction), when mutant α4L617C is challenged to a saturating concentration of MTSET (1 mM) the ACh responses are not affected. In contrast, the remaining potentiation by dFBr found in this mutant is completely abolished after the MTS reaction. Therefore, from these studies $\alpha4^{L617C}\beta2$ was chosen for the protection assays that are described next.

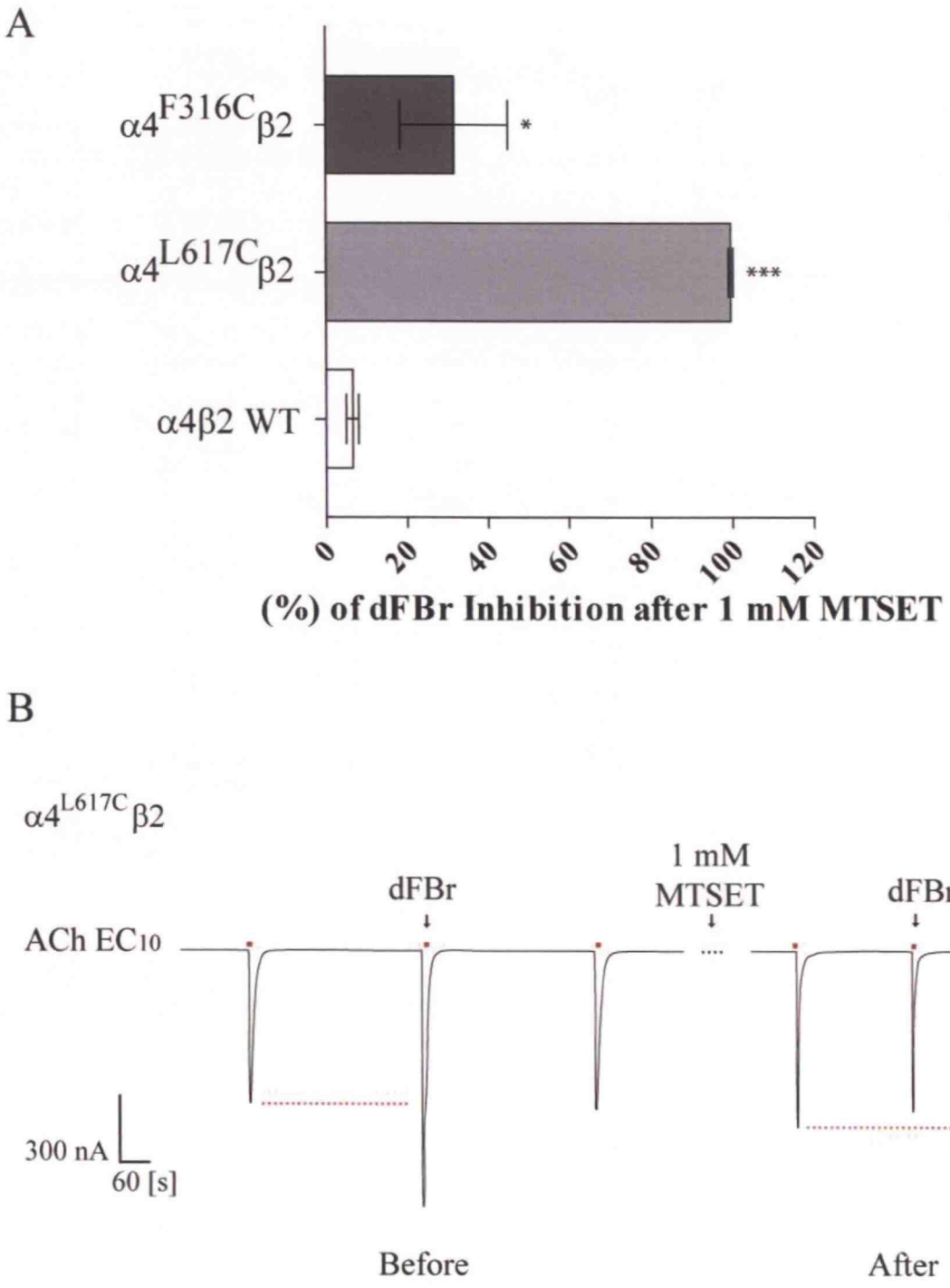

Figure. 4.4. Effect of MTSET on dFBr responses of wild type and mutant α4β2 receptors. A, The percentage of inhibition of the responses elicited by ACh EC_{10} concentrations co-applied with 10 μM dFBr on wild type and mutants $\alpha4^{F316C}\beta2$ and $\alpha4^{L617C}\beta2$ receptors after a 2 min application of 1 mM MTSET is defined as [I(ACh+dFBr) /(I ACh) after MTS/ I(ACh +dFBr) /(I ACh) initial) x 100], where I indicates the current responses. Data represent the mean from at least three independent experiments. *$p < 0.01$ (ANOVA), ***$p < 0.05$. B, Representative traces of dFBr effects on ACh EC_{10} + dFBr current (I_{max}) of mutant $\alpha4^{L617C}\beta2$ before and after application of 1 mM MTSET. Red dots represent ACh EC_{10} applications. dFBr and MTSET applications are indicated with arrows. ACh EC_{10} currents were stabilized (plateau) before and after dFBr and MTSET applications and no differences in ACh EC_{10} currents responses were found post-MTSET.

For the protection assays, the currents elicited by an EC_{10} concentration of ACh at $\alpha4^{L617C}\beta2$ were first stabilised. After stabilisation was achieved, ACh EC_{10} and 10 μM dFBr were co-applied to test receptor maximum potentiation before the MTSET reaction. Next, a sequence of applications (10 seconds) of 20 μM MTSET in presence and absence of 10 μM dFBr was tested for a total time of 40 seconds. After each application ACh EC_{10} + 10 μM dFBr responses were tested for changes in the amplitude of the responses. As shown in Fig. 4.5A, 20 seconds of application of 20 μM MTSET (grey bar) was sufficient to reduce dFBr I_{max} to 50%. However, co-application of MTSET with dFBr (green bar) did not significantly change dFBr I_{max}, suggesting that dFBr protected α4L617C from reacting with MTSET by binding into the putative dFBr pocket. As shown in Fig. 4.5 the reaction rate of MTSET with α4L617C in the absence of dFBr was much faster (k1 0.05 ± 0.01 $M^{-1}s^{-1}$) than in the presence of dFBr (k1 0.004 ± 0.003 $M^{-1}s^{-1}$). These findings show that dFBr protects the free cysteine from reacting with MTSET, which would occur if dFBr bound the region to which α4L617 maps.

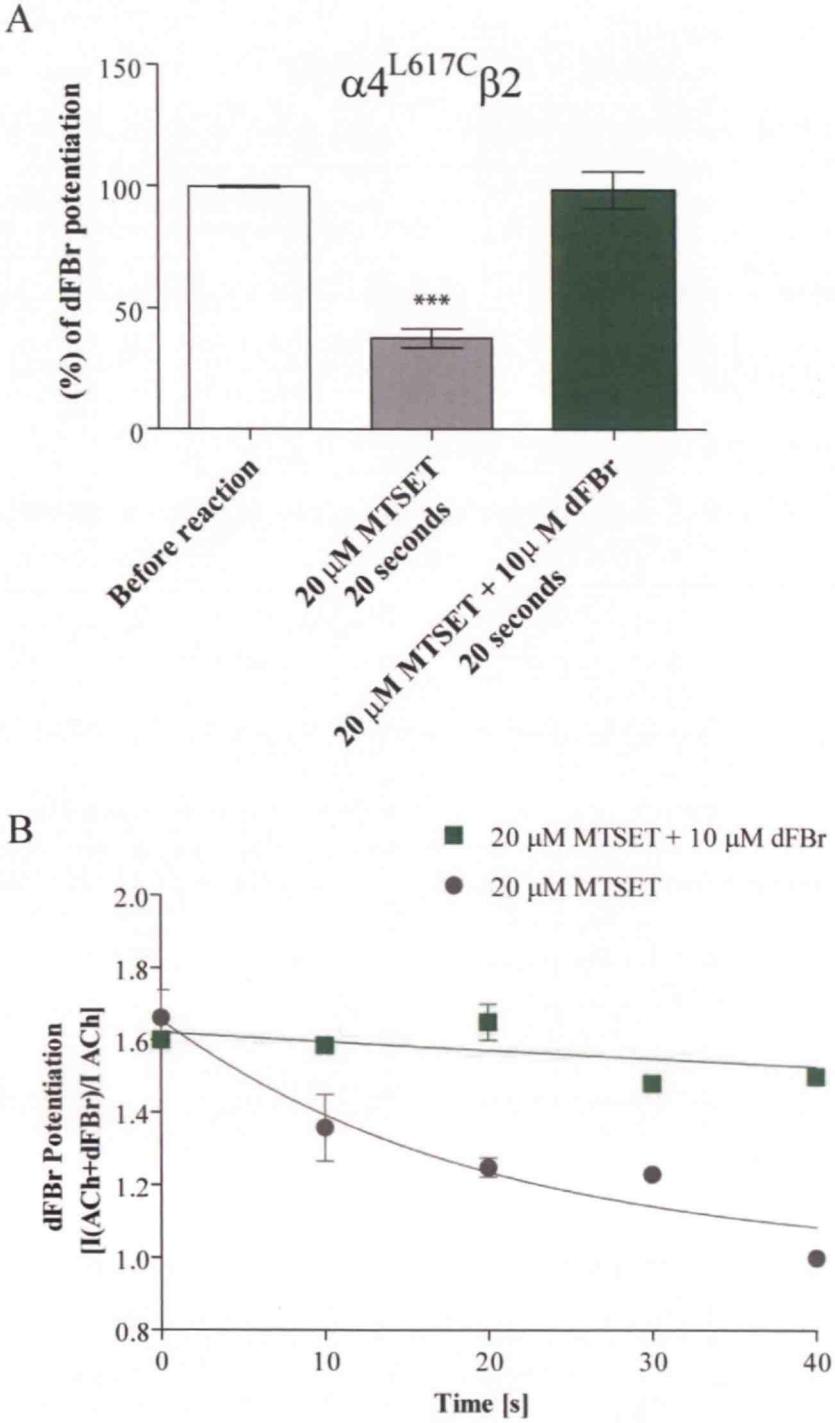

Figure. 4.5. Effect of low concentrations of MTSET in dFBr responses using Protection Assay with and without rates. A) Protection without rates in mutant $\alpha4^{L617C}\beta2$: histogram of % of potentiation elicited by dFBr before MTSET reaction (white), after 20 seconds of application of 20 μM of MTSET (grey) and after 20 seconds co-application of 20 μM MTSET and 10 μM dFBr (green). ***$p<0.01$ (ANOVA). B) Protection with rates in mutant $\alpha4^{L617C}\beta2$. Effects of additive applications (10 seconds each) of 20 μM MTSET in the potentiating effects of dFBr with (■) and without (●) co-application of 10 μM dFBr. Data represent the mean of two to five independent experiments. Data fitted to a One-phase decay plot. k1 values ± SEM: 0.004 ± 0.003 (■) and 0.05 ± 0.01 (●) $M^{-1}s^{-1}$.

4.2.3 The α4 subunit is necessary and sufficient for dFBr potentiation of α4β2 nAChRs.

The studies so far indicate that the potentiating effects of dFBr are mediated through a binding site in the TMD of the α4 subunit. However, the residues that may form the dFBr potentiating site are also conserved in the β2 subunit (Fig 4.6). To examine the possibility that the β2 subunit contributes to the potentiating effects of dFBr, the mutation F303A was introduced into the β2 subunit and the consequences of this mutation on dFBr potentiation were assayed as described in Chapter 2. β2F303 is equivalent to α4F312. Incorporation of β2F303A significantly decreased dFBr efficacy (I_{max}= 3.3 ± 0.31; $p < 0.05$; n = 3) with no changes in dFBr potency (EC_{50} = 2 (0.9-2,5) μM; n =3). In addition, β2F303A increased sensitivity to activation by ACh x 5.3 ($\alpha4\beta2^{F303A}$ ACh EC_{50} = 18.43 (11 – 26) μM). These effects are not consistent with the β2 subunit contributing to a potentiating binding site for dFBr but with disturbing the function of the α4β2 nAChR leading to an indirect effect on dFBr potentiation. Indeed, visual examination of the homology model of the TMD of the β2 subunit suggest that F303 maps to a crevice between M3 and M4 that appears noticeably smaller than the equivalent region in the α4 subunit (Fig. 4.6).

A

	TM3		TM4
α4 (309)	YLLFTMIFVTLSIVITVFVLNV	(601)	IFLWMF IIVCLLGTVG LFL
β2 (300)	YLMFTMVLVTFSIVTSVCVLNV	(461)	DRLFLW IFVFVCVFGT IGMF

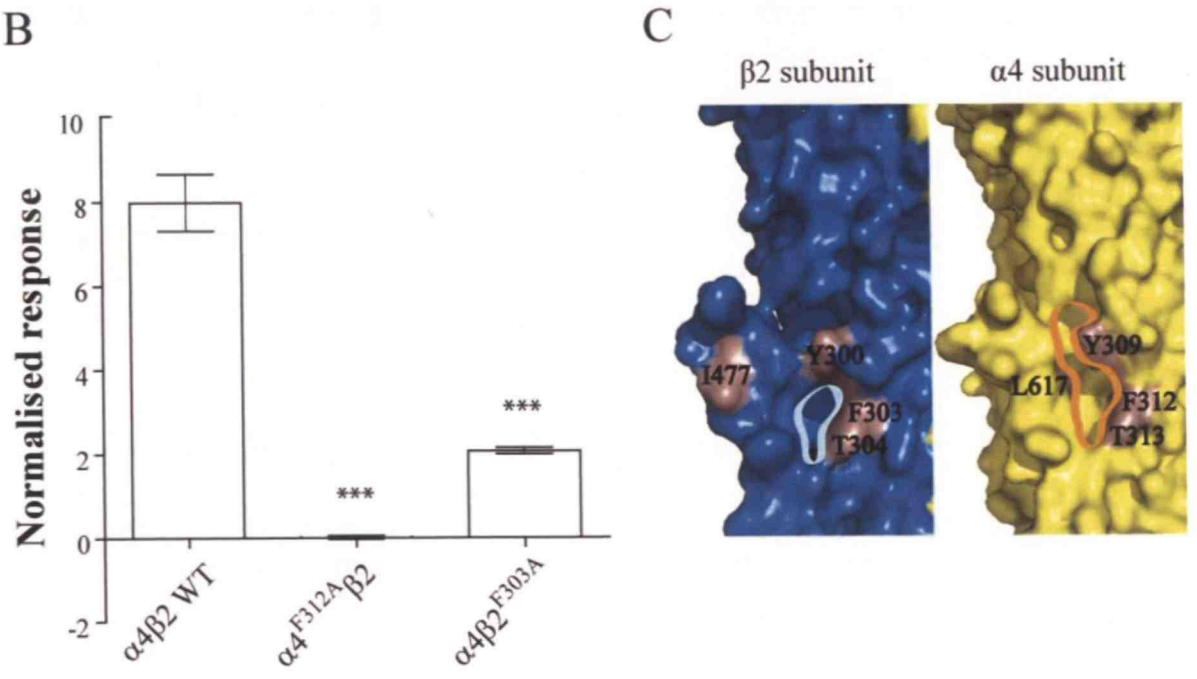

Figure. 4.6. Comparison of the conserved cavity hosting the putative binding site of dFBr in α4 and β2 subunits. In A, sequence alignment of M3 and M4 of both α4 and β2 subunits. Residues that form the crevice are highlighted in grey. In B, histogram of maximal potentiation elicited by dFBr in α4β2 wild type receptors and mutants $\alpha4^{F312A}\beta2$ and $\alpha4\beta2^{F303A}$. ***$p < 0.01$ (ANOVA). In C, Structure of the crevice of both β2 (Blue) and α4 subunits (Yellow), with important residues in M3 and M4 helices. Cavity size is demarked in clear blue for β2 subunit and orange for α4 subunit.

If the potentiating effects of dFBr on α4β2 nAChRs are dependent solely on the binding site housed by the TMD of the α4 subunit, then the number of α4 subunits bearing an intact TMD should influence the extent of dFBr potentiation of ACh responses. To test this possibility, the mutation α4F312A was incorporated into the α4 subunits of concatenated α4β2 nAChRs. For these studies, the mutant concatenated receptors studied were as follows: β2_α4_β2_α4_$\alpha4^{F312A}$, β2_$\alpha4^{F312A}$_β2_$\alpha4^{F312A}$_α4, β2_$\alpha4^{F312A}$_β2_$\alpha4^{F312A}$_$\alpha4^{F312A}$ in and β2_$\alpha4^{F312A}$_β2_$\alpha4^{F312A}$_β2.

The agonist binding sites at α4/β2 interfaces are located at the interface between the first β2 and second α4 subunits and between the third β2 and fourth α4 subunits of both concatemeric receptor (Mazzaferro et al., 2011). In the case of the β2_α4_β2_α4_α4 receptor, the signature third agonist site is located at the interface between the α4 subunit located in the fifth position of the concatenated receptor and the complementary face for this site is contributed by the α4 subunit in the fourth position (Mazzaferro et al., 2011).

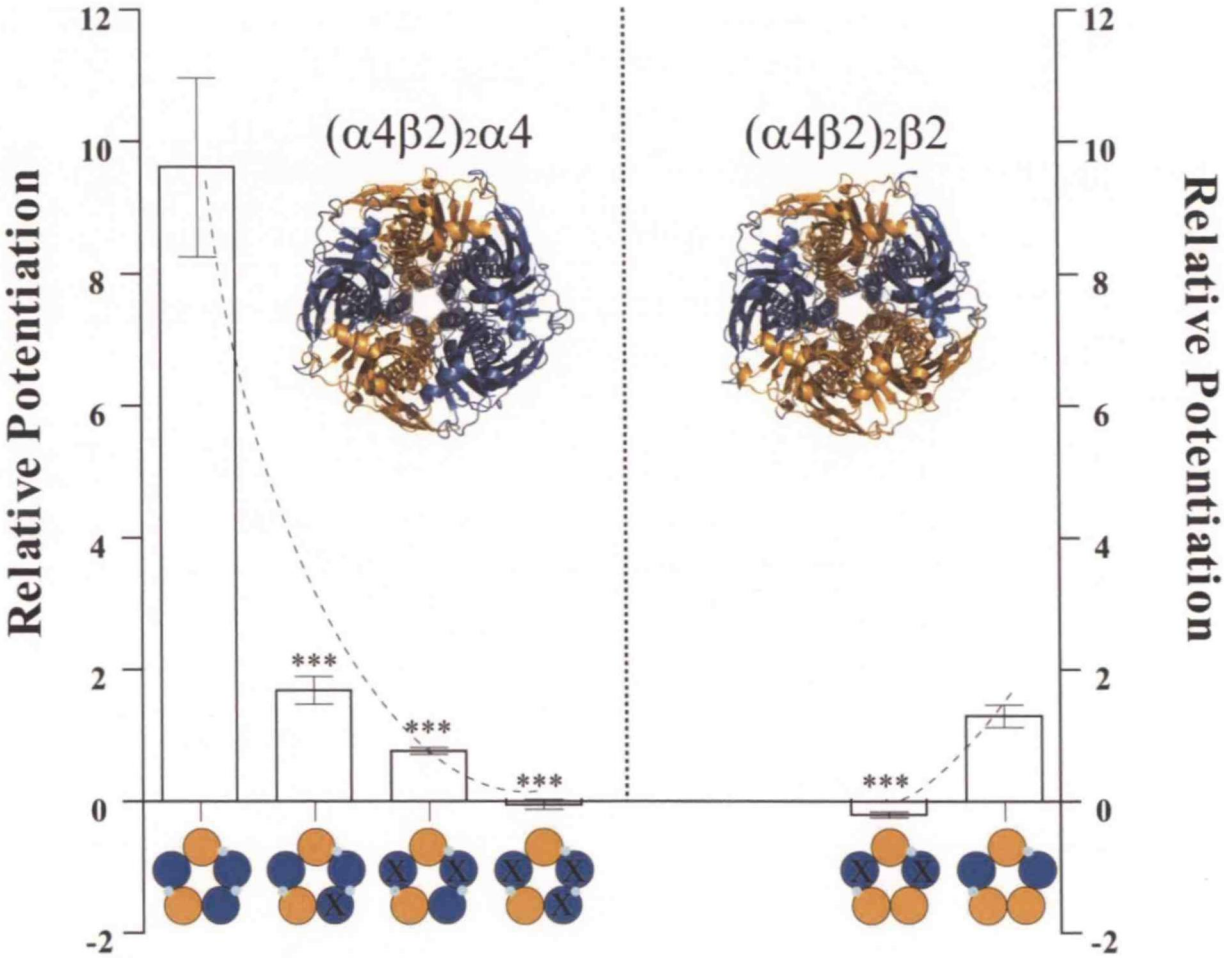

Figure. 4.7. Potentiation of concatenated α4β2 nAChRs is dependent on the number of α4 subunits. The potentiating efficacy of dFBr on wild type and concatenated α4β2 nAChRs was determined as described in the Methods Chapter. Histograms show the maximal potentiating effects of dFBr on wild type and mutant receptors. Values for β2_α4_β2_α4_α4 are shown on the left panels, whilst those for β2_α4_β2_α4_β2 receptors are shown on the right panel. Blue circles marked with an X represent α4F312A subunits. Values represent mean ± SEM of at least 3 independent experiments. Statistical differences were determined using Student's t-tests to compare responses of mutant receptors to each other and one-way analysis of variance to compare all mutant responses to control (wild type). *** $p < 0.001$.

As shown in Figure 4.7, the simultaneous incorporation of F312A mutation into all the α4 subunits of the β2_α4_β2_α4_β2 or β2_α4_β2_α4_α4 receptors completely abolished the potentiating effect of dFBr. However, when dFBr was applied to receptors with intact and mutant α4 subunits, the potentiating effect of dFBr was not fully abolished. Interestingly, in the case of β2_α4_β2_α4_α4 receptor, the subunit that contributes the principal component of the agonist binding site at the α4/α4 interface, appears to play a dominant role in the

potentiating effect of dFBr because the reduction of dFBr potentiation observed in β2_α4_β2_α4_α4^{F312A} was similar to that observed in β2_α4^{F312A}_β2_α4^{F312A}_α4 (Student's t-test). This finding further confirms the view that the agonist binding site at the α4/α4 interface plays a dominant role in determining the functional properties of the β2_α4_β2_α4_α4 receptor (Harpsøe et al., 2011; Mazzaferro et al., 2011; Mazzaferro et al., 2014).

4.3 Discussion

The main finding of the studies reported in this chapter is that a cavity between the top half of the M3 and M4 of the α4 nAChR subunit houses the potentiating binding site of dFBr in the α4β2 nAChR. α4F312, α4Y309 and α4L617 are all predicted to reside in close structural proximity to one another to all be able to bind dFBr, and they all influence dFBr potentiation in accord with a role in binding. These residues likely bind dFBr through hydrophobic interactions (α4F312 and α4L617) and hydrogen bonding (α4Y309) because when their capacity to engage in these types of interactions is impaired by mutagenesis, the sensitivity to potentiation by dFBr was either reduced (α4F312Y, α4L617C, α4L617A) or abolished (α4Y309A, α4Y309F, α4F312A) and these effects are not accompanied by changes in the sensitivity of the α4β2 nAChR to activation by ACh.

Although the residues implicated in the potentiating binding site of dFBr are mostly conserved in the β2 subunit (except for L617), it is the α4 subunit that endows the α4β2 nAChR sensitivity to potentiation by dFBr. Not only TMD α4 residues are critical for potentiation by dFBr, but the number of intact α4 subunits in α4β2 nAChRs determines the extent of potentiation by dFBr. Alanine substitution of β2F303, the residue equivalent to α4F312, decreased the extent of dFBr potentiation, but this effect was accompanied by an increase in sensitivity to ACh, indicating that the effects on dFBr potentiation likely reflect perturbations in receptor function due to structural changes in the β2 subunit. The cavity at the top half of the TMD of β2 is much smaller than the equivalent region in the α4 subunit, bringing the side chains of putative dFBr binding residues structurally closer to one another than in the α4 subunit and this proximity may not tolerate structural changes. The TMD of pLGICs play a pivotal role in gating, and structural integrity in some regions may be critically important for this function. Mutations introduced in this area are not well tolerated,

as suggested by the effects on ACh sensitivity, leading to functional changes. Although the β2 subunit does not contribute with the principal component of the agonist binding site or the agonist binding-gating pathway, each subunit in pLGICs provides structural features that when combined in the whole pLGICs have a functional implication. Examples relevant to this work are the contribution of M3 and M4 of individual subunits in the muscle nAChR to channel gating (Bouzat et al., 2002; De Rosa et al., 2002; Cadugan & Auerbach, 2007).

α4F316A, α4T313A and α4F606A affect potentiation by dFBr but their contribution is consistent with an indirect involvement, likely through their contribution to receptor function. This is likely to be the case of α4F316, a residue highly conserved in the α subunit of nAChR family. Single channel kinetics studies have shown that the mean open time of ACh-induced microscopic is affected by the type of residue present in this position (De Rosa et al., 2002; Cadugan & Auerbach, 2007). Thus, the effect of F316 on dFBr potentiation is likely due to its effects on receptor gating rather than on dFBr binding. Recently, photo-affinity labelling experiments of dFBr in *Torpedo* showed the compound strongly binds the ion channel pore, explaining the inhibitory effects of dFBr in this receptor type (Hamouda et al., 2015). Additionally, dFBr was found to bind both canonical and non-canonical interfaces at the ECD, sites that co-localises with the allosteric sites for physostigmine and galanthamine (Hamouda et al., 2013). The authors speculate these could allocate the potentiating site(s) for dFBr in α4β2 nAChRs. However, the latter is rather speculative since there is no functional data or mutagenesis to confirm it.

The cavity in the top-half of the TMD of pLGICs is a conserved hydrophobic region that houses a wide range of binding sites for modulatory compounds such as propofol (Nury et al., 2011; Ghosh et al., 2013; Jayakar et al., 2013; Sauguet et al., 2014), desfluran (Nury et al.,

2011) and bromoform (Sauguet et al., 2013). Interestingly, comparison of the propofol site in GlyRs and GluCl receptors indicate that the site is highly conserved, yet propofol potentiates GlyR but inhibits GluCl receptors (Ghosh et al., 2013; Jayakar et al., 2013). Furthermore, propofol effects on α4β2 nAChR, and indeed in all nAChRs studied so far, are inhibitory (Tassonyi et al., 2002) and recent work on the *Torpedo* nAChR using a photoreactive propofol analogue and radioligand competition assays showed that propofol binds to an intrasubunit cavity that is equivalent to that present in the bacterial pLGIC GLIC (Jayakar et al., 2013). This raises the question of whether the effector pathways of TMD allosteric modulators rather than their binding sites define the effects of this type of modulator compounds in pLGICs. This issue is explored in detail in Chapter 5 by comparing the effects of dFBr on α4β2 and α3β2 nAChRs.

CHAPTER 5

The C-terminal domain of the α4 subunit as a key determinant of the potentiating effects of dFBr on α4β2 nAChRs

5.1 Introduction

The findings of the previous Chapter are consistent with the presence of a potentiating binding site for dFBr in a cavity between the M3 and M4 regions of the α4 subunit. The residues that likely bind dFBr within this site are α4Y309, α4F312 and α4L617. Interestingly, however, with the exception of the α7 nAChR, these residues are conserved in all α nAChR subunits (Fig. 5.1). This raises the question of how dFBr enhances the agonist responses of only α4- or α2-containing nAChRs. Recent findings on the effects of propofol in GlyRs and nematode GluCl channels suggest that AMs can bind a conserved site across pLGICs and yet display functional diversity by differences in the transduction pathways linked to the binding site (Lynagh & Laube, 2014). Propofol acts as a NAM in cationic-selective receptors and GLIC, but it enhances the agonist responses at $GABA_A$Rs and GlyRs. Divergent experimental evidence has suggested that the potentiating effects is mediated by an inter-subunit cavity in the TMD of anionic pLGICs, whereas the inhibitory effects at cationic pLGICs are mediated by binding to an intra-subunit TMD site (Sauguet et al., 2014). However, recent work on homomeric GlyRs and *C. elegans* GluCl channels has shown that propofol allosterically inhibits GluCl channels and this inhibitory effect is mediated through binding to a TMD site that is the same site that mediates potentiation in GlyRs (Lynagh & Laube, 2014). Interestingly, the opposing effects can be reverted by a single point mutation in position 18' of the M2 segment.

If the C-terminal region (Post-M4 region) is considered in sequence alignments, important differences between the TMD of nAChR subunits are revealed. This segment varies in length and hydrophobicity, with only α4 and α2 subunits presenting an equivalent tail. Previous studies have proposed that the C-terminal region of α4β2 receptors hosts a binding site for

17β-estradiol (Paradiso et al., 2001; Curtis et al., 2002; Jin & Steinbach, 2011). This is not the case for the potentiating binding site of dFBr in α4β2 nAChRs, which is at the top half of a cavity between the M3 and M4 helices of the α4 subunit. However, visual inspection of homology models of the α4β2 nAChR shows the top of the M4 helix of the α4 subunit in structural proximity to the Cys loop, particularly to residues F167 and F170, and these residues map to an area of the Cys loop known to be important in gating (Lee et al., 2009) and studies of modulation of *Torpedo* nAChRs have suggested that interactions between the Cys loop and the C-terminal of the α1 subunit affect the ability of the Cys loop to communicate with the TMD, particularly M2-M3 (daCosta & Baenziger, 2009). Thus, it is tempting to speculate that the short, highly hydrophobic C-terminal of the α4 subunit may be part of the Cys loop – M4 interactions and that binding of dFBr to the TMD simply facilitates or enhances that interaction. This possibility was examined using functional mutagenesis in combination with chimeric receptors assembled from wild type β2 subunits and α subunits made of α4 and α3 subunits with exchanged C-terminal domains or α4 subunits lacking the C-terminal. The findings of these studies suggest the C-terminal of the α4 subunit as a critical part of the transduction pathway linked to the potentiating binding site of dFBr.

5.2 Results

5.2.1 Sequence conservation and dFBr effects in nAChRs.

In an attempt to explain the opposing effects of dFBr on nAChRs (potentiation of α4 or α2-containing receptors vs inhibition of all other nAChR, including the muscle receptor, α7 and α3-containing nAChRs (See Chapters 1 and 3 for key references), the primary sequences of the TMD (location of dFBr binding site) and loops of the ECD (e.g., β1- β2 loop, β6- β7 loop or Cys loop), that may affect the efficacy of dFBr (agonist binding-gating coupling regions) were aligned. Surprisingly, the residues that appear to contribute to the potentiating binding site in the α4 subunit are conserved in all nAChR subunits, except the α7 subunit that has a serine residue in the position equivalent to that occupied by a phenylalanine residue (F312) in the α4 subunit (Fig. 5.1). As shown in Figure 5.1, a triad of residues in the Cys loop are not conserved within α4 and α3 subunits: S/K, F/Y and Q/Y, respectively, although the sequence FPF that is crucial for Cys-loop-TMD interactions is conserved across the nAChR family. Interestingly, the top part of the M4 and the post-M4 region are highly variable, being almost identical only in the α4 and α2 subunits, raising the possibility that the structural determinants of the opposing effects of dFBr in the nAChR reside in this region.

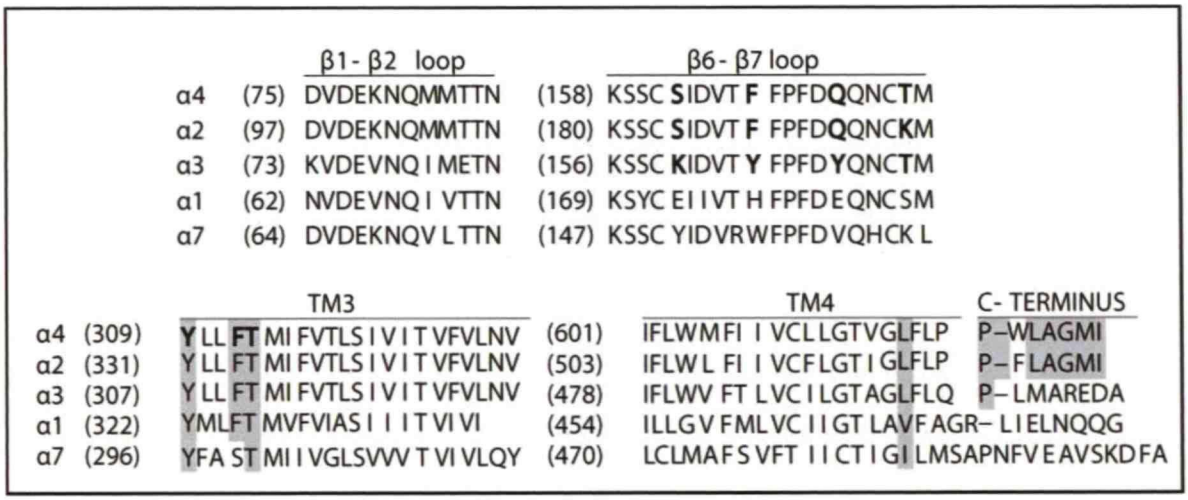

Figure 5.1. Pair-wise Sequence alignment of relevant loops and domains present across α subunits. On top: alignment of β1-β2 loop, β6-β7 loop (Cys loop). Bottom: TM3, TM4 and C-terminal domains. In bold, non-conserved residues. Highlighted in grey key residues for dFBr putative binding site in TM3 and conserved residues in C-terminal domain of α4, α2 and α3 subunits. Sequences were aligned using T-Coffee sequence alignment tool (Notredame et al., 2000).

5.2.2 Role of the C-terminal in the potentiating effects of dFBr in α4β2 nAChRs.

In order to test the possibility that the C-terminal of the α4 subunit may house determinants of the potentiating effects of dFBr, the effects of dFBr on α3β2 receptors assembled with α3 subunits with the α4 C-terminal, or vice versa, were assayed for dFBr potentiation. As shown in Figure 5.1, the α3 subunit has a 8-mer C-terminal tail of primary sequence PLMAREDA, whereas the α4 subunit has a slightly shorter (7-mer) and more hydrophobic tail with a primary sequence of PWLAGMI. As shown in Figure 5.2, α3β2 receptors are only inhibited by dFBr (IC_{50}= 118±16.4). Interestingly, the key residue F310 when mutated to alanine does affect sensitivity to inhibition by dFBr (IC_{50}= 77.9±9.9), suggesting that the region that binds dFBr in the α4 subunit is not involved in inhibition of α3β2 nAChRs. Additionally, just like in α4β2 nAChRs, inhibition of α3β2 nAChRs by dFBr is voltage-dependent, in accord with

channel blockade. Summary of results in Table 5.1, where negative EC_{50} values represent IC_{50} values for receptors only inhibited by dFBr.

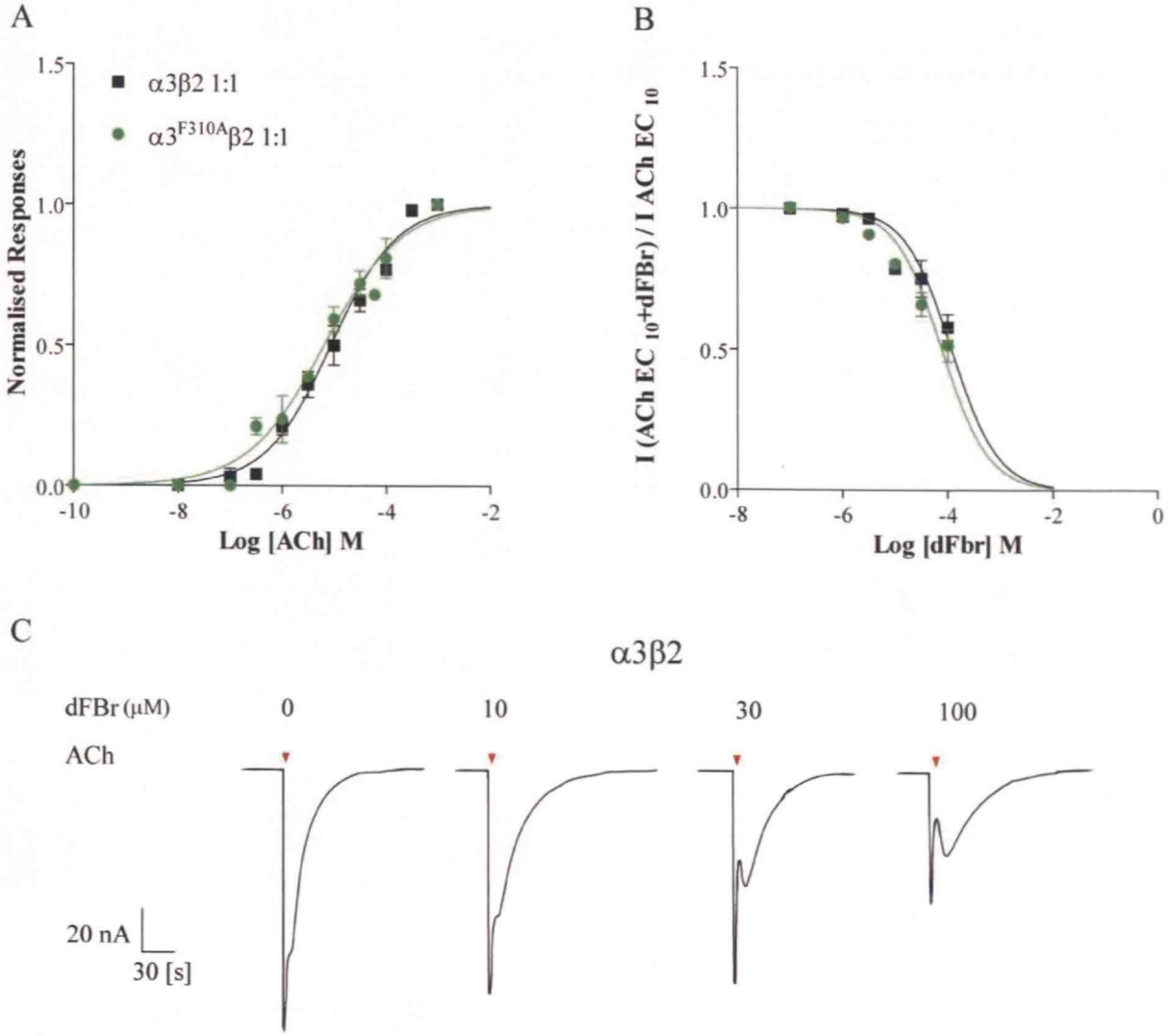

Figure. 5.2. ACh and dFBr concentration response curves for α3β2 wild type and $\alpha3^{F310A}\beta2$ receptors. In A: ACh CRC for α3β2 wild type (■) and $\alpha3^{F310A}\beta2$ (●). B: dFBr Inhibitory profile of α3β2 wild type (■) and $\alpha3^{F310A}\beta2$ (●). In C, representative traces of α3β2 receptors exposed to ACh EC_{10} and increasing concentrations of dFBr (μM). Red arrows (▼) indicate ACh applications.

Next, chimeric receptors containing exchangeable C-terminal tail of either α4 or α3 subunits were tested for sensitivity to potentiation by dFBr. These chimeras were made by substituting the C-tail of the α4 subunit of sequence PWLAGMI by that of the α3 subunit of sequence PLMAREDA ($\alpha4^{\alpha3CT}$) and vice versa to engineer $\alpha3^{\alpha4CT}$. An extra mutant receptor consisting

of a α4 subunit with a knocked out C-terminal was engineered as a control ($\alpha4^{-CT}$). Mutant subunits were co-expressed with wild type β2 subunits in *Xenopus* oocytes using 1:1 cDNA transfection ratios, as for wild type α4β2 or α3β2 nAChRs. All mutant receptors tested yielded functional expression.

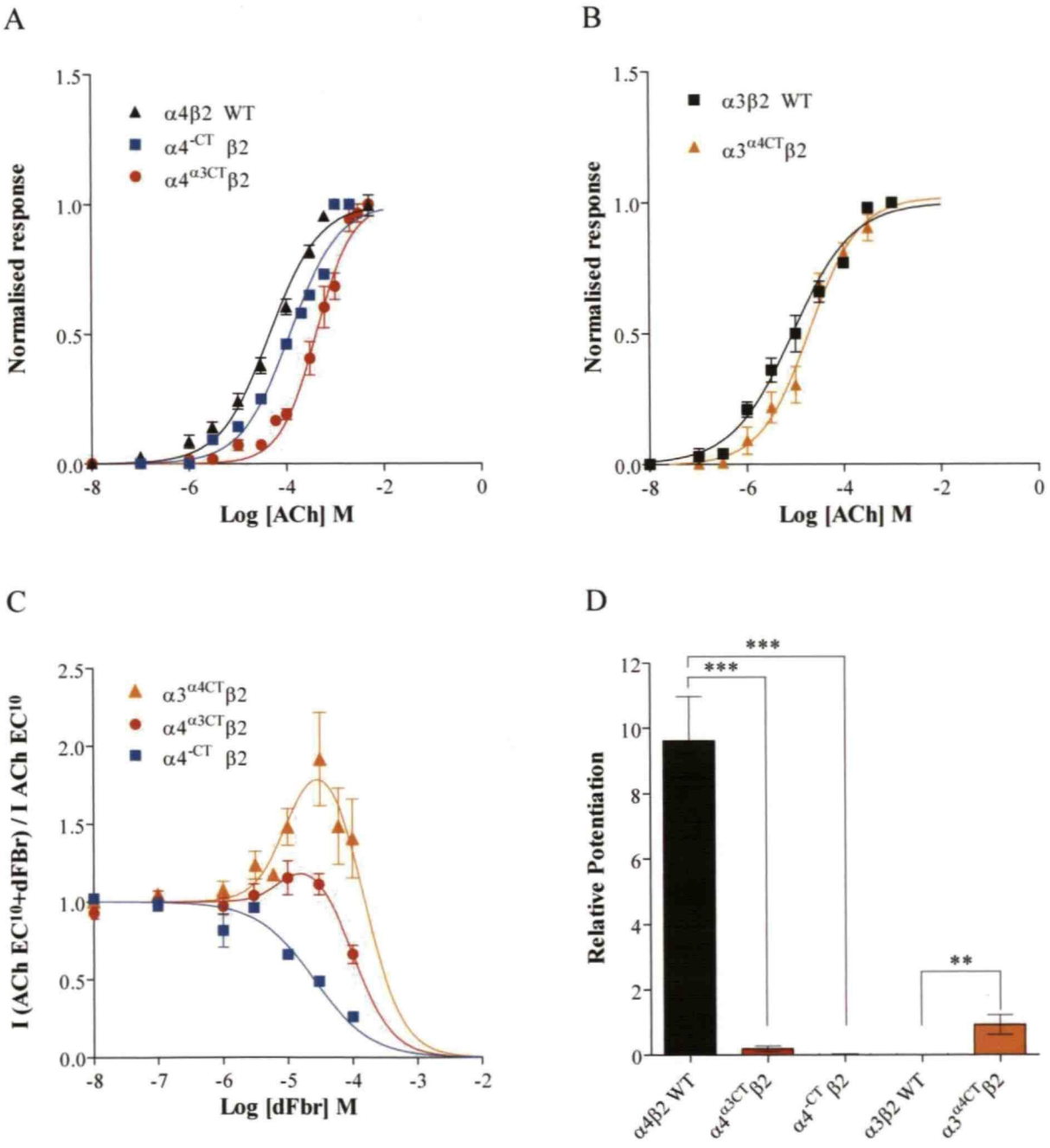

Figure 5.3. Pharmacological profile of α3* and α4* chimeric receptors. A) ACh concentration response curve from α4β2 wild type (▲), $\alpha4^{\alpha3CT}$ β2 (●) and $\alpha4^{-CT}$ β2 (■) receptors. B) ACh concentration response curve from α3β2 wild type (■) and $\alpha3^{\alpha4CT}$ β2 (▲)

receptors. C) dFBr concentration response curves of $\alpha4^{\alpha3CT}\beta2$ (●), $\alpha3^{\alpha4CT}\beta2$ (▲) and $\alpha4^{-CT}\beta2$ (■) chimeric receptors. D) Maximal dFBr potentiation of all wild type and chimeric α3β2 and α4β2 receptors. Relative potentiation represents normalized (I_{max}-1.0) from (I(ACh + dFBr)/ (IACh)). For $\alpha4^{\alpha3CT}\beta2$, $\alpha4^{-CT}\beta2$ and α4β2 receptors: ***p<0.004 (ANOVA). For $\alpha3^{\alpha4CT}\beta2$ and α3β2 receptors: **p<0.01 (t-test).

Table 5.1. Concentration effects of ACh and dFBr on mutant α4β2 and α3β2 nAChRs. EC_{50}, hill slope and I_{max} were estimated from ACh or dFBr, as appropriate, as described in Chapter 2. EC_{50} (95% CI) values represent the mean of 3-6 independent experiments I_{max} and Hill coefficient (nH) are expressed as the mean of 3-6 ± SEM. Statistical differences were determined using Student's t-tests or one way variance. * p < 0.05; **, p <0.001. IC_{50} values are represented as negative EC_{50} values (concentration of dFBr that elicits 50% of the inhibitory response).

Receptor	ACh		dFBr	
	EC_{50} (μM)	nH	EC_{50} (μM)	I_{max}
α4β2	97.99 (81-112)	0.94 ±0.07	1.62 (0.7-2.5)	10.6±2.1
$\alpha4^{-CT}\beta2$	118 (77-160)	0.9±0.11	-25.1** (15.9-34)	
$\alpha4^{\alpha3CT}\beta2$	599.9** (366-833)	0.97±0.16	8.5** (2.0-15)	1.2±0.083**
$\alpha4^{\alpha3CL}\beta2$	467** (399-535)	1.2±0.09	2.1 (1.5-2.8)	5.2±0.54*
$\alpha4^{\alpha3CT,CL}\beta2$	238** (197-280)	1.0±0.04	-124** (93-154)	
$\alpha4^{QPWLAGMI}\beta2$	133* (25-242)	0.63±0.08	8.2 (5.9-10.4)	1.3±0.02**
α3β2	12.8 (6.5-18. bvv9)	0.6±0.06	-118 (83.5-153)	

$\alpha3^{\alpha4CT}\beta2$	20* (10.3-28.6)	0.84±0.14	10.7 (6.9-14.4)	1.92±0.29**
$\alpha3^{PPWLAGMI}\beta2$	22* (18.6-24.9)	0.91±0.05	7.0** (5.7-8.4)	3.88±0.19**
$\alpha3^{F31OA}\beta2$	6.5 (4.0-9.0)	0.57±0.06	-77.9 (56.9-99)	
$\alpha3^{F31OA,PPWLAGMI}\beta2$	28.6* (20.0-37.1)	0.78±0.08	-72.1 (60.6-83.6)	
$\alpha3^{\alpha4CT,CL}\beta2$	13.9 (10.2-17.7)	0.74±0.05	8.4 (7.2-9.7)	2.5±0.11** (2.3-2.8)
$\alpha4^{F167A}\beta2$	142* (101-1200)	1.01±0.18	1.6 (1.1-8.6)	1.1 ±0.05**
$\alpha4^{F167Y}\beta2$	95 (82-110)	0.92±0.05	1.4 (0.3-2.5)	2.2±0.17 (1.82-2.6)
$\alpha4^{F170A}\beta2$	86 (32-223)	0.94±0.06	3.4 (2.4-4.7)	1.8±0.09 (1.63-2.0)
$\alpha4^{F170Y}\beta2$	97 (32-223)	0.99±0.08	1.6±0.48 (0.96-2.4)	5.63 ±0.07 (4.7-6.5)

Oocytes expressing $\alpha4^{-CT}\beta2$ receptors were not sensitive to potentiation by dFBr ($p < 0.001$; n =6), whereas $\alpha4^{\alpha3CT}$, whose α4 subunit has the C-tail of the α3 subunit retained sensitivity to potentiation by dFBr, although the efficacy of dFBr was reduced by 80% ($p < 0.001$; n = 5) (Fig. 5.3; CRC parameters summarised in Table 5.1). dFBr was a modest potentiator of $\alpha3^{\alpha4CT}\beta2$ receptors (I_{max} 1.92±0.083; $p < 0.001$; n = 4). ACh responses for all C-terminal mutant receptors are shifted to the right, suggesting that exchange or removal of the C-

terminal domain affects overall receptor function by reducing ACh sensitivity (Table 5.1).

So far, the findings of this part of the work suggest the C-tail of the α4 subunit as a contributor to sensitivity to potentiation by dFBr. Interestingly, just before the C-tail there is a double proline motif that is only present in the α4 and α2 subunits, both of which confer sensitivity to potentiation by dFBr. Thus, the sequence of the C-tail plus the pre-C-tail is PPWLAGMI in α4, whereas in the α3 subunit is QPLMAREDA. When the QPLMAREDA sequence in the α3 subunit was substituted by PPWLAGMI, the efficacy of dFBr potentiation was tripled in comparison to that on $\alpha3^{QPWLAGMI}\beta2$ nAChRs ($p < 0.001$; $n = 5$) (Fig. 5.4). The possible contribution of the double PP motif to potentiation by dFBr was first tested in α4β2 nAChRs. As shown in Fig. 5.4 replacing the PP motif for QP at the end of the M4 of the α4 subunit (α4QPWLAGMI) almost abolished potentiation by dFBr, as compared to wild type ($p < 0.001$; $n = 5$). The PP motif may affect the mobility of the C-tail such that the C-tail may bend over the top of the M4 segment creating a binding site for dFBr in the α3 subunit, as it has been proposed for the binding site of 17β-estradiol in α4 subunits (Paradiso et al., 2001). Alternatively, the C-tail, forced by the PP motif to remain in close proximity to the top of the M4 helix, may enhance the Cys loop-M4 interactions that govern coupling when dFBr binds its intra-subunit binding site. In the latter possibility, $\alpha3^{F310A,PPWLAGMI}\beta2$ nAChRs should not be sensitive to potentiation by dFBr because α3F310, the α3 residue equivalent to α4F312 is mutated to alanine. As shown in Fig 5.4B, potentiation of α3PPWLAGMI by dFBr was annulled by alanine substitution of F310 ($\alpha3^{F310A,\ PPWLAGMI}\beta2$).

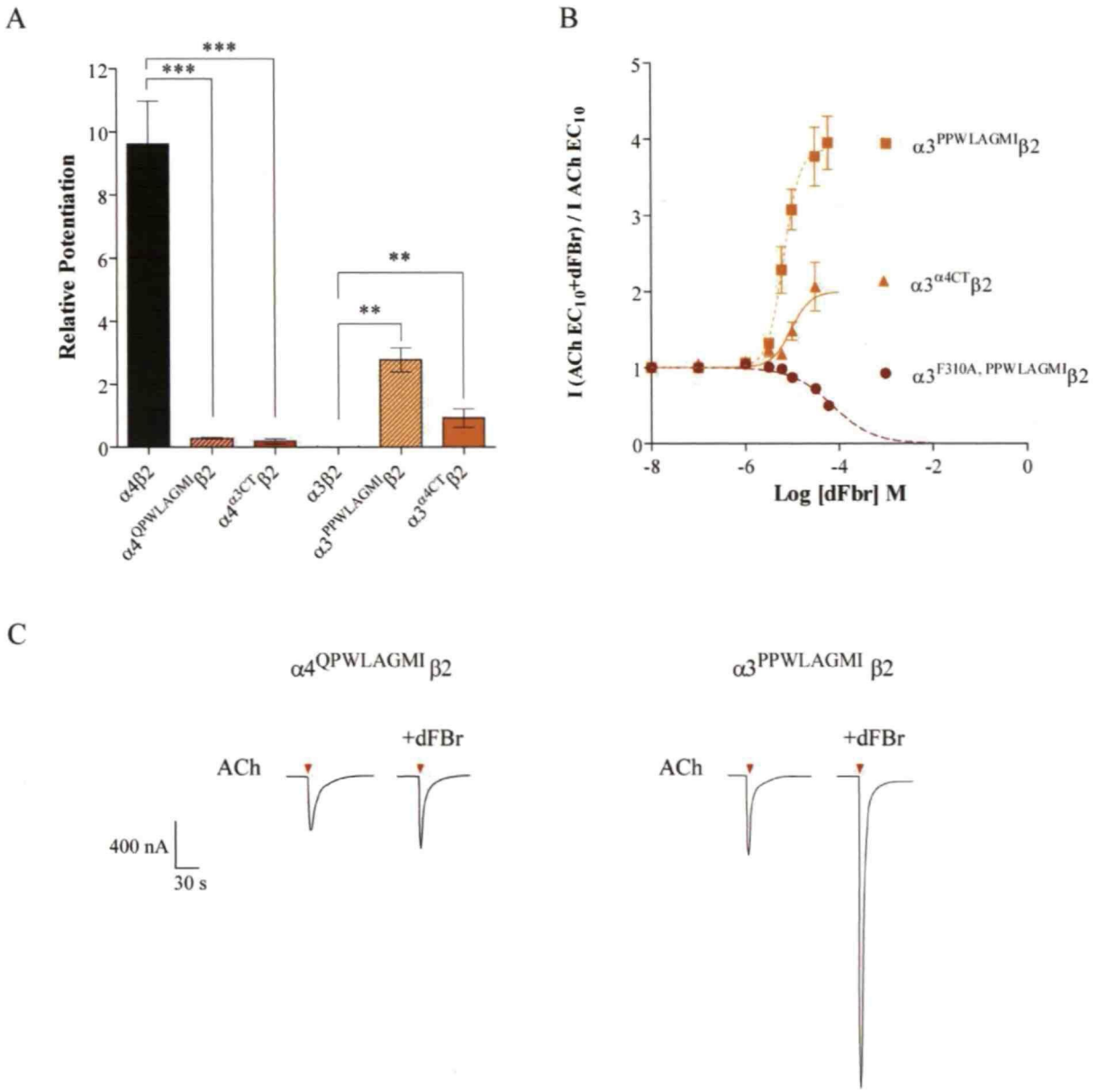

Figure 5.4. Changes in dFBr maximal potentiation by removal or introduction of a PP motif at the top of the M4 helix. A) Maximum potentiation of dFBr for α4β2, $\alpha4^{QPWLAGMI}\beta2$, $\alpha4^{\alpha3CT}\beta2$, α3β2, $\alpha3^{PPWLAGMI}\beta2$ and $\alpha3^{\alpha4CT}\beta2$ receptors: ***p<0.0001 (ANOVA) for α4* constructs and **p<0.01 (t-test) for α3* constructs. Relative potentiation represents normalized (I_{max}-1.0) from (I(ACh + dFBr)/ (IACh)). B) dFBr potentiation of $\alpha3^{PPWLAGMI}\beta2$ (■, dashed line), $\alpha3^{\alpha4CT}\beta2$ (▲)and $\alpha3^{F310A,PPWLAGMI}\beta2$ (●, dashed line) receptors. C) Representative traces of responses in presence and absence of dFBr for $\alpha4^{QPWLAGMI}\beta2$ and $\alpha3^{PPWLAGMI}\beta2$ receptors. Red arrows represent ACh applications (▼).

Single point mutations were performed by exchanging individual amino acids between α4 and α3 subunits (e.g. W to L or L to M) but the lack of dFBr sensitivity found when C-terminals were exchanged or knocked out was not found in those combinations (not shown), in agreement to the described effects of 17β-estradiol by Steinbach and colleagues (Paradiso et al., 2001; Jin & Steinbach, 2011). However, substitution of the last two residues (α4M626 and α4I627) for alanine or cysteine affected dFBr potentiation. In particular, mutants α4I627A, α4I627F and α4I627C significantly reduced dFBr potentiation, with α4I627A completely abolishing the responses. These results suggested this residue is responsible for the effects of C-terminal removal or exchange in α4 subunits (Fig. 5.5).

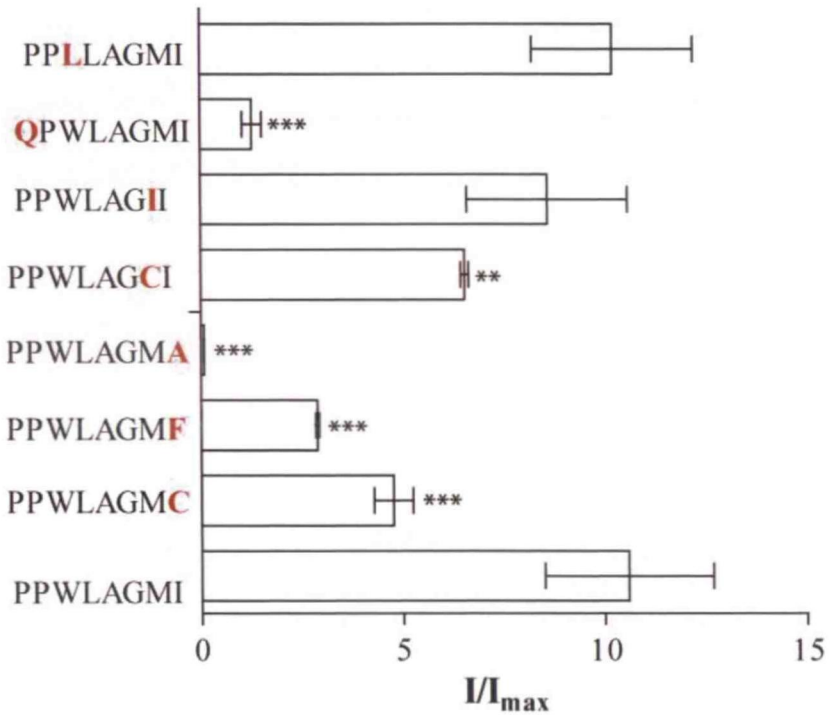

Figure 5.5. Effects of single point mutations in the C-terminal domain on potentiation by dFBr. Histogram of maximum potentiation (I/I_{max}) elicited by dFBr in a series of single amino acid substitutions in the C-terminal tail of α4 subunits. Statistical differences were determined by Student's t-test or one-way analysis of variance of at least 3 individual experiments. $^{**}p < 0.05$; $^{***}p < 0.01$ (ANOVA, compared to control PPWLAGMI).

To rule out the possibility of dFBr binding the C-terminal domain of α4 subunits we tested the effect of co-application of dFBr with 17β-estradiol in oocytes injected with α4β2 wild type receptors in 1:1 ratios. As shown in Figure 5.6, the effects of a co-application of dFBr and 17β-estradiol in the ACh currents are additive, suggesting both compounds elicit potentiating effects in α4β2 receptors via different mechanisms. Previous studies have shown that complete removal of the C-terminal domain of α4 subunits or exchange for that of a α3 subunit removes 17β-estradiol potentiation (Paradiso et al., 2001; Curtis et al., 2002; Jin & Steinbach, 2011), suggesting the molecule is binding this domain. However, all sources of evidence from the presence of this site come from mutagenesis. Additional assays, such as SCAM or Photo-affinity labelling would need to be performed in order to truly correlate this lack of function with the presence of a binding site. Nevertheless, changes in the structure of the C-terminal domain profoundly impair the PAM activity of both compounds, which led us to investigate the possibility of a signal transduction mechanism dependent on this region.

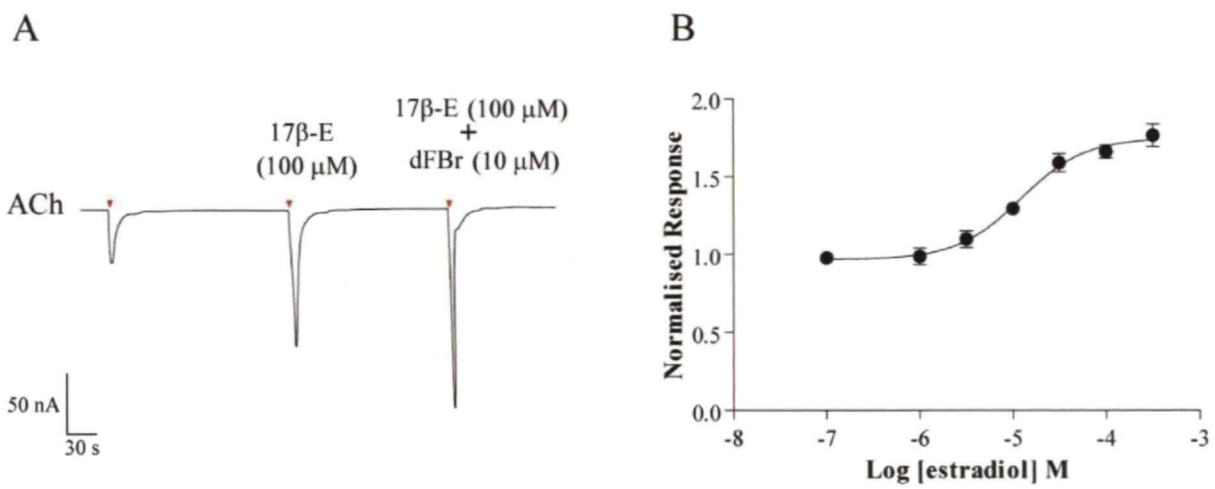

Figure. 5.6. Additive effects of dFBr and 17β-estradiol (17β-E) in α4β2 nAChRs. In A, representative traces of macroscopic currents of α4β2 wild type receptors elicited by EC_{50} ACh (▼) and EC_{50} ACh plus potentiating concentrations of 17β-E (100 μM) and dFBr (10 μM). Red arrows represent ACh applications (▼). In B, 17β-estradiol dose response curve on α4β2 wild type receptors expressed in 1:1 subunit ratios.

5.2.3 Transduction mechanism: C-terminal domain and Cys loop interaction.

As it has been previously described for $GABA_A$Rs and the *Torpedo* nAChR (Estrada-Mondragón et al., 2010; daCosta & Baenziger, 2009) one possible mechanism of signal transduction starting from the C-terminal domain could be a direct interaction with the Cys loop. In Figure 5.7 a close-up of the C-terminal domain and Cys loop of a α4 subunit from our α4β2 model. The short carboxyl domain is incomplete in all available crystal structures, which makes it difficult to understand how it orientates. Additionally the domain is not very conserved across nAChRs and pLGICs.

The Cys loop presents hydrophobic residues pointing outwards and its direction is likely determined by a proline residue (P169 in α4). Two phenylalanine residues seem to be pointing towards the C-terminal domain: F167 and F170. The residue F167 is a tyrosine in α3 subunits.

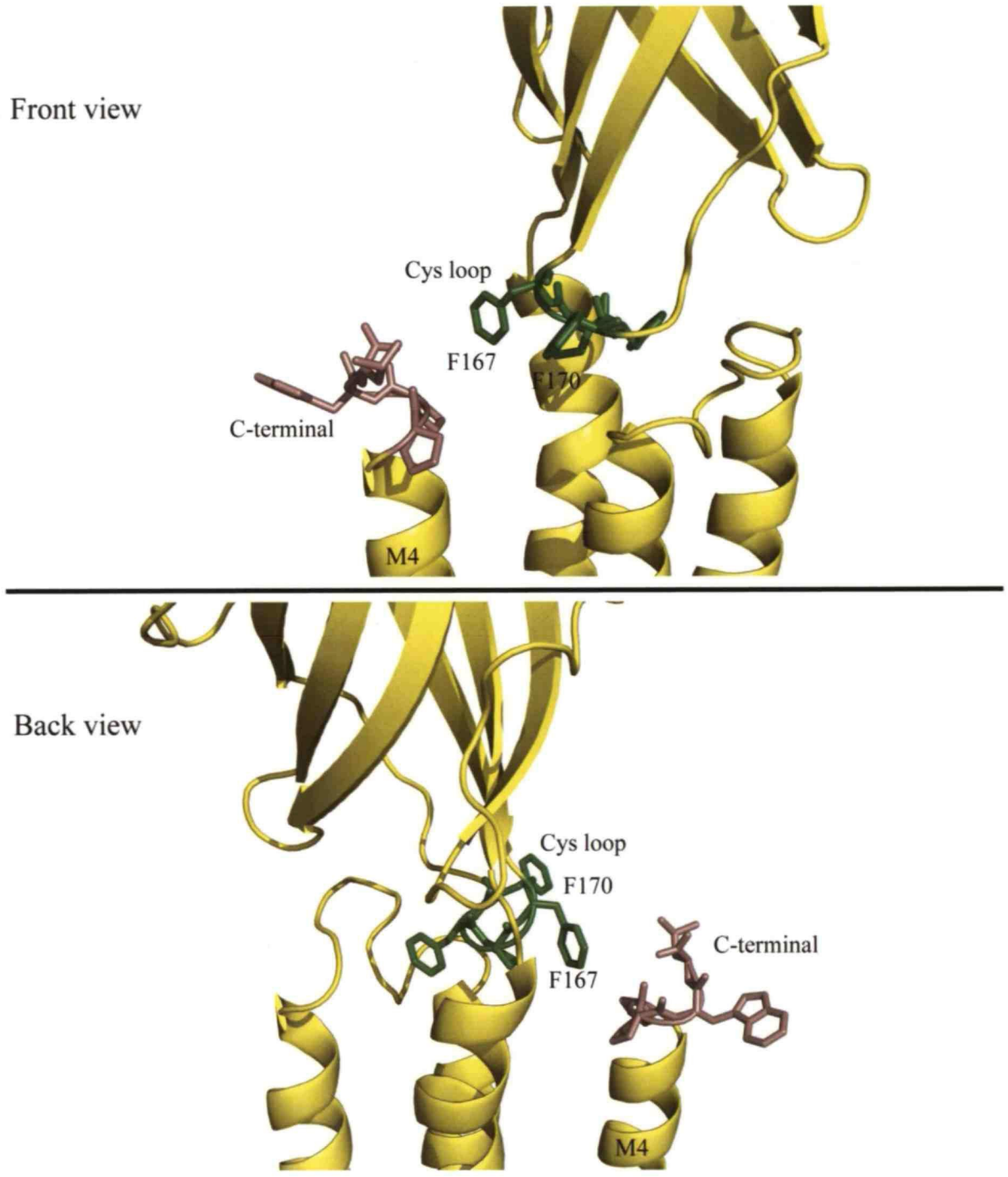

Figure 5.7. Structure of Cys loop and C-terminal domain of an α4 subunit (From α4β2 model adapted from X-ray structure 5-HT$_3$ receptor). Front and back view of Interface between Cys loop (green) and C-terminal domain (dark salmon) of an individual α4 subunit.

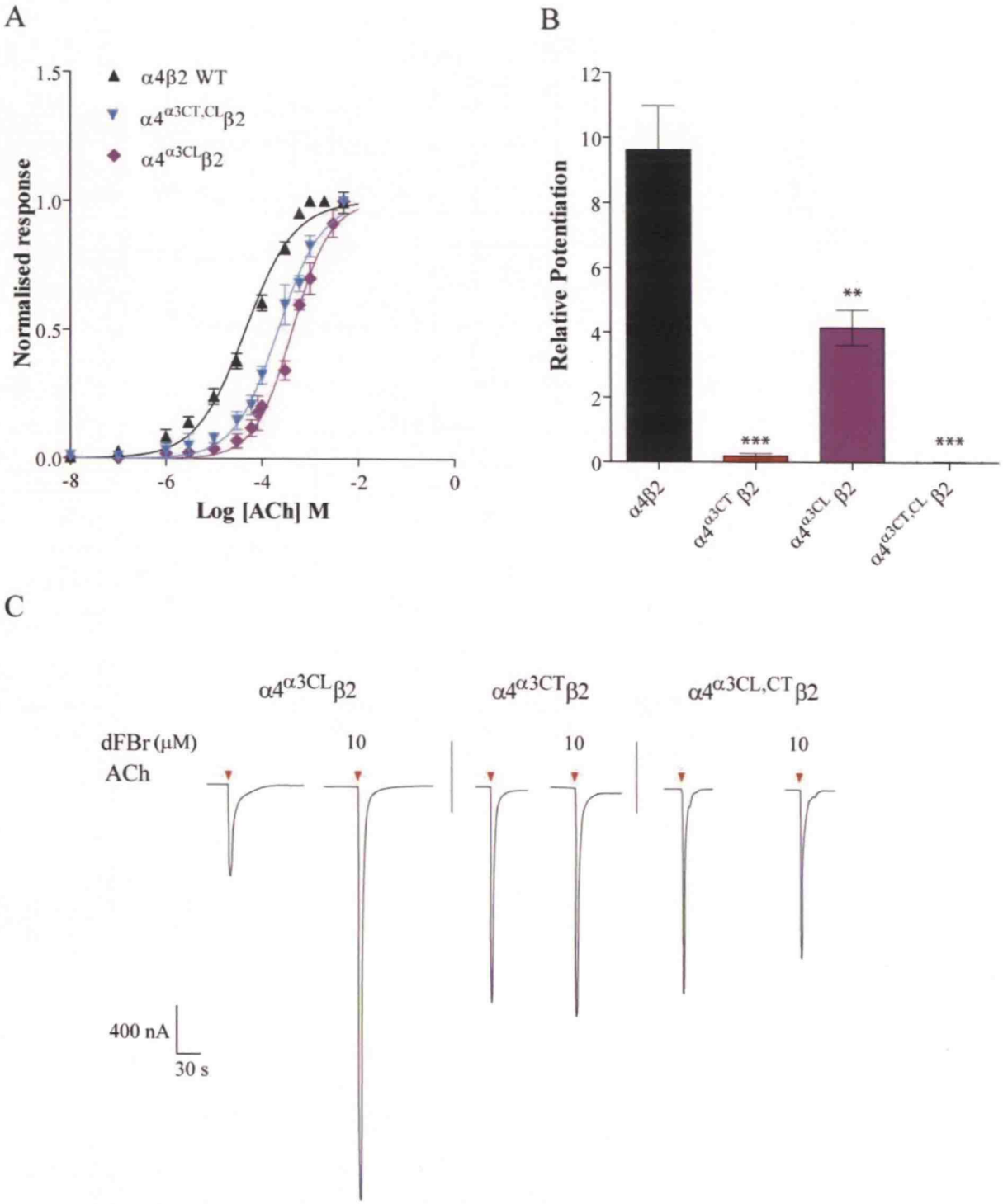

Figure 5.8. ACh and dFBr responses of α4β2 receptors with modified α3 Cys loop and C-terminal domain. A) ACh concentration response curves of α4β2 wild type (▲), the double chimera $\alpha4^{\alpha3CT,CL}\beta2$ (▼) and $\alpha4^{\alpha3CL}\beta2$ (♦) receptors. B) Maximum dFBr potentiation found in α4β2 (black), $\alpha4^{\alpha3CT}\beta2$ (Red), $\alpha4^{\alpha3CL}\beta2$ (Purple) and $\alpha4^{\alpha3CT,CL}\beta2$ receptors (Clear blue).**$p<0.05$, ***$p<0.0001$ (ANOVA). Relative potentiation represents normalized (I_{max}-1.0) from (I(ACh + dFBr)/ (IACh)) C) Representative traces of responses elicited by 10 μM dFBr in $\alpha4^{\alpha3CL}\beta2$, $\alpha4^{\alpha3CT}\beta2$ and $\alpha4^{\alpha3CT,CL}\beta2$ receptors. Red arrows represent ACh applications (▼).

To test if the Cys loop residues may be involved in sensitivity to potentiation, the Cys loop of the α4 subunit was exchanged by that of the α3 subunit ($\alpha4^{\alpha3CL}$) and in $\alpha4^{\alpha3CT}$ subunits ($\alpha4^{\alpha3CT,CL}$) and expressed in oocytes in 1:1 ratios with wild type β2 subunits.

As shown in Figure 5.8, incorporation of the α3 Cys loop reduces dFBr potentiation significantly ($p< 0.001$; $n = 4$), compared to wild type. Importantly the residual potentiation found in $\alpha4^{\alpha3CT}\beta2$ receptors ($I_{max}= 1.92\pm0.083$) was abolished in mutant $\alpha4^{\alpha3CT,CL}\beta2$ nAChR. This suggests a contribution of the Cys loop in the potentiation by dFBr, although the C-terminal domain seems to be more critical.

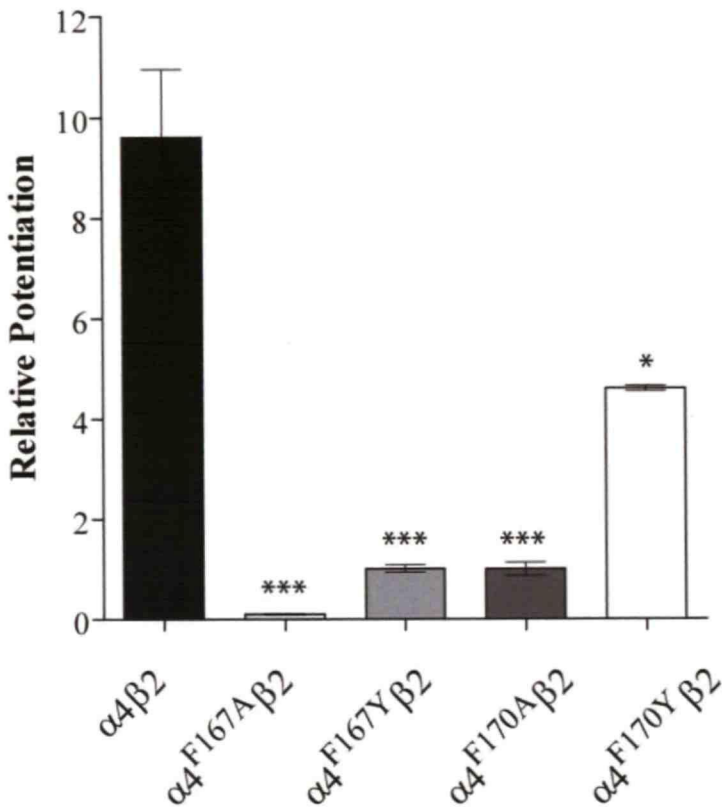

Figure 5.9. Relative potentiation of α4β2 wild type and Cys loop mutants. Histogram of maximum dFBr potentiation found in α4β2 wild type and single mutants of the FPFF motif of Cysloop: α4F167A, α4F167Y, α4F170A and α4F170Y.*$p<0.05$, ***$p<0.0001$ (ANOVA). Relative potentiation represents normalized (I_{max}-1.0) from (I(ACh + dFBr)/ (IACh)).

To examine the contribution of the single residues in Cys loop, a series of single point mutations exchanging F167 and the neighbouring F170 for alanine and tyrosine were performed and co-expressed with wild type β2 subunits in oocytes. As shown in Figure 5.9 (data summarised in Table 5.1), alanine or tyrosine substitutions of F167 or F170 significantly reduced the maximal levels of potentiation by dFBr.

5.3 Discussion

The main finding of this Chapter is that the C-terminal of the α4 subunit is implicated in sensitivity to potentiation by dFBr. Removal of the C-terminal region abolishes the potentiating effects of dFBr on α4β2 nAChRs and exchanging the C-terminal of the α3 for that of the α4 subunit confers sensitivity to potentiation by dFBr to α3β2 nAChRs.

The binding site for dFBr is not located in the C-terminal. Firstly, the ACh sensitivity of the α4β2 and α3β2 nAChRs is affected by changes in the C-terminal and functional mutagenesis in combination with SCAM studies and homology models strongly supported a cavity between the M3 and M4 helices of the α4 subunit as a potentiating binding site for dFBr. Secondly, alanine substitution of α3F310, the residue equivalent to α4F312, abolishes the potentiating effects of dFBr on $\alpha3^{PPWLAGMI}\beta2$ nAChRs, in accord with dFBr binding the TMD in α3PPWLAGMI subunit.

Furthermore, although previous studies using the α4β2 have suggested that the C-terminal of the α4 subunit houses the potentiating binding site of 17β-estradiol (Paradiso et al., 2001; Curtis et al., 2002; Jin & Steinbach, 2011), the additivity of the effects of dFBr and 17β-estradiol are in accord with these compounds binding distinct sites. This domain is thought to contain a binding site for 17β-estradiol. Our data shows that, even though the potentiating effects of dFBr are almost completely abolished by substitution or removal of the C-terminal domain, the effects of both compounds are additive. Indeed, structurally dFBr and 17β-estradiol are too dissimilar to share a common binding site. Additionally, our preliminary data suggests that mutations in TM3 that affect dFBr (F312) do not modify 17β-estradiol potentiation in α4β2 receptors (not shown).

What may the role of the C-terminal in dFBr potentiation of α4β2 nAChRs? The relatively more hydrophobic and short length of the C-terminal of the α4 subunit suggest that this region probably stays in close structural proximity to the top of the M4 segment. Such position is unlikely to be mobile due to the presence of the unique double proline motif right at the beginning of the C-tail. Structural studies of pLGICs show the M4 in close structural proximity to the Cys loop (Unwin, 2005; Unwin & Fujiyoshi, 2012; Hassaine et al., 2014; Miller & Aricescu, 2014; Barrantes, 2015) and it has been suggested that the M4-post M4 region of the α1 subunit may contribute to the transfer of lipid allosteric signals to the ECD via the Cys loop (daCosta & Baenziger, 2009). Thus, it is plausible that the C-tail of the α4 subunit form part of the M4-Cys loop interactions implicated in the coupling of agonist binding to gating and that binding of dFBr to the cavity between the M3 and M4 helices in the TMD of the α4 subunits enhance those interactions, probably by bringing the two regions closer through conformational transitions induced by dFBr binding (Fig. 5.7). This scenario is consistent with the effects of single point mutations of Cys loop residues in close structural proximity to the top end of the M4 helix. Thus, receptor-specific potentiating effects of dFBr reflect differences in the transduction pathway of the allosteric signals generated by binding of dFBr to a site that is highly conserved in the nAChR. The α3β2 is not sensitive to potentiation by dFBr because it lacks the structural apparatus to convey the allosteric signals of bound dFBr to the gate, not because of the absence of a binding site for dFBr.

CHAPTER 6

Final Discussion

Therapeutic strategies based on agonists of nAChRs are often prone to side effects owing to both high amino acid sequence identity and conservation of key structural features (e.g., agonist binding site and TMD) and the widespread distribution of the target nAChR receptor in the body. An advantage of a PAM of nAChRs over its native orthosteric activator (ACh) is that, in principle, greater selectivity can be achieved. PAMs would enhance the action of ACh but might have no effect of its own on the unoccupied receptor. Thus, the ACh or exogenous agonist effect, which might be insufficient in a particular disease state, might be magnified through allosteric modulation. The higher subtype selectivity commonly exerted by AMs, and the fact that the allosteric action is ideally coupled to the simultaneous presence of the endogenous ligand, both help to prevent over-dosage compared with the administration of a conventional, often nonselective, orthosteric agonist.

Interestingly, AMs in the pLGIC family often display opposing effects, depending on receptor type. For example, the general anaesthetic propofol enhances the agonist responses of $GABA_A$Rs and GlyRs (Zeller et al., 2008; Nguyen et al., 2009) but inhibits those of GLIC (Weng et al., 2010; Nury et al., 2011) and 5-HT_3Rs (Rüsch et al., 2007) and nAChRs (Flood et al., 1997). Functional mutagenesis (Krasowski et al., 1998), photo-labelling (Jayakar et al., 2013; Yip et al., 2013) and structural studies of bacterial and eukaryotic pLGICs have suggested that propofol binds an inter-subunit cavity in $GABA_A$Rs and GlyR (Nury et al., 2011; Sauguet et al., 2014) at a site overlapping that of the compound ivermectin in *C elegans* GluCl (Hibbs & Gouaux, 2011). In contrast, in pLGICs inhibited by propofol (GLIC, nAChRs, 5-HT_3Rs), propofol appears to bind an intra-subunit cavity located in the upper part of the TMD (Nury et al., 2010; Jayakar et al., 2013). Both the inter- and intra-subunit cavities are conserved across the pLGICs, but access to the inter-subunit site is restricted in cationic pLGICs and GLIC by the presence of a phenylalanine side in position 14' in M2 (Sauguet et

al., 2013). In pLGICs potentiated by propofol, there is a smaller residue at the equivalent position. Thus, this body of evidence supports the view that the opposing effects of AM on pLGICs are mediated through different binding sites. However, recent studies on the effect of propofol on homomeric human GlyRs and *C. elegans* GluCl channels, have suggested that propofol enhancement and inhibition are mediated by binding to a single site in anion-selective pLGICs, and that the-functional effects (enhancement vs inhibition) depends on a residue located far away from the binding site (M2 18' residue) (Lynagh & Laube, 2014). Thus, AM can exert opposing effects by binding different sites or by binding identical sites but which are linked to different effector systems. This thesis proposes that the opposing effects of dFBr α4- and non-α4 subunit containing nAChRs is due to a unique structural signature in the α4 subunit.

dFBr is a potent PAM of the α4β2 nAChR subtype, with a less efficacious effect in α2β2 receptors. In other nAChRs such as α7 and α3β2 dFBr acts as an inhibitor. At the commencement of this thesis, the binding site of this compound had not been identified. However, as described in Chapters 3, 4 and 5, functional mutagenesis driven largely by both visual examination of homology models of the α4β2 nAChR and docking stimulations provided strong evidence for the presence of a potentiating binding site at a cavity between M3 and M4 helices of the α4 subunit in the top-half part of the TMD. The findings of this thesis strongly suggest that the site is located at an intra-subunit cavity at the top half of the TMD of the α4 subunit. As previously mentioned, photo-labelling studies in *Torpedo* nAChRs published during the writing of this thesis, have shown that dFBr strongly binds a region within the ion channel (Hamouda et al., 2015), in accord with the ion channel blockade effects exerted by high μM concentrations (< than 60-100 μM). dFBr also appeared to bind canonical and non-canonical interfaces in the ECD, but as yet no functional evidence

that these binding is relate to potentiating or any other type of functional effects.

Sequence alignment revealed an important difference between α4 and α3 subunits in a region close to the TMD cavity that houses the potentiating binding site for dFBr. Functional mutagenesis as well as C-terminal-chimeric receptors or removal of the C-terminal demonstrated the importance of this region for the potentiating effects of dFBr. Yet, the presence of the α4 C-terminal does not confer *per se* sensitivity to potentiation by dFBr. An intact M3-M4 cavity is required for potentiation by dFBr and functional mutagenesis and SCAM-based studies strongly supported the TMD as the potentiating binding site for dFBr in α4β2 nAChRs.

What is the role of the C-terminus in dFBr potentiation? The C-terminal has been proposed as the binding site for 17β-estradiol (Paradiso et al., 2001). However, the data presented in Chapter 4 and 5 are not consistent with dFBr binding the C-terminal. Furthermore, the effects of dFBr and 17β-estradiol are additive, in accord with these compounds binding distinct sites. Rather than being a binding site, the C-terminal of the α4 subunit may be part of the effector machinery that translates binding of dFBr to the α4 subunit TMD into potentiation of the α4β2 nAChR. Visual examination of the region around the top-half of the TMD of the α4 subunit reveals that the top end of M4 is in close structural proximity to the Cys loop, and that residue F170 of the conserved (168)FPF(170) motif of the Cys loop orientates towards the top-end of M4. Residue F167 that flanks on the left of the FPF sequence also lies in structural proximity to the α4 subunit TMD, particularly the top half of the M3. Functional mutagenesis of F167 and F170 reveals the importance of these residues for the potentiating effects of dFBr. Interactions between the Cys loop and M4 are known to contribute to gating (For a recent review see Barrantes, 2015; see also DaCosta & Baenziger, 2009) so that one

can speculate that binding of dFBr to the TMD enhances those gating interactions. However, Cys loop-M4 interactions are not unique to the α4β2 nAChR (daCosta & Baenziger, 2009), hence they cannot account for the opposing effects of dFBr on α4β2 nAChRs and other nAChRs such as the α3β2 nAChR. Additionally and as previously mentioned it has been found that function of other PAMs like NS206 is affected by alanine substitution of residues of the Cys loop (Olsen et al., 2013), supporting the idea of a common transduction mechanism of allosteric modulation from a transmembrane binding site. Functional mutagenesis of the α4 subunit C-terminal is consistent with the last residue (I627) being part of the M4-Cys loop interactions that translate binding of dFBr into potentiation. Although more work needs to be carried out to establish whether the C-terminal is involved in gating and in the potentiating effects of dFBr, the data presented in this thesis support the view that the effector machinery of AM, not the binding site of AM, defines the functional diversity of AM binding to highly conserved regions of pLGICs, such as the TMD.

Overall, the data presented in this thesis is in accord with a transmembrane location for the binding site of dFBr and importantly revealed a novel mechanism of signal transduction in pLGICs. This thesis proposes that the conserved cavity in the TMD of the α4 subunit, when bound by dFBr, sends the allosteric binding signal through the C-terminal domain to the Cys loop and from there to the gate. The pathway from the Cys loop to the ion channel remains to be elucidated. Finally, because of the critical role of the C-terminal of the α4 subunit in 17β-estradiol potentiation of α4β2 nAChRs, suggest that both binding and effector structures may be shared, at least partially, by PAMs binding to the TMD of the α4 subunit. Further work needs to be done to clarify this issue. Nevertheless, the work presented in this thesis has provided strong evidence that the C-terminal segment of the M4 helix of the α4 subunit is a unique functional feature that defines the functional effects of dFBr on α4β2 nAChRs.

Acknowledgments

Firstly I would like to thank my supervisor Professor Isabel Bermudez, for her special dedication, patience and support during this 3-year period in her lab. She has been a crucial part of my development as a person and as a scientist and a truly inspiration for the future. Isabel has been my teacher in many aspects in the lab: she taught me all the fundamentals of molecular biology, how to load a gel, how to solder cables, how to dismantle a rig and put it back together, how to be scientifically critic, how to tolerate frustration and most importantly she taught me many lessons of resilience. Through all bitter and sweet moments during these 3 years all I have kept with me are the good memories of hard work, long talks, laughs, custard creams and passion for science. Thank you Isabel for teaching me the importance of hard work, persistence and loving what you do.

Thanks to all the present and past members of the Molecular Neuroscience lab: Stefano Micheloni, Elena Mantione, Nail Benallegue, Karina New, Alexandra Cuevas, Federica Gasparri, Simone Mazzaferro, Silvia Garcia Del Villar, Teresa Minguez, Dr. Jennina Taylor-Wells and Dr. Andrew Jones. Thanks for contributing to this work with positive feedback, ideas, experiments and support.

Thanks to Dr. Patricio Iturriaga for his contribution to the project and for the good moments shared outside the lab.

Thanks to Oxford Brookes University, the members of the Biological and Medical Sciences deparment and Nigel Groome for making possible something otherwise would have been just a dream.

Especially I would like to acknowledge my dearest friend Federica, whose support and true

friendship was essential in this process. Thanks for being there for me in all good and bad moments, always fixing everything with a hug, a good laugh and some delicious food. Thank you also for participating in the correction of this thesis.

Importantly, I would like to thank my students Merve Oncul, Teresa Giordano and Sophie Dubois-Viales. You were an essential piece of my development and I am really grateful I could share with you my passion for science.

I also would like to thank all the friends I met in Oxford, for taking an important part in this period of my life: Lenka, Pierre, Veronika, Mili, Anish, Paul, Alessandra, Gabrielle, Dario, Pietro, Elisa, Merve and Alex. Thanks to my Oxford-Chilean friends Tamara and Nicolas for the happy times doing "once", all the pole dancing and talking mathematics.

Thanks to all those people in Chile who supported me along the way, even in the distance: Valentina Sebastian, Gisela Canedo, Valerie Decap, Isabel Navarrete and Felipe Albornoz. Thanks to my supervisor Dr. Rodrigo Varas, for the many favours, constant support and your friendship. Thanks to Paolo Cevo for giving me the inspiration to become a scientist.

Thanks to my family for supporting my decision of going abroad and always being there for me: Evelyn, Karen, Guillermo, Hector, Pipe and Sole.

Especial thanks to my mother, who I owe all of my achievements, both academic and personal. Thank you for being the hard worker you are, for taking care of me, for teaching me that education is the key to success and that everything can be achieved with effort, passion and dedication. Thanks to my father and to my grandmother who sadly could not make it to see this thesis completed. Thanks to Tata and Lela, to my brothers Diego and Benjamin and

my sisters Catalina and Paola, for making me this cheesy sentimental person by simply always making me feel so loved.

Finally I would like to thank Simone, for all of his dedication, support and for being unconditional to me. You were an essential piece of the project, contributing with great ideas, feedback and good science. Thank you for being my best friend and make me become a better person every day.

Bibliography

Aidley DJ (1996) *Ion Channels: Molecules in Action*. Cambridge University Press

Albuquerque EX, Pereira EFR, Alkondon M and Rogers SW (2009) Mammalian nicotinic acetylcholine receptors: from structure to function. *Physiological reviews*. 89 (1), 73–120.

Althoff T, Hibbs RE, Banerjee S and Gouaux E (2014) X-ray structures of GluCl in apo states reveal a gating mechanism of Cys-loop receptors. *Nature*. 512 (7514), 333–337.

Alves LA, da Silva JHM, Ferreira DNM, Fidalgo-Neto AA, Teixeira PCN, de Souza CAM, Caffarena ER and de Freitas MS (2014) Structural and molecular modeling features of P2X receptors. *International journal of molecular sciences*. 15 (3), 4531–49.

Amin J, Brooks-Kayal A and Weiss DS (1997) Two tyrosine residues on the alpha subunit are crucial for benzodiazepine binding and allosteric modulation of gamma-aminobutyric acidA receptors. *Molecular pharmacology*. 51 (5), 833–41.

Andreasen JT, Nielsen EO and Redrobe JP (2009) Chronic oral nicotine increases brain [3H]epibatidine binding and responsiveness to antidepressant drugs, but not nicotine, in the mouse forced swim test. *Psychopharmacology*. 205 (3), 517–28.

Ashare RL and McKee SA (2012) Effects of varenicline and bupropion on cognitive processes among nicotine-deprived smokers. *Experimental and clinical psychopharmacology*. 20 (1), 63–70.

Auerbach A (2010) The gating isomerization of neuromuscular acetylcholine receptors. *The Journal of physiology*. 588 (Pt 4), 573–86.

Baier CJ, Fantini J and Barrantes FJ (2011) Disclosure of cholesterol recognition motifs in transmembrane domains of the human nicotinic acetylcholine receptor. *Scientific reports*. 1, 69.

Barrantes FJ (2015) Phylogenetic conservation of protein-lipid motifs in pentameric ligand-gated ion channels. *Biochimica et biophysica acta*. 1848 (9), 1796-805.

Beene DL, Price KL, Lester HA, Dougherty DA and Lummis SCR (2004) Tyrosine residues that control binding and gating in the 5-hydroxytryptamine3 receptor revealed by unnatural amino acid mutagenesis. *The Journal of neuroscience : the official journal of the Society for Neuroscience*. 24 (41), 9097–104.

Benallegue N, Mazzaferro S, Alcaino C and Bermudez I (2013) The additional ACh binding site at the α4(+)/α4(-) interface of the (α4β2)2α4 nicotinic ACh receptor contributes to desensitization. *British journal of pharmacology*. 170 (2), 304–16.

Bertrand D, Picard F, Le Hellard S, Weiland S, Favre I, Phillips H, Bertrand S, Berkovic SF, Malafosse A and Mulley J (2002) How mutations in the nAChRs can cause ADNFLE epilepsy. *Epilepsia*. 43 Suppl 5, 112–22.

Bertrand S, Weiland S, Berkovic SF, Steinlein OK and Bertrand D (1998) Properties of neuronal nicotinic acetylcholine receptor mutants from humans suffering from autosomal dominant nocturnal frontal lobe epilepsy. *British journal of pharmacology*. 125 (4), 751–60.

Bianchi MT and Macdonald RL (2001) Agonist Trapping by GABAA Receptor Channels. *The Journal of neuroscience : the official journal of the Society for Neuroscience*. 21 (23), 9083–91.

Billen B, Spurny R, Brams M, van Elk R, Valera-Kummer S, Yakel JL, Voets T, Bertrand D, Smit AB and Ulens C (2012) Molecular actions of smoking cessation drugs at α4β2 nicotinic receptors defined in crystal structures of a homologous binding protein. *Proceedings of the National Academy of Sciences of the United States of America*. 109 (23), 9173–8.

Blount P and Merlie JP (1989) Molecular basis of the two nonequivalent ligand binding sites of the muscle nicotinic acetylcholine receptor. *Neuron*. 3 (3), 349–57.

Bocquet N, Nury H, Baaden M, Le Poupon C, Changeux J-P, Delarue M and Corringer P-J (2009) X-ray structure of a pentameric ligand-gated ion channel in an apparently open conformation. *Nature*. 457 (7225), 111–4.

Bohler S, Gay S, Bertrand S, Corringer PJ, Edelstein SJ, Changeux JP and Bertrand D (2001) Desensitization of neuronal nicotinic acetylcholine receptors conferred by N-terminal segments of the beta 2 subunit. *Biochemistry*. 40 (7), 2066–74.

Bourne Y, Talley TT, Hansen SB, Taylor P and Marchot P (2005) Crystal structure of a Cbtx-AChBP complex reveals essential interactions between snake alpha-neurotoxins and nicotinic receptors. *The EMBO journal*. 24 (8), 1512–22.

Bouzat C, Gumilar F, del Carmen Esandi M and Sine SM (2002) Subunit-selective contribution to channel gating of the M4 domain of the nicotinic receptor. *Biophysical journal*. 82 (4), 1920–9.

Bouzat C, Gumilar F, Spitzmaul G, Wang H-L, Rayes D, Hansen SB, Taylor P and Sine SM (2004) Coupling of agonist binding to channel gating in an ACh-binding protein linked to an ion channel. *Nature*. 430 (7002), 896–900.

Brams M, Gay EA, Sáez JC, Guskov A, van Elk R, van der Schors RC, Peigneur S, Tytgat J, Strelkov S V, Smit AB, Yakel JL and Ulens C (2011) Crystal structures of a cysteine-modified mutant in loop D of acetylcholine-binding protein. *The Journal of biological chemistry*. 286 (6), 4420–8.

Brejc K, van Dijk WJ, Klaassen R V, Schuurmans M, van Der Oost J, Smit AB and Sixma TK (2001) Crystal structure of an ACh-binding protein reveals the ligand-binding domain of nicotinic receptors. *Nature*. 411 (6835), 269–76.

Bren N and Sine SM (1997) Identification of residues in the adult nicotinic acetylcholine receptor that confer selectivity for curariform antagonists. *The Journal of biological chemistry*. 272 (49), 30793–8.

Broad LM (2006) Identification and Pharmacological Profile of a New Class of Selective Nicotinic Acetylcholine Receptor Potentiators. *Journal of Pharmacology and Experimental Therapeutics*. 318 (3), 1108–1117.

Brown RWB, Collins AC, Lindstrom JM and Whiteaker P (2007) Nicotinic alpha5 subunit deletion locally reduces high-affinity agonist activation without altering nicotinic receptor numbers. *Journal of neurochemistry*. 103 (1), 204–15.

Buhr A, Schaerer MT, Baur R and Sigel E (1997) Residues at positions 206 and 209 of the alpha1 subunit of gamma-aminobutyric AcidA receptors influence affinities for benzodiazepine binding site ligands. *Molecular pharmacology*. 52 (4), 676–82.).

Bunders CA, Minvielle MJ, Worthington RJ, Ortiz M, Cavanagh J and Melander C (2011) Intercepting bacterial indole signaling with flustramine derivatives. *Journal of the American Chemical Society*. 133 (50), 20160–3.

Burzomato V, Beato M, Groot-Kormelink PJ, Colquhoun D and Sivilotti LG (2004) Single-channel behavior of heteromeric alpha1beta glycine receptors: an attempt to detect a conformational change before the channel opens. *The Journal of neuroscience : the official journal of the Society for Neuroscience*. 24 (48), 10924–40.

Cadugan DJ and Auerbach A (2007) Conformational dynamics of the alphaM3 transmembrane helix during acetylcholine receptor channel gating. *Biophysical journal*. 93 (3), 859–65.

Cahill K, Stead LF and Lancaster T (2008) Nicotine receptor partial agonists for smoking cessation. *The Cochrane database of systematic reviews*. (3), CD006103.

Cahill K, Stevens S, Perera R and Lancaster T (2013) Pharmacological interventions for smoking cessation: an overview and network meta-analysis. *The Cochrane database of systematic reviews*. 5, CD009329.

Carbone A-L, Moroni M, Groot-Kormelink P-J and Bermudez I (2009) Pentameric concatenated (alpha4)(2)(beta2)(3) and (alpha4)(3)(beta2)(2) nicotinic acetylcholine receptors: subunit arrangement determines functional expression. *British journal of pharmacology*. 156 (6), 970–81.

Cassels BK, Bermúdez I, Dajas F, Abin-Carriquiry JA and Wonnacott S (2005) From ligand design to therapeutic efficacy: the challenge for nicotinic receptor research. *Drug discovery today*. 10 (23-24), 1657–65.

Del Castillo J and Katz B (1957) Interaction at end-plate receptors between different choline derivatives. *Proceedings of the Royal Society of London. Series B, Biological sciences*. 146 (924), 369–81.

Celie PHN, Klaassen R V, van Rossum-Fikkert SE, van Elk R, van Nierop P, Smit AB and Sixma TK (2005) Crystal structure of acetylcholine-binding protein from Bulinus truncatus reveals the conserved structural scaffold and sites of variation in nicotinic acetylcholine receptors. *The Journal of biological chemistry*. 280 (28), 26457–66.

Celie PHN, van Rossum-Fikkert SE, van Dijk WJ, Brejc K, Smit AB and Sixma TK (2004) Nicotine and carbamylcholine binding to nicotinic acetylcholine receptors as studied in AChBP crystal structures. *Neuron*. 41 (6), 907–14.

Cesa LC, Higgins CA, Sando SR, Kuo DW and Levandoski MM (2012) Specificity determinants of allosteric modulation in the neuronal nicotinic acetylcholine receptor: a fine line between inhibition and potentiation. *Molecular pharmacology*. 81 (2), 239–49.

Chakrapani S and Auerbach A (2005) A speed limit for conformational change of an allosteric membrane protein. *Proceedings of the National Academy of Sciences of the United States of America*. 102 (1), 87–92.

Chakrapani S, Bailey TD and Auerbach A (2004) Gating dynamics of the acetylcholine receptor extracellular domain. *The Journal of general physiology*. 123 (4), 341–56.

Changeux J-P (2012) Allostery and the Monod-Wyman-Changeux model after 50 years. *Annual review of biophysics*. 41, 103–33.

Chavez-Noriega LE, Crona JH, Washburn MS, Urrutia A, Elliott KJ and Johnson EC (1997) Pharmacological characterization of recombinant human neuronal nicotinic acetylcholine receptors h alpha 2 beta 2, h alpha 2 beta 4, h alpha 3 beta 2, h alpha 3 beta 4, h alpha 4 beta 2, h alpha 4 beta 4 and h alpha 7 expressed in Xenopus oocytes. *The Journal of pharmacology and experimental therapeutics*. 280 (1), 346–56.

Chiara DC, Xie Y and Cohen JB (1999) Structure of the agonist-binding sites of the Torpedo nicotinic acetylcholine receptor: affinity-labeling and mutational analyses identify gamma Tyr-111/delta Arg-113 as antagonist affinity determinants. *Biochemistry*. 38 (20), 6689–98.

Colquhoun D and Lape R (2012) Perspectives on: conformational coupling in ion channels: allosteric coupling in ligand-gated ion channels. *The Journal of general physiology*. 140 (6), 599–612. Corringer PJ, Le Novère N and Changeux JP (2000) Nicotinic receptors at the amino acid level. *Annual review of pharmacology and toxicology*. 40, 431–58.

Covey LS, Glassman AH and Stetner F (1998) Cigarette smoking and major depression. *Journal of addictive diseases*. 17 (1), 35–46.

Curtis L, Buisson B, Bertrand S and Bertrand D (2002) Potentiation of human alpha4beta2 neuronal nicotinic acetylcholine receptor by estradiol. *Molecular pharmacology*. 61 (1), 127–35.

Cymes GD, Ni Y and Grosman C (2005) Probing ion-channel pores one proton at a time. *Nature*. 438 (7070), 975–80.

Czajkowski C and Karlin A (1995) Structure of the nicotinic receptor acetylcholine-binding site. Identification of acidic residues in the delta subunit within 0.9 nm of the 5 alpha subunit-binding. *The Journal of biological chemistry*. 270 (7), 3160–4.

d'Incamps BL and Ascher P (2014) High affinity and low affinity heteromeric nicotinic acetylcholine receptors at central synapses. *The Journal of physiology*. 592, 4131-6.

daCosta CJB and Baenziger JE (2009) A lipid-dependent uncoupled conformation of the acetylcholine receptor. *The Journal of biological chemistry*. 284 (26), 17819–25.

daCosta CJB, Free CR, Corradi J, Bouzat C and Sine SM (2011) Single-channel and structural foundations of neuronal α7 acetylcholine receptor potentiation. *The Journal of neuroscience : the official journal of the Society for Neuroscience*. 31 (39), 13870–9.

daCosta CJB and Sine SM (2013) Stoichiometry for drug potentiation of a pentameric ion channel. *Proceedings of the National Academy of Sciences of the United States of America*. 110 (16), 6595–600.

Daly JW, Garraffo HM, Spande TF, Decker MW, Sullivan JP and Williams M (2000) Alkaloids from frog skin: the discovery of epibatidine and the potential for developing novel non-opioid analgesics. *Natural product reports*. 17 (2), 131–5.

Dani J a and Bertrand D (2007) Nicotinic acetylcholine receptors and nicotinic cholinergic mechanisms of the central nervous system. *Annual review of pharmacology and toxicology*. 47, 699–729.

Dellisanti CD, Yao Y, Stroud JC, Wang Z-Z and Chen L (2007) Crystal structure of the extracellular domain of nAChR alpha1 bound to alpha-bungarotoxin at 1.94 A resolution. *Nature neuroscience*. 10 (8), 953–62.

Duncalfe LL, Carpenter MR, Smillie LB, Martin IL and Dunn SM (1996) The major site of photoaffinity labeling of the gamma-aminobutyric acid type A receptor by [3H]flunitrazepam is histidine 102 of the alpha subunit. *The Journal of biological chemistry*. 271 (16), 9209–14.

Duret G, Van Renterghem C, Weng Y, Prevost M, Moraga-Cid G, Huon C, Sonner JM and Corringer P-J (2011) Functional prokaryotic-eukaryotic chimera from the pentameric ligand-gated ion channel family. *Proceedings of the National Academy of Sciences of the United States of America*. 108 (29), 12143–8.

Estrada-Mondragón A, Reyes-Ruiz JM, Martínez-Torres A and Miledi R (2010) Structure-function study of the fourth transmembrane segment of the GABAρ1 receptor. *Proceedings of the National Academy of Sciences of the United States of America*. 107 (41), 17780–4.

Fedorov NB, Benson LC, Graef J, Lippiello PM and Bencherif M (2009) Differential pharmacologies of mecamylamine enantiomers: positive allosteric modulation and noncompetitive inhibition. *The Journal of pharmacology and experimental therapeutics*. 328 (2), 525–32.

Flood P, Ramirez-Latorre J and Role L (1997) Alpha 4 beta 2 neuronal nicotinic acetylcholine receptors in the central nervous system are inhibited by isoflurane and propofol, but alpha 7-type nicotinic acetylcholine receptors are unaffected. *Anesthesiology*. 86 (4), 859–65.

Forman SA and Miller KW (2011) Anesthetic sites and allosteric mechanisms of action on Cys-loop ligand-gated ion channels. *Canadian journal of anaesthesia = Journal canadien d'anesthésie*. 58 (2), 191–205.

Frahm S, Ślimak MA, Ferrarese L, Santos-Torres J, Antolin-Fontes B, Auer S, Filkin S, Pons S, Fontaine J-F, Tsetlin V, Maskos U and Ibañez-Tallon I (2011) Aversion to Nicotine Is Regulated by the Balanced Activity of β4 and α5 Nicotinic Receptor Subunits in the Medial Habenula. *Neuron*. 70 (3), 522–535.

Fucile S (2004) Ca2+ permeability of nicotinic acetylcholine receptors. *Cell calcium*. 35 (1), 1–8.

Galzi JL, Devillers-Thiéry A, Hussy N, Bertrand S, Changeux JP and Bertrand D (1992) Mutations in the channel domain of a neuronal nicotinic receptor convert ion selectivity from cationic to anionic. *Nature*. 359 (6395), 500–5.

Gay EA and Yakel JL (2007) Gating of nicotinic ACh receptors; new insights into structural transitions triggered by agonist binding that induce channel opening. *The Journal of physiology*. 584 (Pt 3), 727–33.

George AA, Lucero LM, Damaj MI, Lukas RJ, Chen X and Whiteaker P (2012) Function of human α3β4α5 nicotinic acetylcholine receptors is reduced by the α5(D398N) variant. *The Journal of biological chemistry*. 287 (30), 25151–62.

Ghosh B, Satyshur KA and Czajkowski C (2013) Propofol binding to the resting state of the gloeobacter violaceus ligand-gated ion channel (GLIC) induces structural changes in the inter- and intrasubunit transmembrane domain (TMD) cavities. *The Journal of biological chemistry*. 288 (24), 17420–31.

Gill JK, Savolainen M, Young GT, Zwart R, Sher E and Millar NS (2011) Agonist activation of alpha7 nicotinic acetylcholine receptors via an allosteric transmembrane site. *Proceedings of the National Academy of Sciences of the United States of America*. 108 (14), 5867–72.

Giniatullin R, Nistri A and Yakel JL (2005) Desensitization of nicotinic ACh receptors: shaping cholinergic signaling. *Trends in neurosciences*. 28 (7), 371–8.

Gonzalez-Gutierrez G and Grosman C (2010) Bridging the gap between structural models of nicotinic receptor superfamily ion channels and their corresponding functional states. *Journal of molecular biology*. 403 (5), 693–705.

Gotti C, Clementi F, Fornari A, Gaimarri A, Guiducci S, Manfredi I, Moretti M, Pedrazzi P, Pucci L and Zoli M (2009) Structural and functional diversity of native brain neuronal nicotinic receptors. *Biochemical pharmacology*. 78 (7), 703–11.

Gotti C, Moretti M, Gaimarri A, Zanardi A, Clementi F and Zoli M (2007) Heterogeneity and complexity of native brain nicotinic receptors. *Biochemical pharmacology*. 74 (8), 1102–11.

Gotti C, Zoli M and Clementi F (2006) Brain nicotinic acetylcholine receptors: native subtypes and their relevance. *Trends in pharmacological sciences*. 27 (9), 482–91.

Grady SR, Moretti M, Zoli M, Marks MJ, Zanardi A, Pucci L, Clementi F and Gotti C (2009) Rodent habenulo-interpeduncular pathway expresses a large variety of uncommon nAChR subtypes, but only the alpha3beta4* and alpha3beta3beta4* subtypes mediate acetylcholine release. *The Journal of neuroscience : the official journal of the Society for Neuroscience*. 29 (7), 2272–82.

Grady SR, Salminen O, McIntosh JM, Marks MJ and Collins AC (2010) Mouse striatal dopamine nerve terminals express alpha4alpha5beta2 and two stoichiometric forms of alpha4beta2*-nicotinic acetylcholine receptors. *Journal of molecular neuroscience : MN*. 40 (1-2), 91–5.

Grosman C, Zhou M and Auerbach A (2000) Mapping the conformational wave of acetylcholine receptor channel gating. *Nature*. 403 (6771), 773–6.

Grupe M, Paolone G, Jensen AA, Sandager-Nielsen K, Sarter M and Grunnet M (2013) Selective potentiation of (α4)3(β2)2 nicotinic acetylcholine receptors augments amplitudes of prefrontal acetylcholine- and nicotine-evoked glutamatergic transients in rats. *Biochemical pharmacology*. 86 (10), 1487–96.

Hamouda AK, Kimm T and Cohen JB (2013) Physostigmine and galanthamine bind in the presence of agonist at the canonical and noncanonical subunit interfaces of a nicotinic acetylcholine receptor. *The Journal of neuroscience : the official journal of the Society for Neuroscience*. 33 (2), 485–94.

Hamouda AK, Wang Z-J, Stewart DA, Jain AD, Glennon RA and Cohen JB (2015) Desformylflustrabromine (dFBr) and [3H]dFBr-labeled Binding Sites in a Nicotinic Acetylcholine Receptor. *Molecular pharmacology*. 88 (1), 1-11.

Han S, Yang B-Z, Kranzler HR, Oslin D, Anton R and Gelernter J (2011) Association of CHRNA4 polymorphisms with smoking behavior in two populations. *American Journal of Medical Genetics Part B: Neuropsychiatric Genetics*. 156 (4), 421–429.

Han Z-Y, Zoli M, Cardona A, Bourgeois J-P, Changeux J-P and Le Novère N (2003) Localization of [3H]nicotine, [3H]cytisine, [3H]epibatidine, and [125I]alpha-bungarotoxin binding sites in the brain of Macaca mulatta. *The Journal of comparative neurology*. 461 (1), 49–60.

Hansen SB, Sulzenbacher G, Huxford T, Marchot P, Taylor P and Bourne Y (2005) Structures of Aplysia AChBP complexes with nicotinic agonists and antagonists reveal distinctive binding interfaces and conformations. *The EMBO journal*. 24 (20), 3635–46.

Hansen SB and Taylor P (2007) Galanthamine and non-competitive inhibitor binding to ACh-binding protein: evidence for a binding site on non-alpha-subunit interfaces of

heteromeric neuronal nicotinic receptors. *Journal of molecular biology*. 369 (4), 895–901.

Harpsøe K, Ahring PK, Christensen JK, Jensen ML, Peters D and Balle T (2011) Unraveling the high- and low-sensitivity agonist responses of nicotinic acetylcholine receptors. *The Journal of neuroscience : the official journal of the Society for Neuroscience*. 31 (30), 10759–66.

Harpsøe K, Hald H, Timmermann DB, Jensen ML, Dyhring T, Nielsen EØ, Peters D, Balle T, Gajhede M, Kastrup JS and Ahring PK (2013) Molecular determinants of subtype-selective efficacies of cytisine and the novel compound NS3861 at heteromeric nicotinic acetylcholine receptors. *The Journal of biological chemistry*. 288 (4), 2559–70.

Harvey RJ (2004) GlyR 3: An Essential Target for Spinal PGE2-Mediated Inflammatory Pain Sensitization. *Science*. 304 (5672), 884–887.

Hassaine G, Deluz C, Grasso L, Wyss R, Tol MB, Hovius R, Graff A, Stahlberg H, Tomizaki T, Desmyter A, Moreau C, Li X-D, Poitevin F, Vogel H and Nury H (2014) X-ray structure of the mouse serotonin 5-HT3 receptor. *Nature*. 512 (7514), 276–81.

Hénault CM, Sun J, Therien JPD, daCosta CJB, Carswell CL, Labriola JM, Juranka PJ and Baenziger JE (2014) The role of the M4 lipid-sensor in the folding, trafficking, and allosteric modulation of nicotinic acetylcholine receptors. *Neuropharmacology*. 96, 157-68.

Henderson BJ, Pavlovicz RE, Allen JD, Gonza TF, Orac CM, Bonnell AB, Zhu MX, Boyd RT, Li C, Bergmeier SC and Mckay DB (2010) Negative allosteric modulators that target human alpha4beta2 neuronal nicotinic receptors. *The Journal of Pharmacology and Experimental Therapeutics*. 334 (3), 761–774.

Hibbs RE and Gouaux E (2011) Principles of activation and permeation in an anion-selective Cys-loop receptor. *Nature*. 474 (7349), 54–60.

Hibbs RE, Sulzenbacher G, Shi J, Talley TT, Conrod S, Kem WR, Taylor P, Marchot P and Bourne Y (2009) Structural determinants for interaction of partial agonists with acetylcholine binding protein and neuronal alpha7 nicotinic acetylcholine receptor. *The EMBO journal*. 28 (19), 3040–51.

Hilf RJC and Dutzler R (2009) Structure of a potentially open state of a proton-activated pentameric ligand-gated ion channel. *Nature*. 457 (7225), 115–8.

Hilf RJC and Dutzler R (2008) X-ray structure of a prokaryotic pentameric ligand-gated ion channel. *Nature*. 452 (7185), 375–9.

Hosie AM, Clarke L, da Silva H and Smart TG (2009) Conserved site for neurosteroid modulation of GABA A receptors. *Neuropharmacology*. 56 (1), 149–54.

Hosie AM, Wilkins ME, da Silva HMA and Smart TG (2006) Endogenous neurosteroids regulate GABAA receptors through two discrete transmembrane sites. *Nature*. 444 (7118), 486–9.

Hsiao B, Mihalak KB, Repicky SE, Everhart D, Mederos AH, Malhotra A and Luetje CW (2006) Determinants of zinc potentiation on the alpha4 subunit of neuronal nicotinic receptors. *Molecular pharmacology*. 69 (1), 27–36.

Hu X-Q and Lovinger DM (2008) The L293 residue in transmembrane domain 2 of the 5-HT3A receptor is a molecular determinant of allosteric modulation by 5-hydroxyindole. *Neuropharmacology*. 54 (8), 1153–65.

Hurst RS, Hajós M, Raggenbass M, Wall TM, Higdon NR, Lawson JA, Rutherford-Root KL, Berkenpas MB, Hoffmann WE, Piotrowski DW, Groppi VE, Allaman G, Ogier R, Bertrand S, Bertrand D and Arneric SP (2005) A novel positive allosteric modulator of the alpha7 neuronal nicotinic acetylcholine receptor: in vitro and in vivo characterization. *The Journal of neuroscience : the official journal of the Society for Neuroscience*. 25 (17), 4396–405.

Imoto K, Busch C, Sakmann B, Mishina M, Konno T, Nakai J, Bujo H, Mori Y, Fukuda K and Numa S (1988) Rings of negatively charged amino acids determine the acetylcholine receptor channel conductance. *Nature*. 335 (6191), 645–8.

Iturriaga-Vásquez P, Carbone A, García-Beltrán O, Livingstone PD, Biggin PC, Cassels BK, Wonnacott S, Zapata-Torres G and Bermudez I (2010) Molecular determinants for competitive inhibition of alpha4beta2 nicotinic acetylcholine receptors. *Molecular pharmacology*. 78 (3), 366–75.

Jackson KJ, Marks MJ, Vann RE, Chen X, Gamage TF, Warner JA and Damaj MI (2010) Role of alpha5 nicotinic acetylcholine receptors in pharmacological and behavioral effects of nicotine in mice. *The Journal of pharmacology and experimental therapeutics*. 334 (1), 137–46.

Jadey S and Auerbach A (2012) An integrated catch-and-hold mechanism activates nicotinic acetylcholine receptors. *The Journal of general physiology*. 140 (1), 17–28. Jayakar SS, Dailey WP, Eckenhoff RG and Cohen JB (2013) Identification of propofol binding sites in a nicotinic acetylcholine receptor with a photoreactive propofol analog. *The Journal of biological chemistry*. 288 (9), 6178–89.

Jensen AA, Frølund B, Liljefors T and Krogsgaard-Larsen P (2005) Neuronal nicotinic acetylcholine receptors: structural revelations, target identifications, and therapeutic inspirations. *Journal of medicinal chemistry*. 48 (15), 4705–45.

Jha A, Cadugan DJ, Purohit P and Auerbach A (2007) Acetylcholine receptor gating at extracellular transmembrane domain interface: the cys-loop and M2-M3 linker. *The Journal of general physiology*. 130 (6), 547–58.

Jin X, Bermudez I and Steinbach JH (2014) The nicotinic α5 subunit can replace either an acetylcholine-binding or nonbinding subunit in the α4β2* neuronal nicotinic receptor. *Molecular pharmacology*. 85 (1), 11–7.

Jin X and Steinbach JH (2011) A portable site: a binding element for 17β-estradiol can be placed on any subunit of a nicotinic α4β2 receptor. *The Journal of neuroscience : the official journal of the Society for Neuroscience*. 31 (13), 5045–54.

Jin Y, Yang K, Wang H and Wu J (2011) Exposure of nicotine to ventral tegmental area slices induces glutamatergic synaptic plasticity on dopamine neurons. *Synapse (New York, N.Y.)*. 65 (4), 332–8.

Kamens HM, Corley RP, McQueen MB, Stallings MC, Hopfer CJ, Crowley TJ, Brown SA, Hewitt JK and Ehringer MA (2013) Nominal association with CHRNA4 variants and nicotine dependence. *Genes, brain, and behavior*. 12 (3), 297–304.

Karakas E, Regan MC and Furukawa H (2015) Emerging structural insights into the function of ionotropic glutamate receptors. *Trends in biochemical sciences*. 40 (6), 328–337.

Karlin A and Akabas MH (1998) Substituted-cysteine accessibility method. *Methods in enzymology*. 293, 123–45.

Kash TL, Jenkins A, Kelley JC, Trudell JR and Harrison NL (2003) Coupling of agonist binding to channel gating in the GABA(A) receptor. *Nature*. 421 (6920), 272–5.

Kedmi M, Beaudet AL and Orr-Urtreger A (2004) Mice lacking neuronal nicotinic acetylcholine receptor beta4-subunit and mice lacking both alpha5- and beta4-subunits are highly resistant to nicotine-induced seizures. *Physiological genomics*. 17 (2), 221–9.

Kim J-S, Padnya A, Weltzin M, Edmonds BW, Schulte MK and Glennon RA (2007) Synthesis of desformylflustrabromine and its evaluation as an alpha4beta2 and alpha7 nACh receptor modulator. *Bioorganic & medicinal chemistry letters*. 17 (17), 4855–60.

Konno T, Busch C, Von Kitzing E, Imoto K, Wang F, Nakai J, Mishina M, Numa S and Sakmann B (1991) Rings of anionic amino acids as structural determinants of ion selectivity in the acetylcholine receptor channel. *Proceedings. Biological sciences / The Royal Society*. 244 (1310), 69–79.

Krasowski MD, Koltchine V V, Rick CE, Ye Q, Finn SE and Harrison NL (1998) Propofol and other intravenous anesthetics have sites of action on the gamma-aminobutyric acid type A receptor distinct from that for isoflurane. *Molecular pharmacology*. 53 (3), 530–8.

Krause RM, Buisson B, Bertrand S, Corringer PJ, Galzi JL, Changeux JP and Bertrand D (1998) Ivermectin: a positive allosteric effector of the alpha7 neuronal nicotinic acetylcholine receptor. *Molecular pharmacology*. 53 (2), 283–94.

Kucken AM, Teissére JA, Seffinga-Clark J, Wagner DA and Czajkowski C (2003) Structural requirements for imidazobenzodiazepine binding to GABA(A) receptors. *Molecular pharmacology*. 63 (2), 289–96.

Kuryatov A (2005) Nicotine Acts as a Pharmacological Chaperone to Upregulate Human 4 2 AChRs. *Molecular Pharmacology*. 68 (6), 1839–51.

Kuryatov A, Berrettini W and Lindstrom J (2011) Acetylcholine receptor (AChR) α5 subunit variant associated with risk for nicotine dependence and lung cancer reduces $(\alpha4\beta2)_2\alpha5$ AChR function. *Molecular pharmacology*. 79 (1), 119–25.

Kuryatov A, Onksen J and Lindstrom J (2008) Roles of accessory subunits in alpha4beta2(*) nicotinic receptors. *Molecular pharmacology*. 74 (1), 132–43.

Lape R, Colquhoun D and Sivilotti LG (2008) On the nature of partial agonism in the nicotinic receptor superfamily. *Nature*. 454 (7205), 722–7.

Laviolette SR and van der Kooy D (2004) The neurobiology of nicotine addiction: bridging the gap from molecules to behaviour. *Nature reviews. Neuroscience*. 5 (1), 55–65.

Lee C-H, Zhu C, Malysz J, Campbell T, Shaughnessy T, Honore P, Polakowski J and Gopalakrishnan M (2011) α4β2 neuronal nicotinic receptor positive allosteric modulation: an approach for improving the therapeutic index of α4β2 nAChR agonists in pain. *Biochemical pharmacology*. 82 (8), 959–66.

Lee WY, Free CR and Sine SM (2009) Binding to gating transduction in nicotinic receptors: Cys-loop energetically couples to pre-M1 and M2-M3 regions. *The Journal of neuroscience : the official journal of the Society for Neuroscience*. 29 (10), 3189–99.

Lee WY and Sine SM (2005) Principal pathway coupling agonist binding to channel gating in nicotinic receptors. *Nature*. 438 (7065), 243–7.

Lester HA, Xiao C, Srinivasan R, Son CD, Miwa J, Pantoja R, Banghart MR, Dougherty DA, Goate AM and Wang JC (2009) Nicotine is a selective pharmacological chaperone of acetylcholine receptor number and stoichiometry. Implications for drug discovery. *The AAPS journal*. 11 (1), 167–77.

Levin ED and Simon BB (1998) Nicotinic acetylcholine involvement in cognitive function in animals. *Psychopharmacology*. 138 (3-4), 217–30.

Li S-X, Huang S, Bren N, Noridomi K, Dellisanti CD, Sine SM and Chen L (2011) Ligand-binding domain of an α7-nicotinic receptor chimera and its complex with agonist. *Nature neuroscience*. 14 (10), 1253–9.

Lindstrom J, Merlie J and Yogeeswaran G (1979) Biochemical properties of acteylcholine receptor subunits from Torpedo californica. *Biochemistry*. 18 (21), 4465–70.

Liu X (2013) Positive allosteric modulation of α4β2 nicotinic acetylcholine receptors as a new approach to smoking reduction: evidence from a rat model of nicotine self-administration. *Psychopharmacology*. 230 (2), 203–13.

Lohmann TH, Torrão AS, Britto LR, Lindstrom J and Hamassaki-Britto DE (2000) A comparative non-radioactive in situ hybridization and immunohistochemical study of the distribution of alpha7 and alpha8 subunits of the nicotinic acetylcholine receptors in visual areas of the chick brain. *Brain research*. 852 (2), 463–9.

Lummis SCR, Beene DL, Lee LW, Lester HA, Broadhurst RW and Dougherty DA (2005) Cis-trans isomerization at a proline opens the pore of a neurotransmitter-gated ion channel. *Nature*. 438 (7065), 248–52.

Lynagh T and Laube B (2014) Opposing effects of the anesthetic propofol at pentameric ligand-gated ion channels mediated by a common site. *The Journal of neuroscience : the official journal of the Society for Neuroscience*. 34 (6), 2155–9.

Lynagh T and Pless SA (2014) Principles of agonist recognition in Cys-loop receptors. *Frontiers in physiology*. 5, 160.

Lynch JW (2004) Molecular structure and function of the glycine receptor chloride channel. *Physiological reviews*. 84 (4), 1051–95.

Mansvelder HD and McGehee DS (2002) Cellular and synaptic mechanisms of nicotine addiction. *Journal of neurobiology*. 53 (4), 606–17.

Mantione E, Micheloni S, Alcaino C, New K, Mazzaferro S and Bermudez I (2012) Allosteric modulators of alpha4beta2 nicotinic acetylcholine receptors: a new direction for antidepressant drug discovery. *Future Med Chem*. 4 (17), 2217–2230.

Marks MJ, Meinerz NM, Drago J and Collins AC (2007) Gene targeting demonstrates that alpha4 nicotinic acetylcholine receptor subunits contribute to expression of diverse [3H]epibatidine binding sites and components of biphasic 86Rb+ efflux with high and low sensitivity to stimulation by acetylcholine. *Neuropharmacology*. 53 (3), 390–405.

Marks MJ, Whiteaker P, Calcaterra J, Stitzel JA, Bullock AE, Grady SR, Picciotto MR, Changeux JP and Collins AC (1999) Two pharmacologically distinct components of nicotinic receptor-mediated rubidium efflux in mouse brain require the beta2 subunit. *The Journal of pharmacology and experimental therapeutics*. 289 (2), 1090–103.

Marotta CB, Dilworth CN, Lester HA and Dougherty DA (2014) Probing the non-canonical interface for agonist interaction with an α5 containing nicotinic acetylcholine receptor. *Neuropharmacology*. 77, 342–9.

Maskos U, Molles BE, Pons S, Besson M, Guiard BP, Guilloux J-P, Evrard A, Cazala P, Cormier A, Mameli-Engvall M, Dufour N, Cloëz-Tayarani I, Bemelmans A-P, Mallet J, Gardier AM, David V, Faure P, Granon S and Changeux J-P (2005) Nicotine reinforcement and cognition restored by targeted expression of nicotinic receptors. *Nature*. 436 (7047), 103–7.

Mazzaferro S, Benallegue N, Carbone A, Gasparri F, Vijayan R, Biggin PC, Moroni M and Bermudez I (2011) Additional acetylcholine (ACh) binding site at alpha4/alpha4 interface of (alpha4beta2)2alpha4 nicotinic receptor influences agonist sensitivity. *The Journal of biological chemistry*. 286 (35), 31043–54.

Mazzaferro S, Gasparri F, New K, Alcaino C, Faundez M, Vasquez PI, Vijayan R, Biggin PC and Bermudez I (2014) Non-equivalent ligand selectivity of agonist sites in (α4β2)2α4 nicotinic acetylcholine receptors: A key determinant of agonist efficacy. *Journal of Biological Chemistry*. 289 (31), 21795-806.

McCormack TJ, Melis C, Colón J, Gay EA, Mike A, Karoly R, Lamb PW, Molteni C and Yakel JL (2010) Rapid desensitization of the rat α7 nAChR is facilitated by the presence

of a proline residue in the outer β-sheet. *The Journal of physiology*. 588 (Pt 22), 4415–29.

Millar NS and Gotti C (2009) Diversity of vertebrate nicotinic acetylcholine receptors. *Neuropharmacology*. 56 (1), 237–46.

Miller PS and Aricescu AR (2014) Crystal structure of a human GABAA receptor. *Nature*. 512 (7514), 270–5.

Miller PS and Smart TG (2010) Binding, activation and modulation of Cys-loop receptors. *Trends in pharmacological sciences*. 31 (4), 161–74.

Mineur YS, Abizaid A, Rao Y, Salas R, DiLeone RJ, Gündisch D, Diano S, De Biasi M, Horvath TL, Gao X-B and Picciotto MR (2011) Nicotine decreases food intake through activation of POMC neurons. *Science (New York, N.Y.)*. 332 (6035), 1330–2.

Mineur YS, Einstein EB, Seymour PA, Coe JW, O'neill BT, Rollema H and Picciotto MR (2011) α4β2 nicotinic acetylcholine receptor partial agonists with low intrinsic efficacy have antidepressant-like properties. *Behavioural pharmacology*. 22 (4), 291–9.

Mineur YS and Picciotto MR (2010) Nicotine receptors and depression: revisiting and revising the cholinergic hypothesis. *Trends in pharmacological sciences*. 31 (12), 580–6.

Miwa JM, Freedman R and Lester HA (2011) Neural systems governed by nicotinic acetylcholine receptors: emerging hypotheses. *Neuron*. 70 (1), 20–33.

Miyazawa A, Fujiyoshi Y and Unwin N (2003) Structure and gating mechanism of the acetylcholine receptor pore. *Nature*. 423 (6943), 949–55.

Moretti M, Vailati S, Zoli M, Lippi G, Riganti L, Longhi R, Viegi A, Clementi F and Gotti C (2004) Nicotinic acetylcholine receptor subtypes expression during rat retina development and their regulation by visual experience. *Molecular pharmacology*. 66 (1), 85–96.

Moroni M, Vijayan R, Carbone A, Zwart R, Biggin PC and Bermudez I (2008) Non-agonist-binding subunit interfaces confer distinct functional signatures to the alternate stoichiometries of the alpha4beta2 nicotinic receptor: an alpha4-alpha4 interface is required for Zn2+ potentiation. *The Journal of neuroscience : the official journal of the Society for Neuroscience*. 28 (27), 6884–94.

Moroni M, Zwart R, Sher E, Cassels BK and Bermudez I (2006) α4β2 nicotinic receptors with high and low acetylcholine sensitivity: pharmacology , stoichiometry , and sensitivity to long-term exposure to nicotine. *Molecular Pharmacology*. 70 (2), 755–768.

Mukhtasimova N, Free C and Sine SM (2005) Initial coupling of binding to gating mediated by conserved residues in the muscle nicotinic receptor. *The Journal of general physiology*. 126 (1), 23–39.

Mukhtasimova N, Lee WY, Wang H-L and Sine SM (2009) Detection and trapping of intermediate states priming nicotinic receptor channel opening. *Nature*. 459 (7245), 451–4.

Nelson ME, Kuryatov A, Choi CH, Zhou Y and Lindstrom J (2003) Alternate stoichiometries of alpha4beta2 nicotinic acetylcholine receptors. *Molecular pharmacology*. 63 (2), 332–41.

Nemecz A and Taylor P (2011) Creating an α7 nicotinic acetylcholine recognition domain from the acetylcholine-binding protein: crystallographic and ligand selectivity analyses. *The Journal of biological chemistry*. 286 (49), 42555–65.

Newman MB, Nazian SJ, Sanberg PR, Diamond DM and Shytle RD (2001) Corticosterone-attenuating and anxiolytic properties of mecamylamine in the rat. *Progress in neuro-psychopharmacology & biological psychiatry*. 25 (3), 609–20.

Nguyen HT, Li K, daGraca RL, Delphin E, Xiong M and Ye JH (2009) Behavior and cellular evidence for propofol-induced hypnosis involving brain glycine receptors. *Anesthesiology*. 110 (2), 326–32.

Niessen K V, Seeger T, Tattersall JEH, Timperley CM, Bird M, Green C, Thiermann H and Worek F (2013) Affinities of bispyridinium non-oxime compounds to [(3)H]epibatidine binding sites of Torpedo californica nicotinic acetylcholine receptors depend on linker length. *Chemico-biological interactions*. 206 (3), 545–54.

Notredame C, Higgins DG and Heringa J (2000) T-Coffee: A novel method for fast and accurate multiple sequence alignment. *Journal of molecular biology*. 302 (1), 205–17.

Nury H, Bocquet N, Le Poupon C, Raynal B, Haouz A, Corringer P-J and Delarue M (2010) Crystal Structure of the Extracellular Domain of a Bacterial Ligand-Gated Ion Channel. *Journal of Molecular Biology*. 395 (5), 1114–1127.

Nury H, Van Renterghem C, Weng Y, Tran A, Baaden M, Dufresne V, Changeux J-P, Sonner JM, Delarue M and Corringer P-J (2011) X-ray structures of general anaesthetics bound to a pentameric ligand-gated ion channel. *Nature*. 469 (7330), 428–31.

Nys M, Kesters D and Ulens C (2013) Structural insights into Cys-loop receptor function and ligand recognition. *Biochemical pharmacology*. 86 (8), 1042–53.

O'Neill AB and Brioni JD (1994) Benzodiazepine receptor mediation of the anxiolytic-like effect of (-)-nicotine in mice. *Pharmacology, biochemistry, and behavior*. 49 (3), 755–7.

Olsen JA, Ahring PK, Kastrup JS, Gajhede M and Balle T (2014) Structural and Functional Studies of the Modulator NS9283 Reveal Agonist-Like Mechanism of Action at α4β2 Nicotinic Acetylcholine Receptors. *The Journal of biological chemistry*. 289 (36), 24911–21.

Olsen JA, Kastrup JS, Peters D, Gajhede M, Balle T and Ahring PK (2013) Two distinct allosteric binding sites at α4β2 nicotinic acetylcholine receptors revealed by NS206 and

NS9283 give unique insights to binding activity-associated linkage at Cys-loop receptors. *The Journal of biological chemistry*. 288 (50), 35997–6006.

Pandya A and Yakel JL (2011) Allosteric modulator Desformylflustrabromine relieves the inhibition of α2β2 and α4β2 nicotinic acetylcholine receptors by β-amyloid(1-42) peptide. *Journal of molecular neuroscience : MN*. 45 (1), 42–7.

Paradiso K, Zhang J and Steinbach JH (2001) The C terminus of the human nicotinic alpha4beta2 receptor forms a binding site required for potentiation by an estrogenic steroid. *The Journal of neuroscience : the official journal of the Society for Neuroscience*. 21 (17), 6561–8.

Pavlovicz RE, Henderson BJ, Bonnell AB, Boyd RT, McKay DB and Li C (2011) Identification of a negative allosteric site on human α4β2 and α3β4 neuronal nicotinic acetylcholine receptors. *PloS one*. 6 (9), e24949.

Peters L, König GM, Terlau H and Wright AD (2002) Four new bromotryptamine derivatives from the marine bryozoan Flustra foliacea. *Journal of natural products*. 65 (11), 1633–7.

Phillips HA, Favre I, Kirkpatrick M, Zuberi SM, Goudie D, Heron SE, Scheffer IE, Sutherland GR, Berkovic SF, Bertrand D and Mulley JC (2001) CHRNB2 is the second acetylcholine receptor subunit associated with autosomal dominant nocturnal frontal lobe epilepsy. *American journal of human genetics*. 68 (1), 225–31.

Picciotto MR, Caldarone BJ, Brunzell DH, Zachariou V, Stevens TR and King SL (2001) Neuronal nicotinic acetylcholine receptor subunit knockout mice: physiological and behavioral phenotypes and possible clinical implications. *Pharmacology & therapeutics*. 92 (2-3), 89–108.

Picciotto MR and Zoli M (2008) Neuroprotection via nAChRs: the role of nAChRs in neurodegenerative disorders such as Alzheimer's and Parkinson's disease. *Frontiers in bioscience : a journal and virtual library*. 13, 492–504.

Preskorn SH, Gawryl M, Dgetluck N, Palfreyman M, Bauer LO and Hilt DC (2014) Normalizing effects of EVP-6124, an alpha-7 nicotinic partial agonist, on event-related potentials and cognition: a proof of concept, randomized trial in patients with schizophrenia. *Journal of psychiatric practice*. 20 (1), 12–24.

Purohit P and Auerbach A (2009) Unliganded gating of acetylcholine receptor channels. *Proceedings of the National Academy of Sciences of the United States of America*. 106 (1), 115–20.

Purohit P, Mitra A and Auerbach A (2007) A stepwise mechanism for acetylcholine receptor channel gating. *Nature*. 446 (7138), 930–3.

Quik M and Jeyarasasingam G (2000) Nicotinic receptors and Parkinson's disease. *European Journal of Pharmacology*. 393 (1-3), 223–230.

Quik M, O'Neill M and Perez X a (2007) Nicotine neuroprotection against nigrostriatal damage: importance of the animal model. *Trends in pharmacological sciences*. 28 (5), 229–35.

Quik M, Zhang D, Perez XA and Bordia T (2014) Role for the nicotinic cholinergic system in movement disorders; therapeutic implications. *Pharmacology & therapeutics*. 144 (1), 50–59.

Rabenstein RL, Caldarone BJ and Picciotto MR (2006) The nicotinic antagonist mecamylamine has antidepressant-like effects in wild-type but not beta2- or alpha7-nicotinic acetylcholine receptor subunit knockout mice. *Psychopharmacology*. 189 (3), 395–401.

Raber J, Koob GF and Bloom FE (1995) Interleukin-2 (IL-2) induces corticotropin-releasing factor (CRF) release from the amygdala and involves a nitric oxide-mediated signaling; comparison with the hypothalamic response. *The Journal of pharmacology and experimental therapeutics*. 272 (2), 815–24.

Revah F, Galzi JL, Giraudat J, Haumont PY, Lederer F and Changeux JP (1990) The noncompetitive blocker [3H]chlorpromazine labels three amino acids of the acetylcholine receptor gamma subunit: implications for the alpha-helical organization of regions MII and for the structure of the ion channel. *Proceedings of the National Academy of Sciences of the United States of America*. 87 (12), 4675–9.

Reynolds JA and Karlin A (1978) Molecular weight in detergent solution of acetylcholine receptor from Torpedo californica. *Biochemistry*. 17 (11), 2035–8.

Rode F, Munro G, Holst D, Nielsen EØ, Troelsen KB, Timmermann DB, Rønn LCB and Grunnet M (2012) Positive allosteric modulation of α4β2 nAChR agonist induced behaviour. *Brain research*. 1458, 67–75.

Rohde LAH, Ahring PK, Jensen ML, Nielsen EØ, Peters D, Helgstrand C, Krintel C, Harpsøe K, Gajhede M, Kastrup JS and Balle T (2012) Intersubunit bridge formation governs agonist efficacy at nicotinic acetylcholine α4β2 receptors: unique role of halogen bonding revealed. *The Journal of biological chemistry*. 287 (6), 4248–59.

Rollema H, Wilson GG, Lee TC, Folgering JHA and Flik G (2011) Effect of co-administration of varenicline and antidepressants on extracellular monoamine concentrations in rat prefrontal cortex. *Neurochemistry international*. 58 (1), 78–84.

De Rosa MJ, Rayes D, Spitzmaul G and Bouzat C (2002) Nicotinic receptor M3 transmembrane domain: position 8' contributes to channel gating. *Molecular pharmacology*. 62 (2), 406–14.

Rucktooa P, Smit AB and Sixma TK (2009) Insight in nAChR subtype selectivity from AChBP crystal structures. *Biochemical pharmacology*. 78 (7), 777–87.

Rudolph U and Knoflach F (2011) Beyond classical benzodiazepines: novel therapeutic potential of GABAA receptor subtypes. *Nature reviews. Drug discovery*. 10 (9), 685–97.

Rüsch D, Braun HA, Wulf H, Schuster A and Raines DE (2007) Inhibition of human 5-HT(3A) and 5-HT(3AB) receptors by etomidate, propofol and pentobarbital. *European journal of pharmacology*. 573 (1-3), 60–4.

Sala F, Mulet J, Reddy KP, Bernal JA, Wikman P, Valor LM, Peters L, König GM, Criado M and Sala S (2005) Potentiation of human alpha4beta2 neuronal nicotinic receptors by a Flustra foliacea metabolite. *Neuroscience letters*. 373 (2), 144–9.

Samochocki M, Höffle A, Fehrenbacher A, Jostock R, Ludwig J, Christner C, Radina M, Zerlin M, Ullmer C, Pereira EFR, Lübbert H, Albuquerque EX and Maelicke A (2003) Galantamine is an allosterically potentiating ligand of neuronal nicotinic but not of muscarinic acetylcholine receptors. *The Journal of pharmacology and experimental therapeutics*. 305 (3), 1024–36.

Sancar F, Ericksen SS, Kucken AM, Teissére JA and Czajkowski C (2007) Structural determinants for high-affinity zolpidem binding to GABA-A receptors. *Molecular pharmacology*. 71 (1), 38–46.

Sarter M, Nelson CL and Bruno JP (2005) Cortical cholinergic transmission and cortical information processing in schizophrenia. *Schizophrenia bulletin*. 31 (1), 117–38.

Sauguet L, Howard RJ, Malherbe L, Lee US, Corringer P-J, Harris RA and Delarue M (2013) Structural basis for potentiation by alcohols and anaesthetics in a ligand-gated ion channel. *Nature communications*. 4, 1697.

Sauguet L, Shahsavar A and Delarue M (2014) Crystallographic studies of pharmacological sites in pentameric ligand-gated ion channels. *Biochimica et biophysica acta*.

Schaerer MT, Buhr A, Baur R and Sigel E (1998) Amino acid residue 200 on the alpha1 subunit of GABA(A) receptors affects the interaction with selected benzodiazepine binding site ligands. *European journal of pharmacology*. 354 (2-3), 283–7.

Seo S, Henry JT, Lewis AH, Wang N and Levandoski MM (2009) The positive allosteric modulator morantel binds at noncanonical subunit interfaces of neuronal nicotinic acetylcholine receptors. *The Journal of neuroscience : the official journal of the Society for Neuroscience*. 29 (27), 8734–42.

Shahsavar A, Kastrup JS, Nielsen EØ, Kristensen JL, Gajhede M and Balle T (2012) Crystal structure of Lymnaea stagnalis AChBP complexed with the potent nAChR antagonist DHβE suggests a unique mode of antagonism. *PloS one*. 7 (8), e40757.

Shytle RD, Penny E, Silver AA, Goldman J and Sanberg PR (2002) Mecamylamine (Inversine): an old antihypertensive with new research directions. *Journal of human hypertension*. 16 (7), 453–7.

Sine SM (1993) Molecular dissection of subunit interfaces in the acetylcholine receptor: identification of residues that determine curare selectivity. *Proceedings of the National Academy of Sciences of the United States of America*. 90 (20), 9436–40.

Sine SM (2002) The nicotinic receptor ligand binding domain. *Journal of neurobiology*. 53 (4), 431–46.

Sine SM and Claudio T (1991) Gamma- and delta-subunits regulate the affinity and the cooperativity of ligand binding to the acetylcholine receptor. *The Journal of biological chemistry*. 266 (29), 19369–77.

Slater YE, Houlihan LM, Maskell PD, Exley R, Bermúdez I, Lukas RJ, Valdivia AC and Cassels BK (2003) Halogenated cytisine derivatives as agonists at human neuronal nicotinic acetylcholine receptor subtypes. *Neuropharmacology*. 44 (4), 503–15.

Smulders CJGM, Zwart R, Bermudez I, van Kleef RGDM, Groot-Kormelink PJ and Vijverberg HPM (2005) Cholinergic drugs potentiate human nicotinic alpha4beta2 acetylcholine receptors by a competitive mechanism. *European journal of pharmacology*. 509 (2-3), 97–108.

Spurny R, Ramerstorfer J, Price K, Brams M, Ernst M, Nury H, Verheij M, Legrand P, Bertrand D, Bertrand S, Dougherty D a, de Esch IJP, Corringer P-J, Sieghart W, Lummis SCR and Ulens C (2012) Pentameric ligand-gated ion channel ELIC is activated by GABA and modulated by benzodiazepines. *Proceedings of the National Academy of Sciences of the United States of America*. 109 (44), E3028–34.

Srinivasan R, Pantoja R, Moss FJ, Mackey EDW, Son CD, Miwa J and Lester HA (2011) Nicotine up-regulates alpha4beta2 nicotinic receptors and ER exit sites via stoichiometry-dependent chaperoning. *The Journal of general physiology*. 137 (1), 59–79.

Staley JK, Krishnan-Sarin S, Cosgrove KP, Krantzler E, Frohlich E, Perry E, Dubin JA, Estok K, Brenner E, Baldwin RM, Tamagnan GD, Seibyl JP, Jatlow P, Picciotto MR, London ED, O'Malley S and van Dyck CH (2006) Human tobacco smokers in early abstinence have higher levels of beta2* nicotinic acetylcholine receptors than nonsmokers. *The Journal of neuroscience : the official journal of the Society for Neuroscience*. 26 (34), 8707–14.

Steinlein O, Sander T, Stoodt J, Kretz R, Janz D and Propping P (1997) Possible association of a silent polymorphism in the neuronal nicotinic acetylcholine receptor subunit alpha4 with common idiopathic generalized epilepsies. *American journal of medical genetics*. 74 (4), 445–9.

Steinlein OK, Mulley JC, Propping P, Wallace RH, Phillips HA, Sutherland GR, Scheffer IE and Berkovic SF (1995) A missense mutation in the neuronal nicotinic acetylcholine receptor alpha 4 subunit is associated with autosomal dominant nocturnal frontal lobe epilepsy. *Nature genetics*. 11 (2), 201–3.

Taly A, Corringer P-J, Guedin D, Lestage P and Changeux J-P (2009) Nicotinic receptors: allosteric transitions and therapeutic targets in the nervous system. *Nature reviews. Drug discovery*. 8 (9), 733–50.

Taly A, Delarue M, Grutter T, Nilges M, Le Novère N, Corringer P-J and Changeux J-P (2005) Normal mode analysis suggests a quaternary twist model for the nicotinic receptor gating mechanism. *Biophysical journal*. 88 (6), 3954–65.

Tapia L, Kuryatov A and Lindstrom J (2007) Ca2+ permeability of the (alpha4)3(beta2)2 stoichiometry greatly exceeds that of (alpha4)2(beta2)3 human acetylcholine receptors. *Molecular pharmacology*. 71 (3), 769–76.

Tapper AR, McKinney SL, Marks MJ and Lester HA (2007) Nicotine responses in hypersensitive and knockout alpha 4 mice account for tolerance to both hypothermia and locomotor suppression in wild-type mice. *Physiological genomics*. 31 (3), 422–8.

Tapper AR, McKinney SL, Nashmi R, Schwarz J, Deshpande P, Labarca C, Whiteaker P, Marks MJ, Collins AC and Lester HA (2004) Nicotine activation of alpha4* receptors: sufficient for reward, tolerance, and sensitization. *Science (New York, N.Y.)*. 306 (5698), 1029–32.

Tassonyi E, Charpantier E, Muller D, Dumont L and Bertrand D (2002) The role of nicotinic acetylcholine receptors in the mechanisms of anesthesia. *Brain research bulletin*. 57 (2), 133–50.

Teissére JA and Czajkowski C (2001) A (beta)-strand in the (gamma)2 subunit lines the benzodiazepine binding site of the GABA A receptor: structural rearrangements detected during channel gating. *The Journal of neuroscience : the official journal of the Society for Neuroscience*. 21 (14), 4977–86.

Timmermann DB, Grønlien JH, Kohlhaas KL, Nielsen EØ, Dam E, Jørgensen TD, Ahring PK, Peters D, Holst D, Christensen JK, Chrsitensen JK, Malysz J, Briggs CA, Gopalakrishnan M and Olsen GM (2007) An allosteric modulator of the alpha7 nicotinic acetylcholine receptor possessing cognition-enhancing properties in vivo. *The Journal of pharmacology and experimental therapeutics*. 323 (1), 294–307.

Timmermann DB, Sandager-Nielsen K, Dyhring T, Smith M, Jacobsen A-M, Nielsen EØ, Grunnet M, Christensen JK, Peters D, Kohlhaas K, Olsen GM and Ahring PK (2012) Augmentation of cognitive function by NS9283, a stoichiometry-dependent positive allosteric modulator of α2- and α4-containing nicotinic acetylcholine receptors. *British journal of pharmacology*. 167 (1), 164–82.

Unwin N (1993) Nicotinic acetylcholine receptor at 9 A resolution. *Journal of molecular biology*. 229 (4), 1101–24.

Unwin N (2005) Refined structure of the nicotinic acetylcholine receptor at 4A resolution. *Journal of molecular biology*. 346 (4), 967–89.

Unwin N and Fujiyoshi Y (2012) Gating movement of acetylcholine receptor caught by plunge-freezing. *Journal of molecular biology*. 422 (5), 617–34.

Venkatachalan SP and Czajkowski C (2008) A conserved salt bridge critical for GABA(A) receptor function and loop C dynamics. *Proceedings of the National Academy of Sciences of the United States of America*. 105 (36), 13604–9.

Vincler M and Eisenach JC (2004) Plasticity of spinal nicotinic acetylcholine receptors following spinal nerve ligation. *Neuroscience research*. 48 (2), 139–45.

Wang Q and Lynch JW (2011) Activation and desensitization induce distinct conformational changes at the extracellular-transmembrane domain interface of the glycine receptor. *The Journal of biological chemistry*. 286 (44), 38814–24.

Weiland S, Witzemann V, Villarroel A, Propping P and Steinlein O (1996) An amino acid exchange in the second transmembrane segment of a neuronal nicotinic receptor causes partial epilepsy by altering its desensitization kinetics. *FEBS letters*. 398 (1), 91–6.

Weltzin MM, Huang Y and Schulte MK (2014) Allosteric modulation of alpha4beta2 nicotinic acetylcholine receptors by HEPES. *European journal of pharmacology*. 732, 159–68.

Weltzin MM and Schulte MK (2010) Pharmacological characterization of the allosteric modulator desformylflustrabromine and its interaction with alpha4beta2 neuronal nicotinic acetylcholine receptor orthosteric ligands. *Journal of Pharmacology and Experimental Therapeutics*. 334 (3), 917–926.

Weng Y, Yang L, Corringer P-J and Sonner JM (2010) Anesthetic sensitivity of the Gloeobacter violaceus proton-gated ion channel. *Anesthesia and analgesia*. 110 (1), 59–63.

Wieland HA, Lüddens H and Seeburg PH (1992) A single histidine in GABAA receptors is essential for benzodiazepine agonist binding. *The Journal of biological chemistry*. 267 (3), 1426–9.

Wilkins JN, Carlson HE, Van Vunakis H, Hill MA, Gritz E and Jarvik ME (1982) Nicotine from cigarette smoking increases circulating levels of cortisol, growth hormone, and prolactin in male chronic smokers. *Psychopharmacology*. 78 (4), 305–8.

Wilson GG and Karlin A (1998) The location of the gate in the acetylcholine receptor channel. *Neuron*. 20 (6), 1269–81.

Wingrove PB, Thompson SA, Wafford KA and Whiting PJ (1997) Key amino acids in the gamma subunit of the gamma-aminobutyric acidA receptor that determine ligand binding and modulation at the benzodiazepine site. *Molecular pharmacology*. 52 (5), 874–81.

Wolstenholme AJ and Rogers AT (2005) Glutamate-gated chloride channels and the mode of action of the avermectin/milbemycin anthelmintics. *Parasitology*. 131 Suppl, S85–95.

Wonnacott S, Barik J, Dickinson J and Jones IW (2006) Nicotinic receptors modulate transmitter cross talk in the CNS: nicotinic modulation of transmitters. *Journal of molecular neuroscience : MN*. 30 (1-2), 137–40.

Wonnacott S, Kaiser S, Mogg A, Soliakov L and Jones IW (2000) Presynaptic nicotinic receptors modulating dopamine release in the rat striatum. *European journal of pharmacology*. 393 (1-3), 51–8.

Wyllie DJA and Chen PE (2007) Taking the time to study competitive antagonism. *British journal of pharmacology*. 150 (5), 541–51.

Xiao Y, Fan H, Musachio JL, Wei Z-L, Chellappan SK, Kozikowski AP and Kellar KJ (2006) Sazetidine-A, a novel ligand that desensitizes alpha4beta2 nicotinic acetylcholine receptors without activating them. *Molecular pharmacology*. 70 (4), 1454–60.

Xiu X, Puskar NL, Shanata JAP, Lester HA and Dougherty DA (2009) Nicotine binding to brain receptors requires a strong cation-pi interaction. *Nature*. 458 (7237), 534–7.

Ye Q, Koltchine V V, Mihic SJ, Mascia MP, Wick MJ, Finn SE, Harrison NL and Harris RA (1998) Enhancement of glycine receptor function by ethanol is inversely correlated with molecular volume at position alpha267. *The Journal of biological chemistry*. 273 (6), 3314–9.

Yip GMS, Chen Z-W, Edge CJ, Smith EH, Dickinson R, Hohenester E, Townsend RR, Fuchs K, Sieghart W, Evers AS and Franks NP (2013) A propofol binding site on mammalian GABAA receptors identified by photolabeling. *Nature chemical biology*. 9 (11), 715–20.

Yoshimura RF, Hogenkamp DJ, Li WY, Tran MB, Belluzzi JD, Whittemore ER, Leslie FM and Gee KW (2007) Negative allosteric modulation of nicotinic acetylcholine receptors blocks nicotine self-administration in rats. *The Journal of pharmacology and experimental therapeutics*. 323 (3), 907–15.

Young GT, Zwart R, Walker AS, Sher E and Millar NS (2008) Potentiation of alpha7 nicotinic acetylcholine receptors via an allosteric transmembrane site. *Proceedings of the National Academy of Sciences of the United States of America*. 105 (38), 14686–91.

Zeller A, Jurd R, Lambert S, Arras M, Drexler B, Grashoff C, Antkowiak B and Rudolph U (2008) Inhibitory ligand-gated ion channels as substrates for general anesthetic actions. *Handbook of experimental pharmacology*. (182), 31–51.

Zhang H and Karlin A (1997) Identification of acetylcholine receptor channel-lining residues in the M1 segment of the beta-subunit. *Biochemistry*. 36 (50), 15856–64.

Zhang J, Xiao Y-D, Jordan KG, Hammond PS, Van Dyke KM, Mazurov AA, Speake JD, Lippiello PM, James JW, Letchworth SR, Bencherif M and Hauser TA (2012) Analgesic effects mediated by neuronal nicotinic acetylcholine receptor agonists: correlation with desensitization of α4β2* receptors. *European journal of pharmaceutical sciences : official journal of the European Federation for Pharmaceutical Sciences*. 47 (5), 813–23.

Zhang T, Zhang L, Liang Y, Siapas AG, Zhou F-M and Dani J a (2009) Dopamine signaling differences in the nucleus accumbens and dorsal striatum exploited by nicotine. *The Journal of neuroscience : the official journal of the Society for Neuroscience*. 29 (13), 4035–43.

Zhong W, Gallivan JP, Zhang Y, Li L, Lester HA and Dougherty DA (1998) From ab initio quantum mechanics to molecular neurobiology: a cation-pi binding site in the nicotinic

receptor. *Proceedings of the National Academy of Sciences of the United States of America*. 95 (21), 12088–93..

Zhou Y, Nelson ME, Kuryatov A, Choi C, Cooper J and Lindstrom J (2003) Human alpha4beta2 acetylcholine receptors formed from linked subunits. *The Journal of neuroscience : the official journal of the Society for Neuroscience*. 23 (27), 9004–15.

Zimmermann I and Dutzler R (2011) Ligand activation of the prokaryotic pentameric ligand-gated ion channel ELIC. *PLoS biology*. 9 (6), e1001101.

Zouridakis M, Giastas P, Zarkadas E, Chroni-Tzartou D, Bregestovski P and Tzartos SJ (2014) Crystal structures of free and antagonist-bound states of human α9 nicotinic receptor extracellular domain. *Nature structural & molecular biology*. 21 (11), 976–80.

Zwart R, Broad LM, Xi Q, Lee M, Moroni M, Bermudez I and Sher E (2006) 5-I A-85380 and TC-2559 differentially activate heterologously expressed alpha4beta2 nicotinic receptors. *European journal of pharmacology*. 539 (1-2), 10–7.

Zwart R, Carbone AL, Moroni M, Bermudez I, Mogg AJ, Folly EA, Broad LM, Williams AC, Zhang D, Ding C, Heinz BA and Sher E (2008) Sazetidine-A is a potent and selective agonist at native and recombinant alpha 4 beta 2 nicotinic acetylcholine receptors. *Molecular pharmacology*. 73 (6), 1838–43.

Zwart R, De Filippi G, Broad LM, McPhie GI, Pearson KH, Baldwinson T and Sher E (2002) 5-Hydroxyindole potentiates human alpha 7 nicotinic receptor-mediated responses and enhances acetylcholine-induced glutamate release in cerebellar slices. *Neuropharmacology*. 43 (3), 374–84.